Senior Design Project

USRA/NASA/VPI&SU

Design of a Pressurized Lunar Rover

Final Report

24 APRIL 1992

SUBMITTED BY:

MANOJ BHARDWAJ
VATSAL BULSARA
DAVID KOKAN
SHAUN SHARIFF
ERIC SVARVERUD
RICHARD WIRZ

DEPARTMENT OF AEROSPACE AND OCEAN ENGINEERING

VIRGINIA POLYTECHNIC INSTITUTE AND STATE UNIVERSITY

ADVISORS:

PROFESSOR ANTONY JAKUBOWSKI
DEPARTMENT OF AEROSPACE AND OCEAN ENGINEERING
VIRGINIA POLYTECHNIC INSTITUTE AND STATE UNIVERSITY

DAVY A. HAYNESS
SPACE EXPLORATION INITIATIVE
NASA LANGLEY RESEARCH CENTER

CONTENTS

i. LIST OF TABLES

ii. LIST OF FIGURES

iii. ABSTRACT

A pressurized lunar rover is necessary for future long-term habitation of the moon. The rover must be able to safely perform many tasks, ranging from transportation and reconnaissance to exploration and rescue missions.

Numerous designs were considered in an effort to maintain a low overall mass and good mobility characteristics. The configuration adopted consists of two cylindrical pressure hulls passively connected by a pressurized flexible passageway. The vehicle has an overall length of 11 meters and a total mass of seven metric tons. The rover is driven by eight independently powered two meter diameter wheels. The dual-cylinder concept allows a combination of articulated frame and double Ackermann steering for executing turns. In an emergency, the individual drive motors allow the option of skid steering as well. Two wheels are connected to either side of each cylinder through a pinned bar which allows constant ground contact. Together, these systems allow the rover to easily meet its mobility requirements.

A dynamic isotope power system (DIPS), in conjunction with a closed Brayton cycle, supplies the rover with a continuous supply of 8.5 kW. The occupants are well protected from the DIPS system's radiation by a shield of tantalum. The large amount of heat produced by the DIPS and other rover systems is rejected by thermal radiators. The thermal radiators and solar collectors are located on the top of the rear cylinder. The solar collectors are used to recharge batteries for peak power periods.

The rover's shell is made of graphite-epoxy coated with multi-layer insulation (MLI). The graphite-epoxy provides strength while the thermally resistant MLI gives protection from the lunar environment. An elastomer separates the two materials to compensate for the thermal mismatch.

The communications system allows for communication with the lunar base, with an option for direct communication with earth via a lunar satellite link. The various links are combined into one signal broadcast in the S-band at 2.3 GHz. The rover is fitted with a parabolic reflector dish for S-band transmission, and an omnidirectional antenna for local EVA communication.

The rover's guidance, navigation, and control subsystem consists of an inertial guidance system, an orbiting lunar satellite, and an obstacle avoidance system. In addition, the rover is equipped with a number of external fixtures including two telerobotic arms, lights, cameras, EVA storage, manlocks, a docking fixture, solar panels, thermal radiators, and a scientific airlock.

In conclusion, this rover at a minimum meets all of the design requirements and clearly surpasses them in the areas of mobility and maneuverability.

1. INTRODUCTION

1.1 Why a Pressurized Lunar Rover (PLR)? Man's return to the Moon will involve a permanent manned lunar base and outposts. These facilities will be supported by manned and unmanned rovers. Pressurized rovers will provide safe and comfortable transportation to areas in the vicinity of these outposts. Furthermore, they will perform extended missions far from their base. A pressurized rover operating on the Moon may also provide experience and technology for similar operations on Mars. This paper describes a design of a pressurized lunar rover.

By the time that the PLR will be implemented, lunar settlements will have reached the lunar base stage. There will be a network of lunar outposts and other unmanned facilities. The PLR will transport personnel and supplies at the base, and between bases and outposts. It will also serve in search and rescue operations for other rovers, and will perform survey and exploration missions.

Since the late 1950's, many papers have been written on unpressurized rovers. These papers outline many ideas especially in the areas of mobility and power. After the success of the Apollo program, pressurized, as well as unpressurized rovers, have been designed for future lunar missions. Many mobility schemes such as walkers and track-driven vehicles have been considered. The most common type of pressurized rover consists of a cylindrical pressure hull propelled by four to eight wheels. This general configuration was used as a basis for comparison of the various design options.

Alternatives to the basic cylindrical design can introduce advantages. In light of the rugged terrain that the rover will encounter, the performance of the mobility system is critical. Due to the high cost of transporting mass to the Moon, it is also important to minimize weight. Many of the missions required of the PLR take place far from the base so the rover must be very reliable and safe.

The design philosophy involved comparing different types of configurations that introduced advantages over the standard single cylinder. The importance of a low mass has already been mentioned. Mobility is critical since the primary functions of the rover are transportation and exploration of remote areas. The lunar surface is an extremely varied terrain, and the rover must be able to handle numerous conditions. Safety and reliability are also critical, since there will be no immediately available assistance for rovers on medium to long range missions. Simplicity is important for ease of repair and maintenance in the lunar environment.

1.2 General Performance Requirements. The following is a list of the key design requirements for a PLR (Haynes):

1. A nominal operational radius of 500 km (1,000 km range) per mission (lunar day).
2. A nominal operational radius of 50 km (100 km range) for lunar night operations.
3. Able to support a nominal crew of four.
4. A nominal operational time of 14 days per mission.
5. An airlock to allow EVA and which is compatible with the lunar surface habitat.
6. An emergency one-time range of 2,000 km with a crew of two.
7. Able to support a crew of six in an emergency with no range requirement (lunar safe-haven).
8. Storage and consumable provisions to support two EVA suits for 28 hours of use each per mission.
9. Direct communications capability with the Earth (audio, visual, and data).
10. PLR shall be able to tow utility trailers with a mass of up to two metric tons.

1.3 Lunar Environmental Design Considerations. A great deal of knowledge of the lunar environment resulted from the intensive studies and experiences of the Apollo program.

The following sections examine features important to the design of a vehicle for lunar operations.

1.3.1 Temperature. Essentially the Moon is devoid of atmosphere. Unlike the Earth, radiation to and from the lunar surface is not hindered by an atmospheric blanket. This causes severe temperature ranges and gradients. Temperature extremes on the surface range from -233°C within shadowed polar craters to 123°C in the equatorial regions. Mean temperatures are about 107°C during the day and -153°C at night (Heiken et al). Temperature is a critical consideration for many subsystems. The thermal control system must be able to accommodate this wide range of conditions. Furthermore, it is important to avoid thermal mismatches between bonded materials.

1.3.2 Gravity. The gravitational acceleration at the lunar equator is 1.62 m/sec^2, about one-sixth that of earth. This is critical to the design of the mobility system since weight is a primary variable in determining vehicle performance. The human factors associated with this lower gravity are also important. Apollo 12 astronauts explained that the characteristic "loping" gait seen in films was the most natural way to move; heel-to-toe "Earth" walking was more difficult and energy consuming (Heiken et al). It is therefore critical that the vehicle's inner layout accommodate the astronauts as they deal with this environment. In lunar gravity, a 0.4 to 1.25 meter vertical hop is easier than using conventional stairs. This allows steps to be much larger. Also, seats that support the knees and buttocks are often used considering the posture people maintain.

1.3.3 Radiation. The Moon is exposed to many types of ionizing radiation that can be biologically harmful. The three dominant types are the solar wind, solar flare associated particles (also called solar energetic particles or solar cosmic rays), and galactic cosmic rays. These forms of radiation consist mainly of protons and neutrons with some heavier nuclei.

Radiation levels vary with time and usually reflect solar activity. Obviously, the vehicle must protect its occupants from these harmful types of radiation.

1.3.4 Micrometeoroids. A meteoroid is a naturally occurring solid body traveling through space smaller than a comet or asteroid. Micrometeoroids are those meteoroids with diameters less than approximately one millimeter. These evaporate upon entering Earth's atmosphere but are an important consideration for lunar activities. From size and frequency distributions, it can be estimated that a micrometeoroid of about one milligram mass should be expected to strike the rover yearly, with smaller objects being more frequent and larger ones rarer. Velocities have been calculated to range from 13 to 18 km/sec. It has been suggested that two to three millimeters of a tough composite material would provide effective shielding against damage by micrometeoroids in the milligram mass range. Another option is to use a buffer zone behind a less tough material. This would cause the micrometeoroid to disperse so that it cannot penetrate the hull.

The rarer impacts of larger meteoroids pose a more significant hazard, especially to critical components. These components should be protected (by placing them where they cannot be struck) to ensure their safety.

1.3.5 Trafficability. Trafficability is defined as the capacity of a soil to support a vehicle and to provide sufficient traction for movement. Many elaborate walking machines were developed prior to actual landings because it was assumed that trafficability would be poor. However, from the experience of both Apollo and Lunakod missions, it is now known that almost any vehicle with round wheels can perform satisfactorily on the lunar surface, provided that the ground contact pressure is no greater than 7-10 kPa. The energy consumed by wheeled vehicles can be estimated. Important parameters include the wheel load, wheel footprint area, chord length of wheel ground contact, width of wheel ground contact, and various previously measured soil characteristics.

1.3.6 Dust. The lunar regolith has grainy characteristics very similar to silty sand. Many of the particles are sharp and glassy (Heiken et al). Accumulation and adhesion to equipment was experienced on previous missions. "Sandblasting" can occur, especially in the presence of takeoffs and landings. Exposed or delicate equipment will have to be protected from the harmful effects of lunar dust. Also, dust removal equipment must be used after extra-vehicular activity.

2. CONFIGURATION SELECTION

2.1 Initial Configurations. The first step of the design process was to establish the basic configuration of the rover. The major subsystems and their relationships had to be agreed upon before in-depth work could begin. Preliminary studies showed that the pressure structure shape and mobility subsystem should be selected first because these elements have significant effects on other aspects of the design. This led to the selection of four initial configurations.

One of the first designs considered was a slightly longer variation on the single cylinder often seen in literature. This design has a low center of gravity and a simple interior (Figure 2.1). A second design used tracks for enhanced mobility performance but was ruled out due to its high mass and power requirements. A single spherical pressure hull was also considered because of its optimum volume per unit mass. However, significant disadvantages included a high center of gravity and the utilization of available interior space. Therefore the fourth option of a multi-segmented spherical configuration was also considered (Figure 2.2).

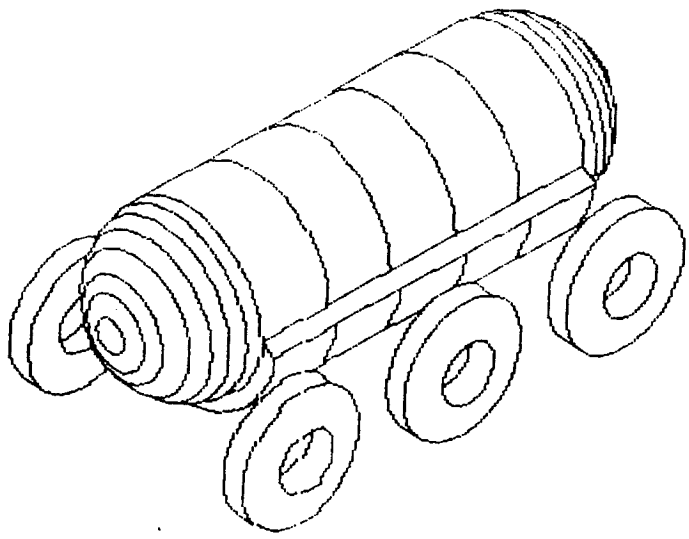

Figure 2.1 - Single Cylinder

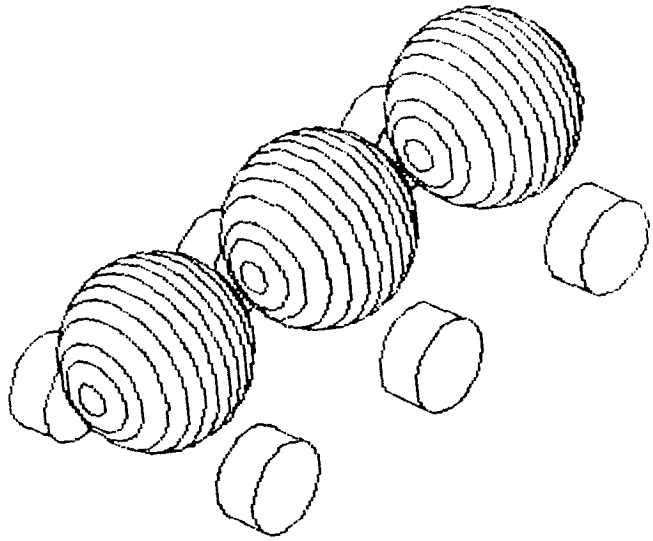

Figure 2.2 - Multi-segmented Spherical Configuration

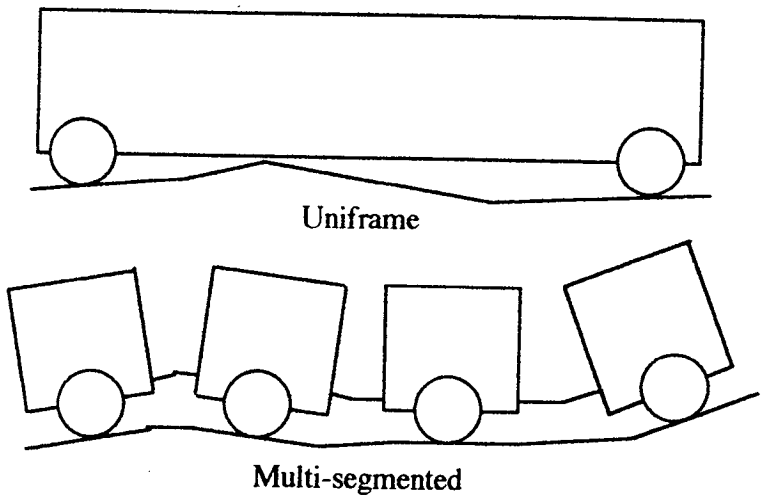

Figure 2.3 - Frame Options

The frame option was basically a choice between a uniframe configuration and a multi-segmented one (Figure 2.3). The uniframe, a standard one-piece frame, would be the simplest to construct and the most reliable. However, it needs more ground clearance, and therefore a higher center of gravity which decreases stability. Multiframe designs consist of a train of multiple segments, which allow pivoting at their connections. Increased maneuverability is achieved because the vehicle can conform to terrain conditions.

2.2 HLLV and Shuttle C Evolution Effects. The cargo bay diameter of the launch vehicle affects the rover design. By completing most of the rover's construction on Earth, in-space assembly can be minimized. The projected dimensions of the National Launch System Derived Heavy Lift Launch Vehicles (HLLVs) and Shuttle C limit the size and shape of the pressure hull (Cook). For the lunar phase of space exploration, the HLLV's dimensions will be 7.62 meters (diameter) by 27.4 meters (length), and Shuttle C's dimensions will be 6.7 by 22 meters. Only one launch is required to bring the mass of the rover to the moon, using either launch system.

2.3 Intermediate Configurations. As a result of preliminary analysis, three intermediate configurations were considered. To utilize the mass advantages of a spherical pressure hull, a multi-segmented dual sphere design was considered. The dual sphere configuration avoided the HLLV limitations of the single sphere. Utilizing the interior space of a spherical hull is difficult. Therefore, a simpler dual cylinder configuration was also considered (Figure 2.4). It maintained the mobility advantages of a segmented configuration without a significant mass increase over the dual sphere.

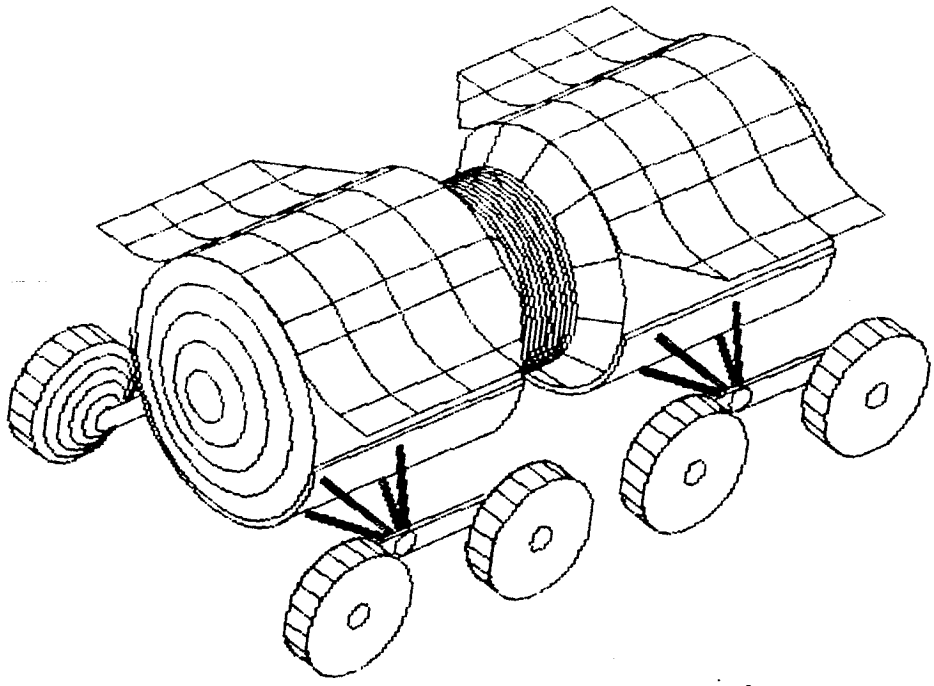

Figure 2.4 - Dual Cylinder Configuration

2.4 Final Configuration.

2.4.1 Selection. Establishing the final configuration was reduced to a choice between three options: a dual sphere, a dual cylinder, and the standard single cylinder. Both of the segmented frame designs used a flexible pressurized passageway to passively connect the two pressure hulls. The flexible passageway increased the mass and complexity of the vehicle, but the mobility advantages were significant. The dual cylinder was chosen as the final configuration due to its increased mobility over the single cylinder and its simplicity compared to the dual spheres. It is a compromise between a uniframe and a many-segmented frame.

2.4.2 Design Features. The final dual cylinder configuration can be seen in Figure 2.5. Its specifications are shown in Table 2.1. Table 2.2 is the mass statement, Table 2.3 displays the vehicle's performance characteristics, and Table 2.4 lists the primary power consumers.

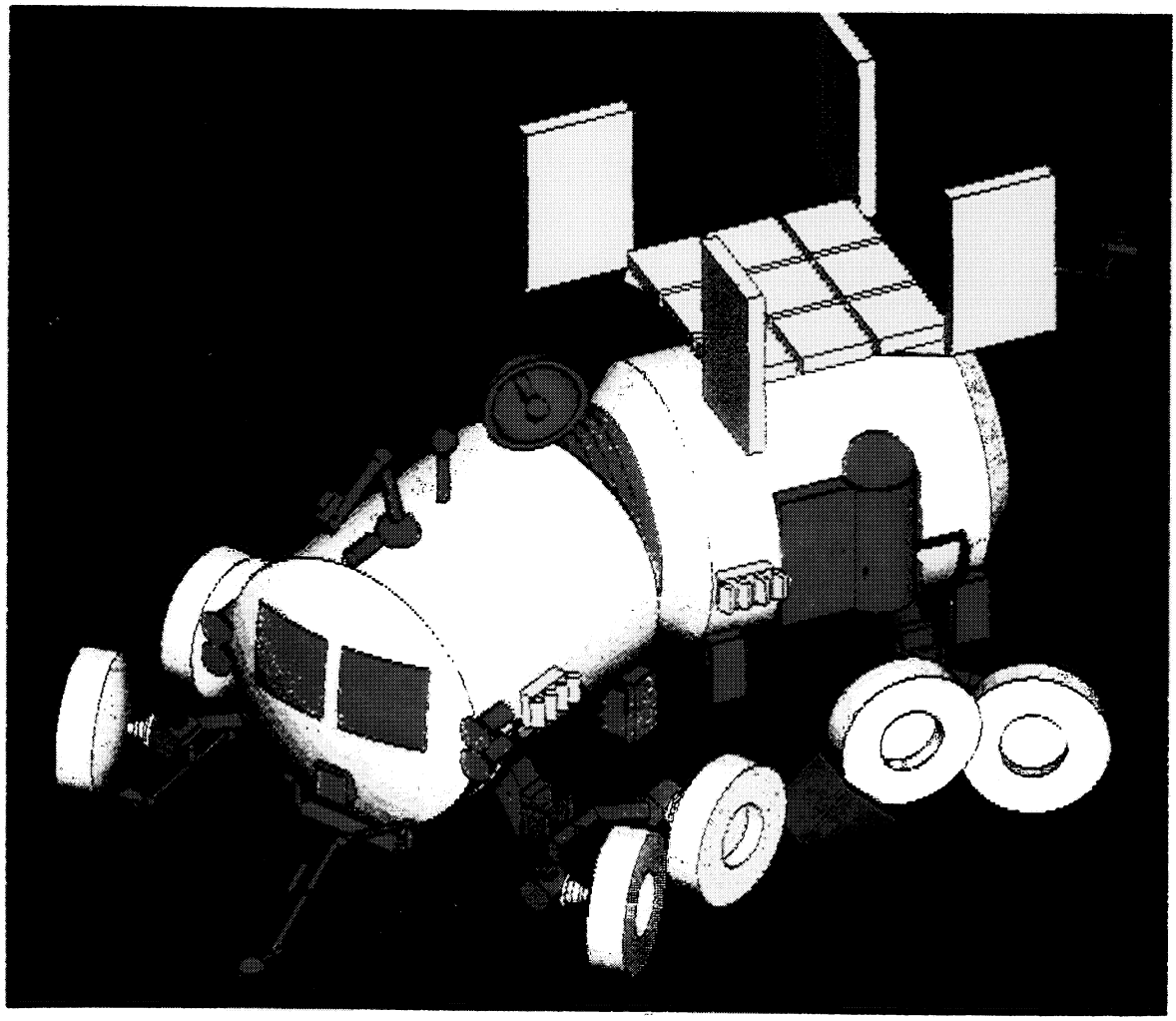

Figure 2.5(a) - Final Configuration (top view)

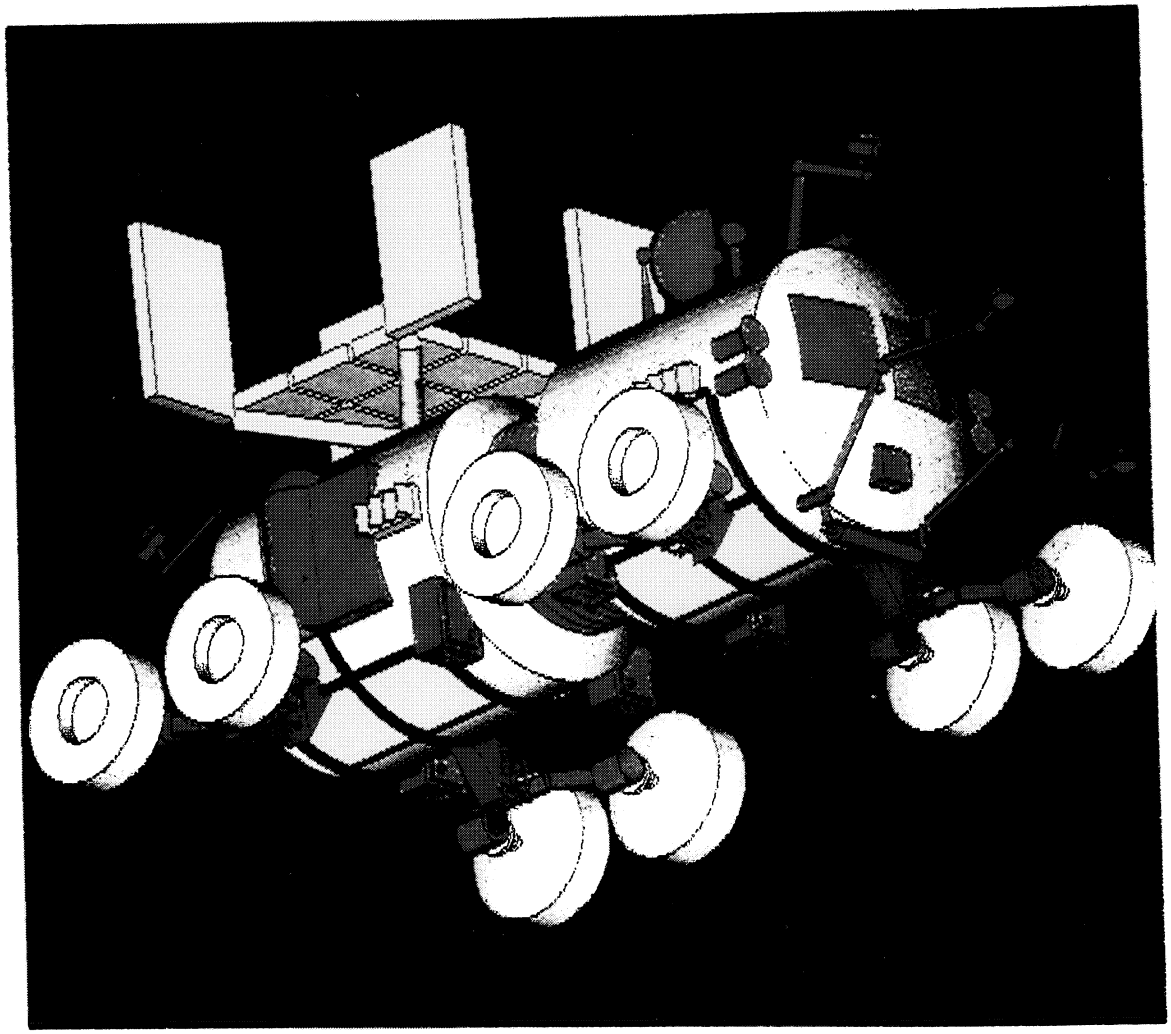

Figure 2.5(b) - Final Configuration (bottom view)

Table 2.1 - Final Configuration Specifications

Primary dimensions:	
Total vehicle length	11 m
Cylinder length	5 m
Cylinder diameter	4 m
Flexible passage length	1 m
Wheel diameter	2 m
Wheelbase	7.5 m

Primary power source: Dynamic Isotope Power System (closed Brayton cycle)
Secondary power source: Sodium-sulfur batteries with photovoltaic array

External fixtures:
- 1 1.2 meter parabolic reflector antenna
- 1 omnidirectional VHF antenna
- 6 exterior storage bins and tool boxes
- 4 visibility and maintenance cameras with lights
- 4 driving lights
- 2 robotic arms
- 1 scientific airlock
- 2 manlocks
- 1 towing hitch
- 1 docking fixture
- 2 EVA seats
- 1 high resolution landscape camera
- 1 9 m^2 directable solar collector array
- 2 7.5 m^2 directable thermal radiators
- 4 second surface mirror radiators

Table 2.2 - Mass Statement

SYSTEM	**MASS (kg)**
Structure and Pressure Vessel	
Inner Graphite/Epoxy Shell	553
NOMEX Core (Honeycomb)	84
Outer Graphite/Epoxy Shell	559
Elastomer Layer (for Thermal Mismatch)	130
Aluminum Coating	378
Flexible Connection	238
Saddle	652
KEVLAR 29 Micrometeoroid Shielding	240
Thermal Control System	
Insulation	130

Radiator	90
Pumps	20
Heat Exchanger	50
Piping	100
Refrigerant	50
Power system	
Engines	200
Structure	60
Heat Source Blocks	200
Radiation & Housing	500
Power Distribution	40
Sodium Sulfur Batteries	16
Solar Collectors	18
Mobility	
Tires (8)	240
Motors (9)	36
Gearing Sets (9)	36
Suspension Groups (4)	60
Steering	
Articulated Frame Joint & Connection	50
Environmental Control/Life Support	
Atmospheric Control & Supply	80
Atmospheric Revitalization	20
Fire Detection & Suppression	10
Water Recovery & Management	120
Waste Management	20
Extra-vehicular Activity & Support	20
Manlocks	230
Internal Facilities	
Communications	25
Guidance and Navigation	10
Galley	70
Personal Hygiene	90
Emergency Equipment	30
Drive Stations	80
Work Stations	40
Sleep Quarters	60
External Fixtures	
Visibility & Maintenance Cameras (2)	8
High Resolution Landscape Camera	4
Lights	4
Antenna	15
Telerobotics	22
Drill Coring	10
Winch	5
Hitch	2
EVA Suits	450
Crew	360
Payload	500
TOTAL MASS	**7,015**

Table 2.3 - Mobility Performance Characteristics

Maximum Velocity	(4 wheels), 14.7 km/hr (8 wheels), 29.4 km/hr
Nominal Power Requirement	(4 wheels) 1.36 kW/wheel (8 wheels) 0.68 kW/wheel
Maximum Allowable Power	1.5 kW/wheel
Maximum Gross Pull	900 N/wheel
Maximum Vehicle Acceleration	0.64 m/s^2
Soil Compaction Resistance	
Normal Soil	22 N/wheel
Soft Soil	81 N/wheel
Hard Soil	4.0 N/wheel
Minimum Turn Radius (in percent of vehicle length)	
Neutral Steer	78.3%
Oversteer	60%
Range	2,000 km
Maximum Gradient	26.5°
Wheel Sinkage	
Normal Soil	1.03 cm
Soft Soil	2.86 cm
Hard Soil	0.21 cm
Climbable Step Height	0.53 M
Crossable Crevice	1.7 M

Table 2.4 - Subsystem Power Requirements

SYSTEM	POWER REQUIRED (W)
Drive Motors	
Normal Operations	5,452
Maximum	12,000
ECLSS	160
Operation (computers, communication, etc.)	600
Thermal Control	
Average	800
Maximum	1,356
Internal Requirements (includes lights, galley, hygiene, etc.)	1,500
External Lighting	1,000
Experiments	1,000
Miscellaneous	1,000

2.4.3 Internal Layout And Features. The interior layout of the rover is shown in Figures 2.6-2.17. The 4-man crew occupies the rover for up to two weeks while performing various missions including driving, EVA, sampling and data collection, and other tasks. The interior will provide a comfortable working environment with ample radiation and solar flare protection.

The interior is separated into four areas: driving, living, working, and EVA. The driving and living areas are located in the front section of the rover while the EVA and work areas are in the rear. The Environmental Control & Life Support Systems (ECLSS) are located overhead to provide an ample amount of mass overhead for general radiation protection. The power systems and other utilities are primarily located under the floor of the rover.

2.4.3.1 Driving Area. The driving area, located in the front of the rover, has two driving stations. It is elevated to give the driver a good view of the landscape, aiding navigation (Figures 2.7, 2.8 and 2.9). The window placement minimizes the drivers' blind spots allowing a good view of the lunar surface (Figures 2.10 and 2.11). A transparent sheet is stretched between two spools across the windows. When lunar dust accumulates on the sheet, a clean section is rolled down over the window, replacing the dirty one. Overhead video monitors give the drivers additional visual assistance. The seats can recline to a sleeping position and are free to translate and rotate to allow access to the side mounted work stations. These stations are used for vehicle guidance, navigation, control, systems monitoring, data management, communications, and mission-specific tasks.

The telerobotics in the front of the rover are controlled from the drive stations and are equipped with cameras for visual aid (Figure 2.5). They are able to cover a large area from one stopped position. The robotic arms can perform many tasks such as scooping, scraping, drilling, and digging into the lunar surface for samples. The samples are collected

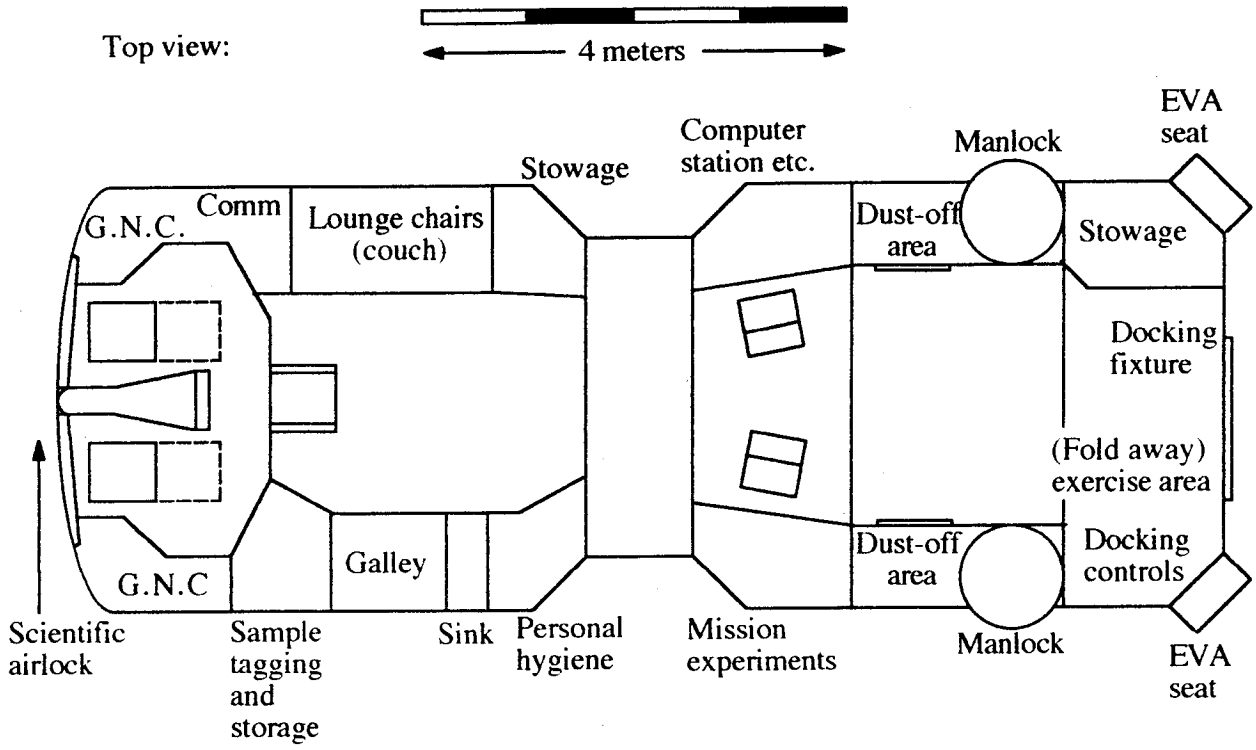

Figure 2.6 - Internal Layout

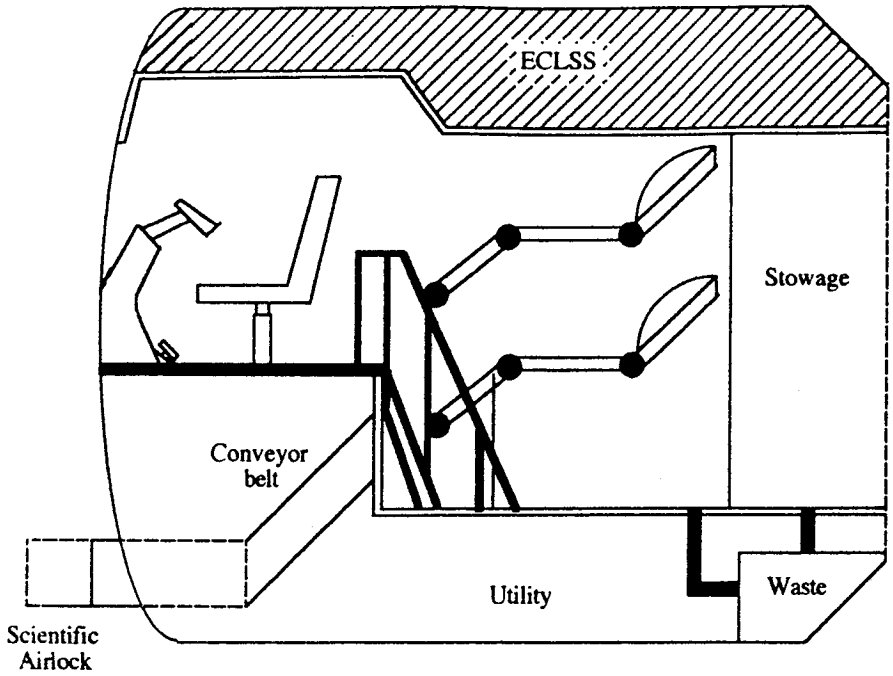

Figures 2.7 - Forward Cylinder, Starboard View

2 Meters

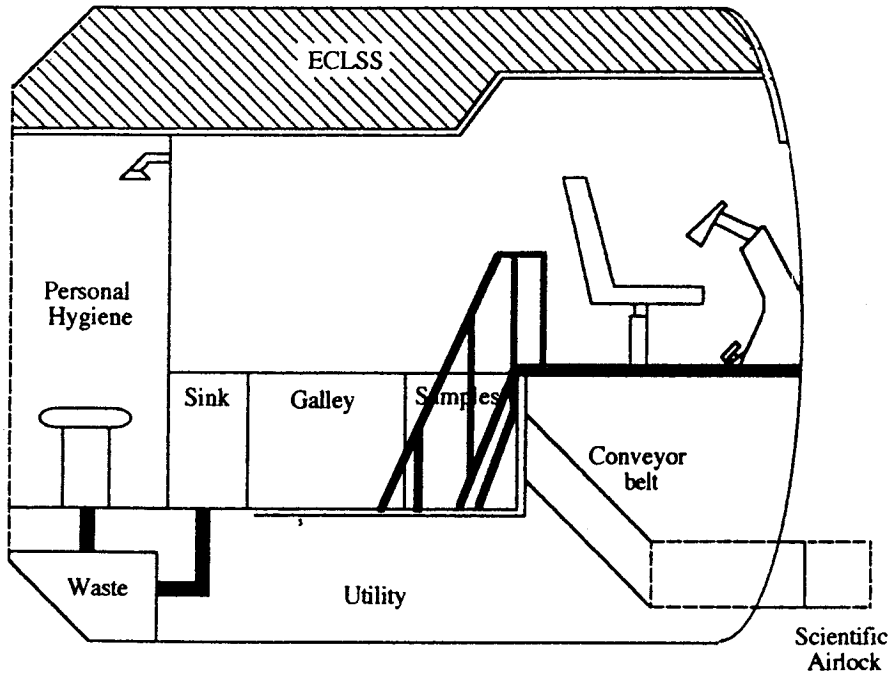

Figure 2.8 - Forward Cylinder, Port View

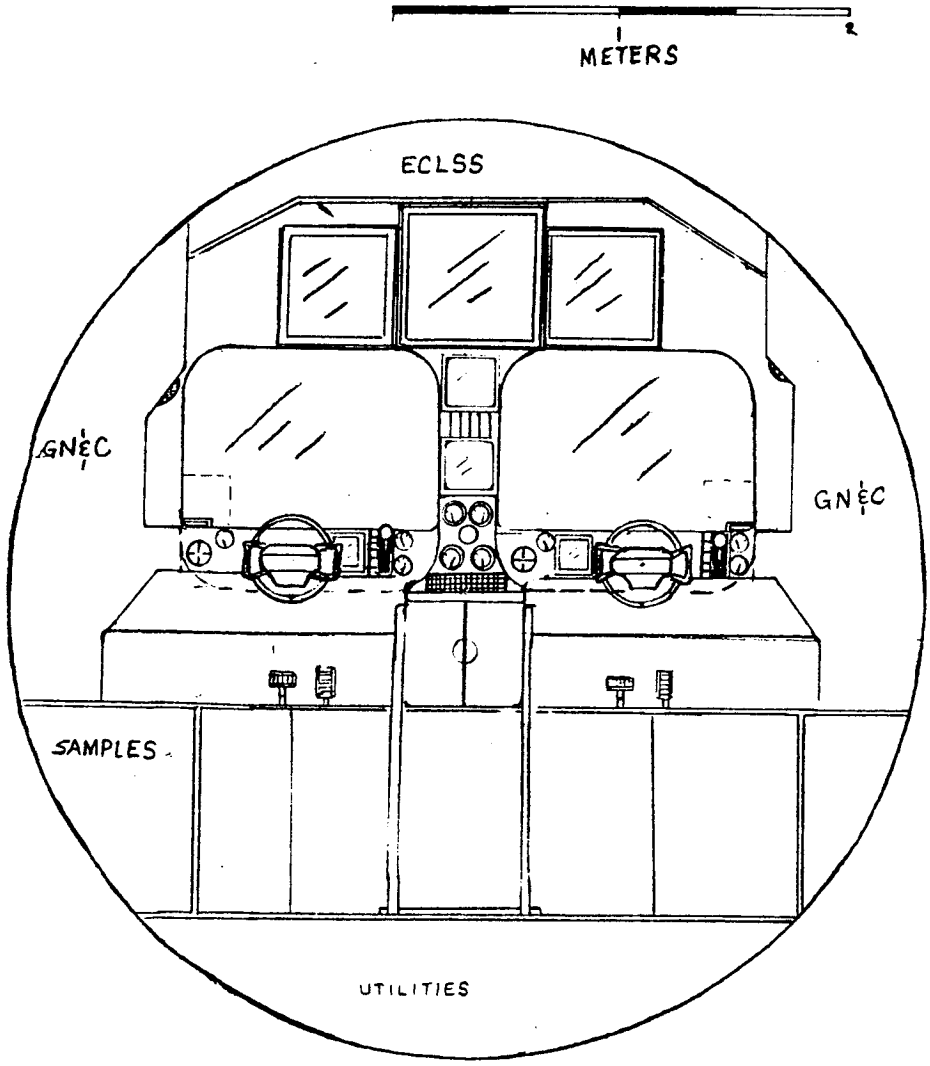

Figure 2.9 - Driving Area

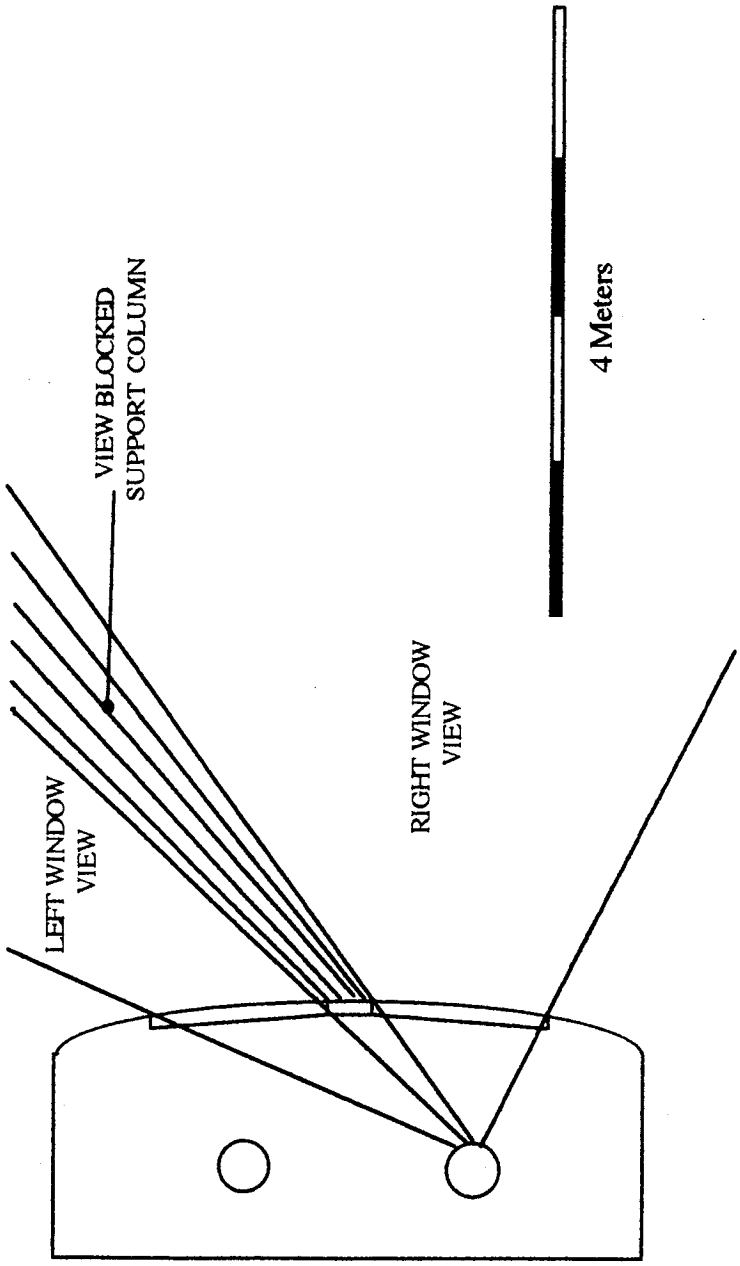

Figure 2.10 - Horizontal Visibility

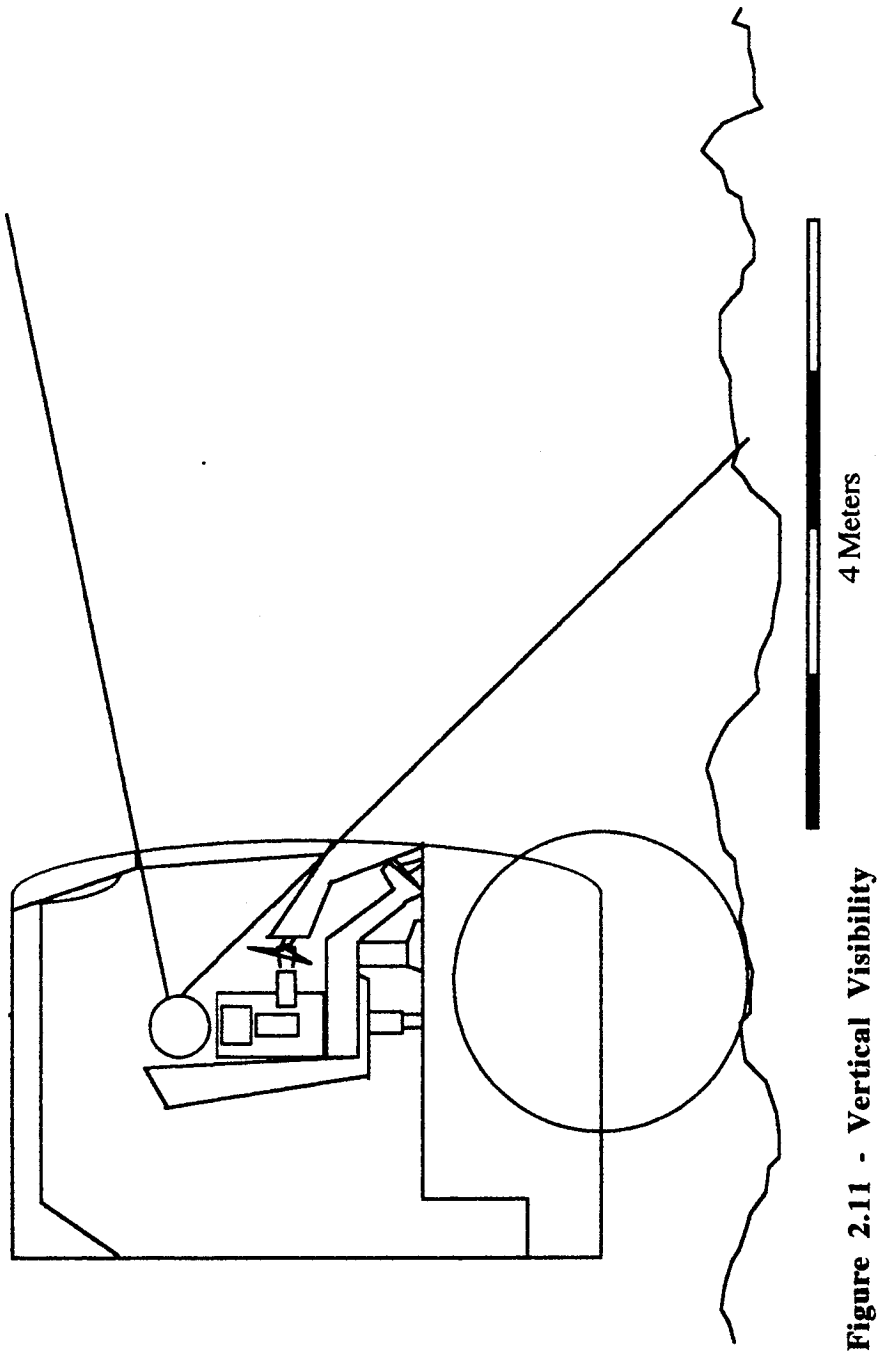

Figure 2.11 - Vertical Visibility

by a scientific airlock which is also accessed by the drill corer located underneath the rover. After the samples are collected they are brought to the sample storage bin by a hand-powered conveyor belt. Here they are tagged and stored in a vacuum or in nitrogen-filled containers for future examination.

2.4.3.2 Living Area. Immediately aft of the driving area is the living area (Figures 2.7, 2.8, and 2.12). This allows the front of the rover to be an open area for crew meetings. The lounge chairs can be assembled for use as beds or a couch. A sound/light curtain can be drawn around the lounge chairs for privacy. The compact galley and a multi-purpose sink are located next to the personal hygiene facilities. The personal hygiene room is also a shower, which is provided because of the possibility of several EVA excursions during missions.

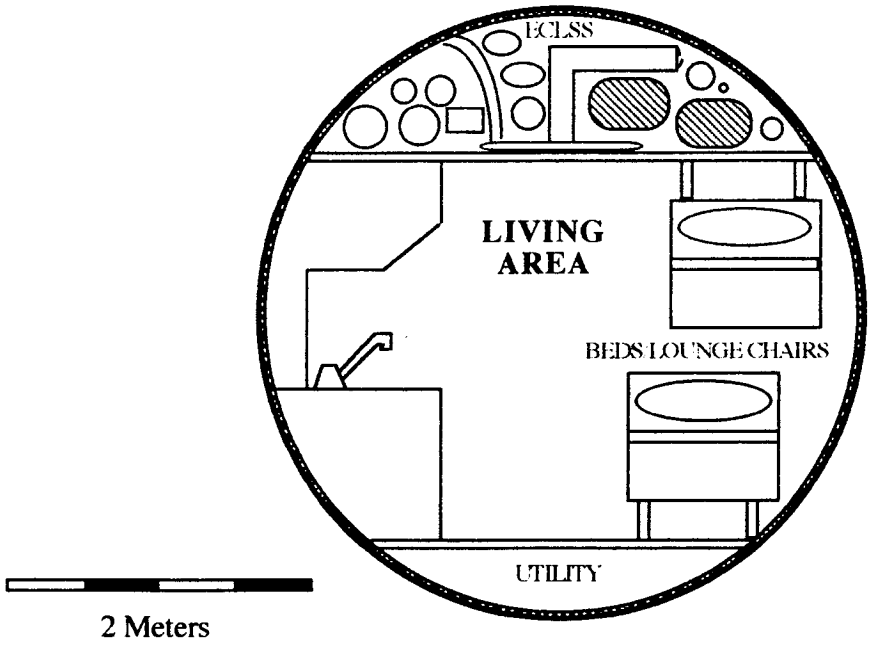

Figure 2.12 - Living Area

2.4.3.3 EVA Area. The EVA area splits the work area so the exterior portion to the manlocks does not interfere with the vertical translation of the wheels (Figures 2.13-2.15). A manlock is a type of form-fitting airlock. By using a pressurized volume of 1.57 m^3, the manlock conserves energy for EVA ingress and egress. A folding bridge and ladder allow the lunarnauts to avoid the wheel group (Figure 2.16). The suits are stored inside the manlocks. A post-EVA dust-off area is provided to prevent lunar dust from contaminating the interior.

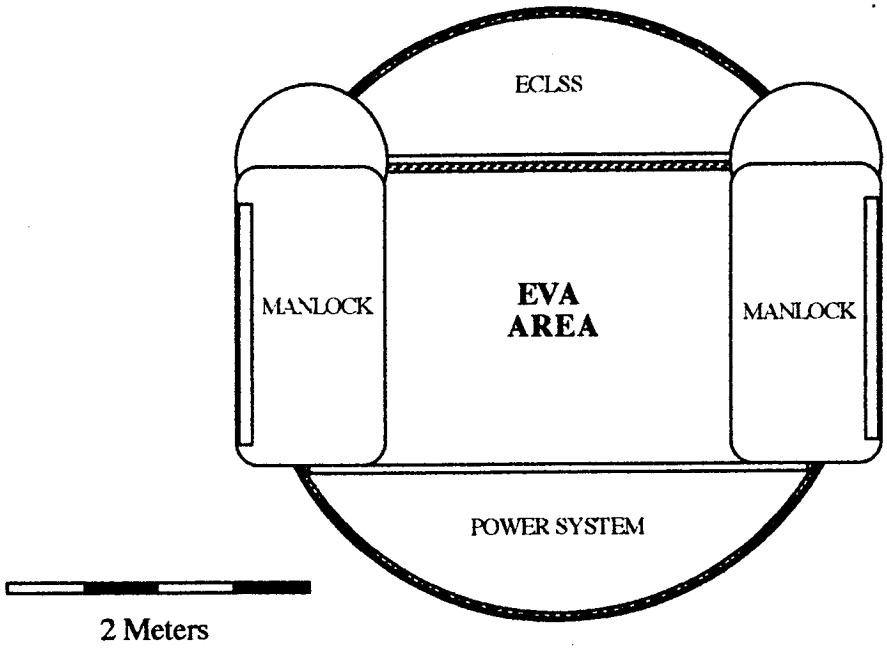

Figure 2.13 - EVA Area

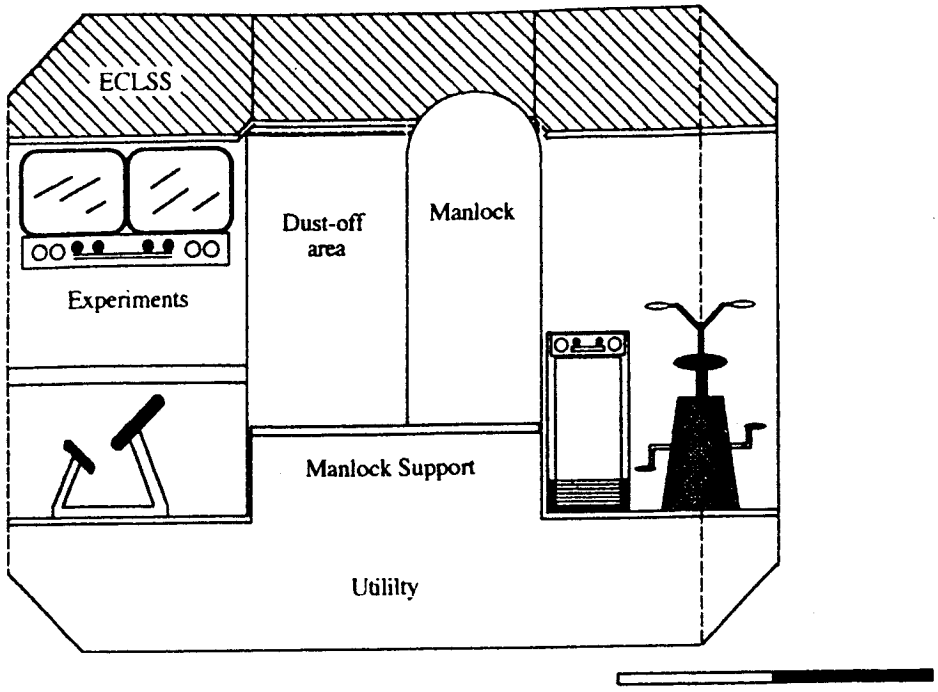

Figures 2.14 - Rear Cylinder, Starboard View

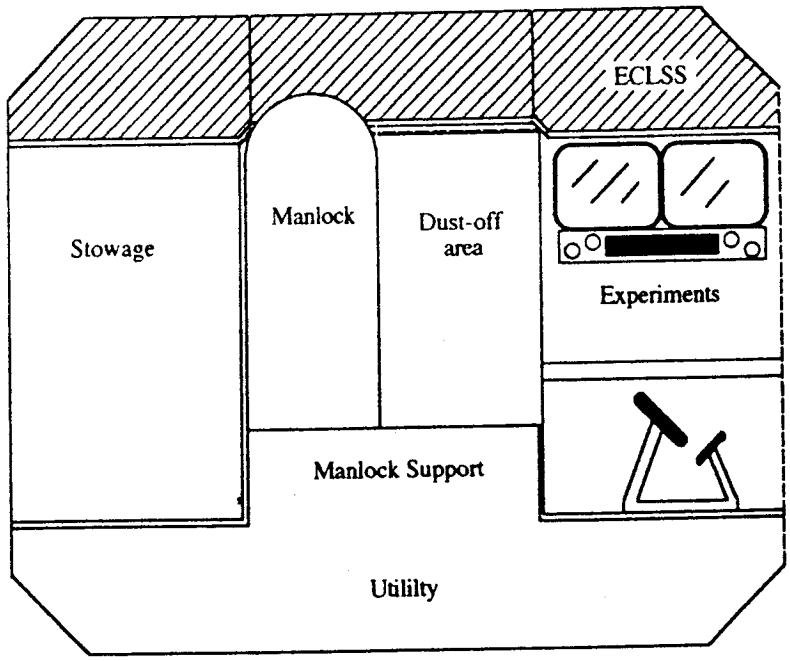

Figure 2.15 - Rear Cylinder, Port View

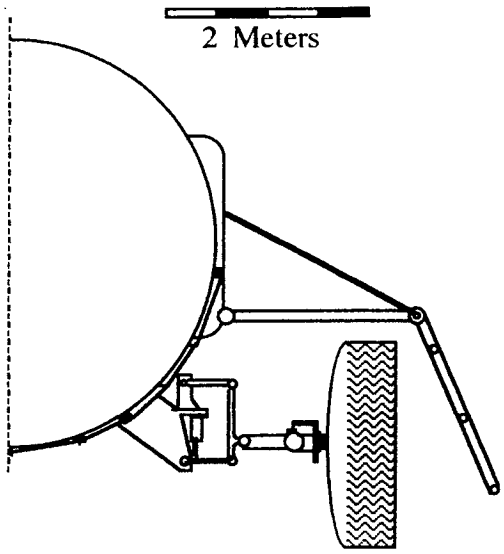

Figure 2.16 - EVA Ingress and Egress

A protection area is required to shield the occupants during periods of high solar flare activity. One study of space radiation protection examined the lunar regolith itself as a possible radiation shield for lunar base surface systems (Nealy et al). The proposed design called for about a 0.5 meter thick shield, an unrealistic mass for a transport vehicle. More appropriate materials such as water and aluminum have been investigated. For galactic cosmic rays, 3 g/cm^2 of water or 6 g/cm^2 of aluminum would provide sufficient protection. For solar flares, 15 g/cm^2 of water or 18 g/cm^2 of aluminum are necessary (Townsend et al). However, the mass of a material dedicated solely for the purpose of providing radiation protection becomes unreasonably large for a crew of three or four. The solution is to use consumables such as water, radiators, and trash to provide shielding. Shielding on the order of 20 g/cm^2 can be assumed sufficient for solar flare protection (NASA Memorandum 4170, Volume III). The EVA area is surrounded by relatively massive equipment such as the solar

collectors and thermal radiators overhead and the manlocks on either side. Therefore, the EVA area is used to protect the occupants during solar flares.

A docking fixture to mate with the base is located in the very back of the rover. The base uses its airlock to transfer the rover passengers. The docking fixture allows direct passage between the rover and the base.

2.4.3.4 Work Area. The work area is made up of several parts (Figures 2.14, 2.15, and 2.17). Computer and mission experiments stations are used to perform mission specific tasks. At the mission experiments station, samples and observations obtained during the mission can be analyzed. In-depth system and maintenance checks as well as data relays can be carried out at the computer station. Minimal controls which are located in the very rear of the rover are used to aid docking. Interior storage and emergency facilities are also found in the rear. A fold-away exercise area that can aid in charging the batteries is provided and can be easily stowed, depending on mission needs.

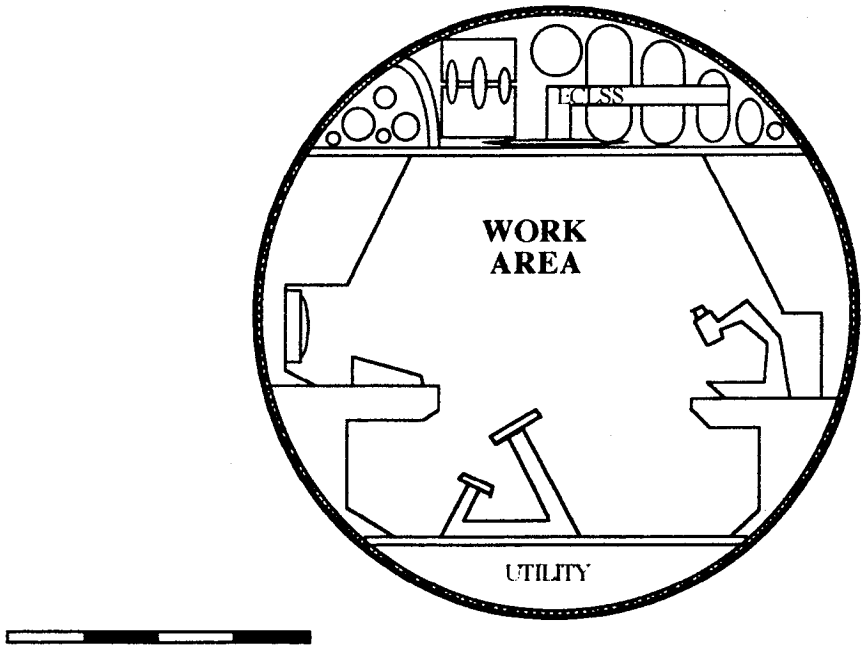

Figure 2.17 - Work Area

3. MATERIALS SELECTION

When selecting materials for the rover structure, the harsh lunar environment must be considered. Important criteria include large temperature extremes (-233°C to 123°C), thermal cycling with sharp temperature gradients, solar radiation, and micrometeoroids (see §1.0). Materials must be chosen that can withstand these harsh conditions and minimize mass. Also, the internal and external loadings on the rover will require the selection of extremely durable materials. High modulus, graphite/reinforced epoxy type materials are the leading candidates for most large spacecraft systems (Blankenship et al). The use of a graphite/epoxy composite has many advantages. The material is strong, lightweight, thermally stable, and like most other composites, can be tailored to meet particular needs.

3.1 Thermal Characteristics. With large, divergent temperature extremes, the material on the exterior of the pressure hull will expand and contract. The magnitude of expansion is related to the material's coefficient of thermal expansion. Ideally, a material that has a negligible coefficient such as a graphite/epoxy should be used.

Thermal cycling is a greater problem than temperature extremes. Repeated cycling over a prolonged period can cause severe microdamage, altering both the stability and stiffness of the graphite/epoxy (Blankenship et al). The particular microdamage that degrades the integrity of the material is called microcracking. A solution to this problem is to place multilayer insulation (MLI) over the graphite/epoxy. It minimizes the temperature cycling range by increasing the heat capacity of the shell.

3.2 Solar Radiation. The MLI also provides an excellent defense against solar radiation. If the graphite/epoxy is exposed to radiation, chemical reactions begin to occur. These reactions severely alter the graphite/epoxy's material properties. Some of the adverse results include a reduction in the transverse strength and modulus of elasticity, increased

volatility, and a reduction in thermal stability (Sykes et al). By simply protecting the graphite/epoxy with MLI, the harmful effects due to solar radiation are reduced.

3.3 Thermal Mismatch. There is a thermal mismatch between the MLI and the graphite/epoxy. Since the coefficients of thermal expansion are considerably different, their expansions are unequal. If the mismatch problem is not corrected, the MLI may crack or separate from the graphite/epoxy. The solution to this problem is to put an elastomer layer between the aluminum and the graphite/epoxy (Kander). The elastomer, having rubber like characteristics, will yield to the thermal mismatch (Figure 3.1). A good elastomer candidate is isobutylene isoprene because of its high continuous use temperature of 150°C.

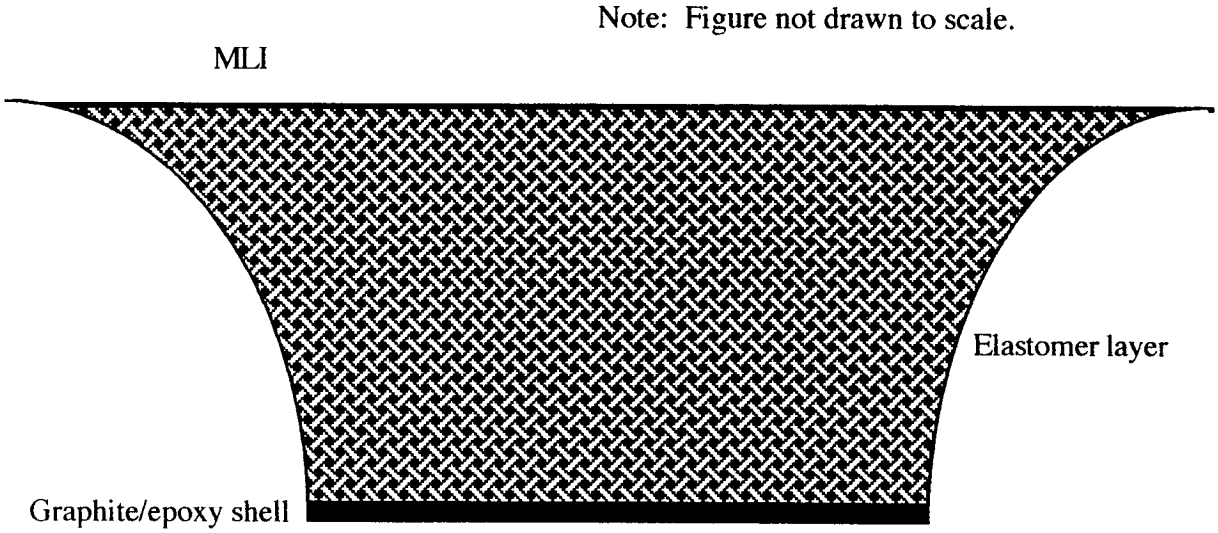

Figure 3.1 - Thermal Mismatch

3.4 Micrometeoroids. Ballistic impacts on the rover by micrometeoroids could prove catastrophic. A bumper shield system will be used to combat impact damage. The system entails the use of a bumper shield, spacing, and a back wall. The principle behind this scheme is that as a micrometeoroid breaks through the bumper shield, it disintegrates. The spacing behind the bumper provides room for the disintegrated particles to disperse. The back wall stops the dispersed material. The critical parameters to this design are the bumper shield thickness (t_s), the spacing (S), and the back wall thickness (t_b)

According to NASA standards, the bumper thickness is 10 to 20% of the impacting particle's length (Wertz). For the lunar environment, the average micrometeoroid will have a diameter of one millimeter. Based on safety and manageability, the bumper shield will be made of the conventional Al 7075-T6 with a one millimeter thickness.

Although the MLI and elastomer layers of the shell are the outermost, they do not serve well as the back wall. Therefore, the outer graphite/epoxy shell of 0.25 cm thickness will essentially serve as the back wall.

According to the equation

$$t_b = (Cmv)/2S$$

where

t_b = back wall thickness = 0.25 cm

m = micrometeoroid mass = 0.001 g

C = 41.5 ± 14.0

v = micrometeoroid velocity = 13 to 18 km/s

S = spacing thickness (cm)

the spacing thickness may be calculated (Wertz). Using a factor of safety of two, the spacing thickness was found to equal four centimeters.

Due to the relatively high frequency of micrometeoroid impacts in the lunar environment, rather than having one large bumper shield, a panelling scheme will be used.

This allows for individual panels to be replaced if considerable damage has occurred. Strips of KEVLAR 29 I-beams will be wrapped circumferentially around the rover. The aluminum panels will be fastened onto the I-beams thus providing the four centimeter spacing (Figure 3.2).

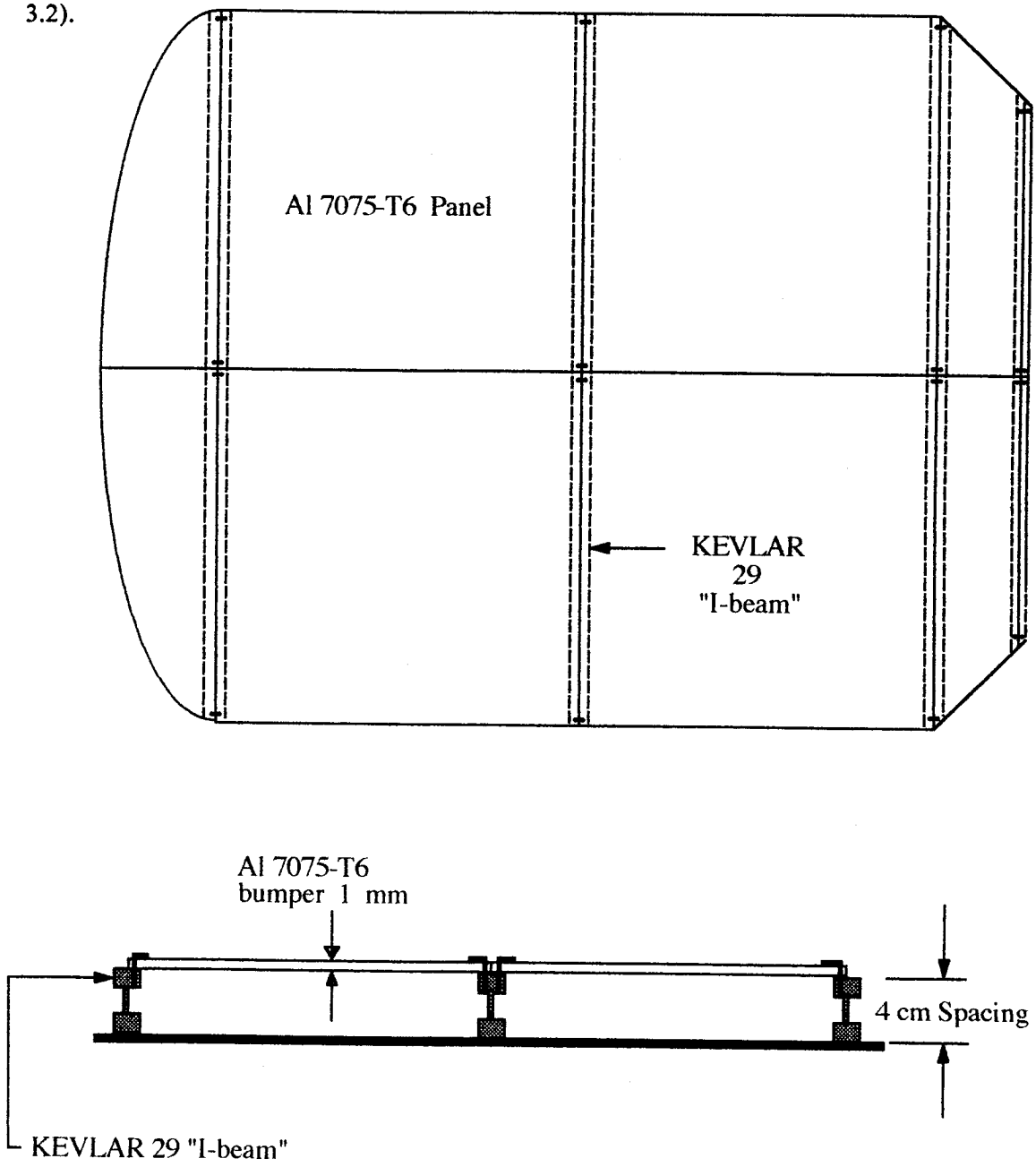

Figure 3.2 - Micrometeoroid Protection

3.5 Honeycomb Core (NOMEX). Since the occupants' safety is of great concern, two graphite/epoxy pressure hulls will be used rather than one. A material will separate the shells and increase the stiffness and strength without significant mass increase. Options included honeycombs of balsa, aluminum, or NOMEX, as well as urethane or PVC foams. The material most appropriate for this duty is NOMEX honeycomb core (Kander). NOMEX has high thermal tolerance, specific shear strength, and toughness. It is light weight and a good thermal insulator. These characteristics as well as its fire resistance also make it a prime candidate for the interior cabin.

3.6 Flexible Material. The articulated frame dual-cylinder requires a flexible material to join the segments. A strong, highly flexible tube with a circular cross-section, having "accordion-like" characteristics is needed. The purpose of the flexible connection is to join the two structures, making essentially one continuous cabin. The rear structure is pulled by the articulated frame and not the flexible connection. An elastomer in the form of a thick solid, reinforced with KEVLAR 49 fibers, is a good candidate (Kander). One elastomer that may be used due to its favorable thermal properties is isobutylene isoprene (*CRC Practical Handbook of Materials Science*). However, lunar atmospheric effects on the material will have to be investigated.

3.7 Graphite/Epoxy Selection. Merely stating that graphite/epoxy will be the material used for the structure is inadequate. Properties can vary quite drastically from one graphite/epoxy to another. Thornel, a subsidiary of Amoco, fabricates several candidates which have been used in space structural components. The tensile, compressive, and shear strengths as well as the modulus of elasticity should be high. The material should be thermally favorable, implying a very low coefficient of thermal expansion as well as a low thermal conductivity for insulation purposes. Finally, since mass is critical, the density should be minimized.

A bar graph (Figure 3.3) was prepared comparing the different materials. Each material property was normalized against the best material in that category. To calculate the overall rating, an average of the ratings was taken. Each category was weighted equally and the best material was T-650/35/Epoxy. Its material properties are presented in Table 3.1 (Thornel).

Table 3.1 - Properties of T-650/35/Epoxy

Density	1,600 kg/m^3
Tensile Strength	2,068 MPa
Modulus	152 GPa
Thermal Conductivity	8.73 $W/(m \cdot K)$
Expansion Coefficient	$-0.1 \times 10^{-6}/°F$
Compressive Strength	1,724 MPa
Shear Strength	124 MPa

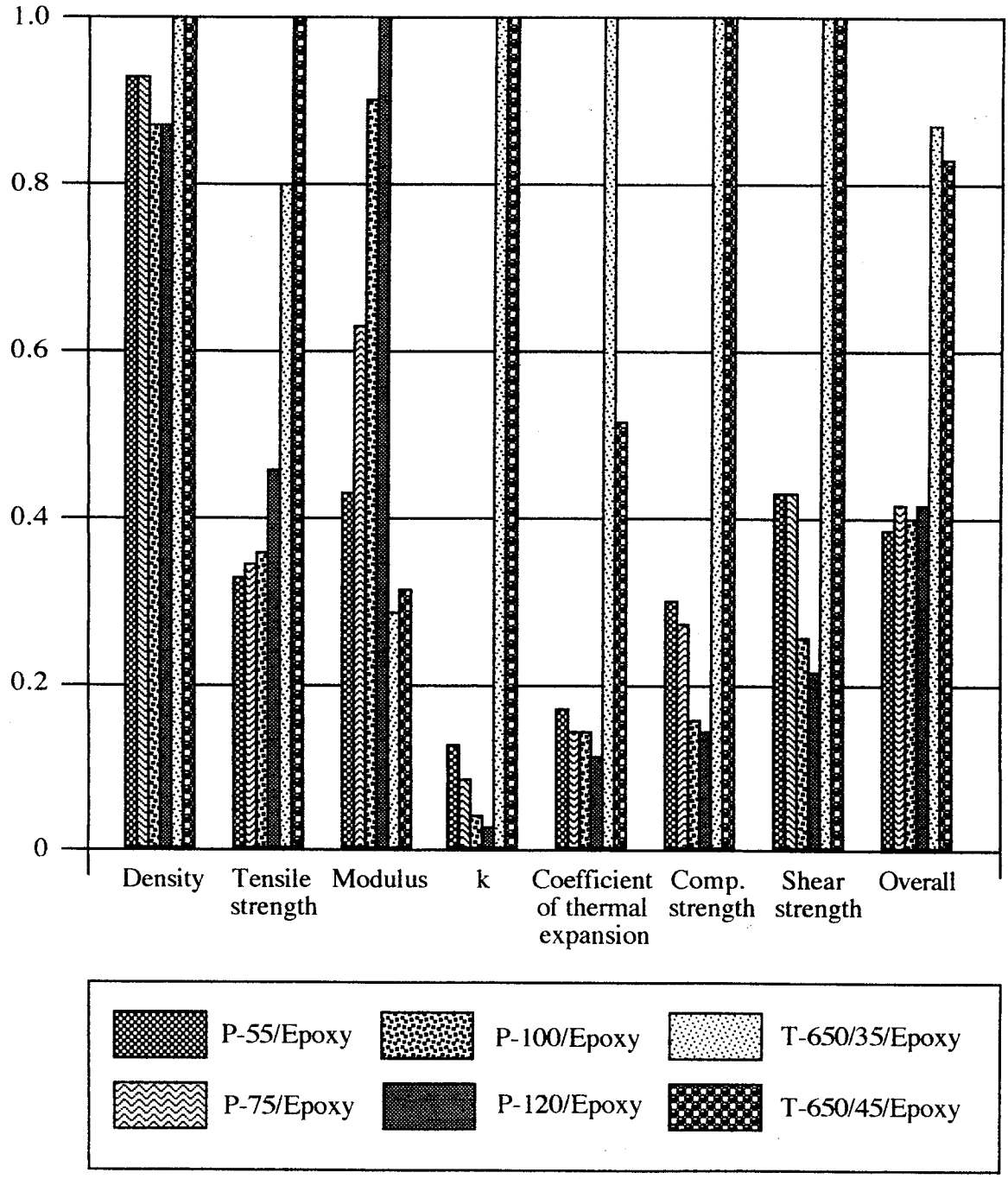

Figure 3.3 - Graphite/Epoxy Candidates

3.8 Material Selection For Vehicle Substructure. The primary variable used in selecting a material for the saddle was weight. The lightest engineering metal, with the exceptions of magnesium and beryllium, is aluminum. Aluminum alloys are about one-third the weight of steel. They possess a high strength-to-weight ratio, are weldable, and can be easily machined. Thus an aluminum alloy will be used for the saddle.

3.9 Conclusions. The materials selection and thicknesses for the rover's shell are presented in Table 3.2. Table 3.3 is the mass statement. Figure 3.4 is an illustration of the shell cross section. Structural analyses should be performed to check the validity of the materials and thicknesses chosen.

Table 3.2 - Pressurized Lunar Rover Shell

MATERIAL	DENSITY (kg/m^3)	THICKNESS (cm)
Graphite/Epoxy	1,600	0.25
NOMEX Honeycomb Core	40	1.50
Graphite/Epoxy	1,600	0.25
Elastomer (Isobutylene Isoprene)	920	0.10
MLI	1.21 (kg/m^2)	3.00
Aluminum	2,700	0.10

Table 3.3 - Materials Mass Statement

COMPONENT	MASS (kg)
Graphite/Epoxy	553
NOMEX Honeycomb Core	84
Graphite/Epoxy	550
Elastomer (Isobutylene Isoprene)	130
MLI	130
Aluminum	378
Flexible connection	238
Saddle	652

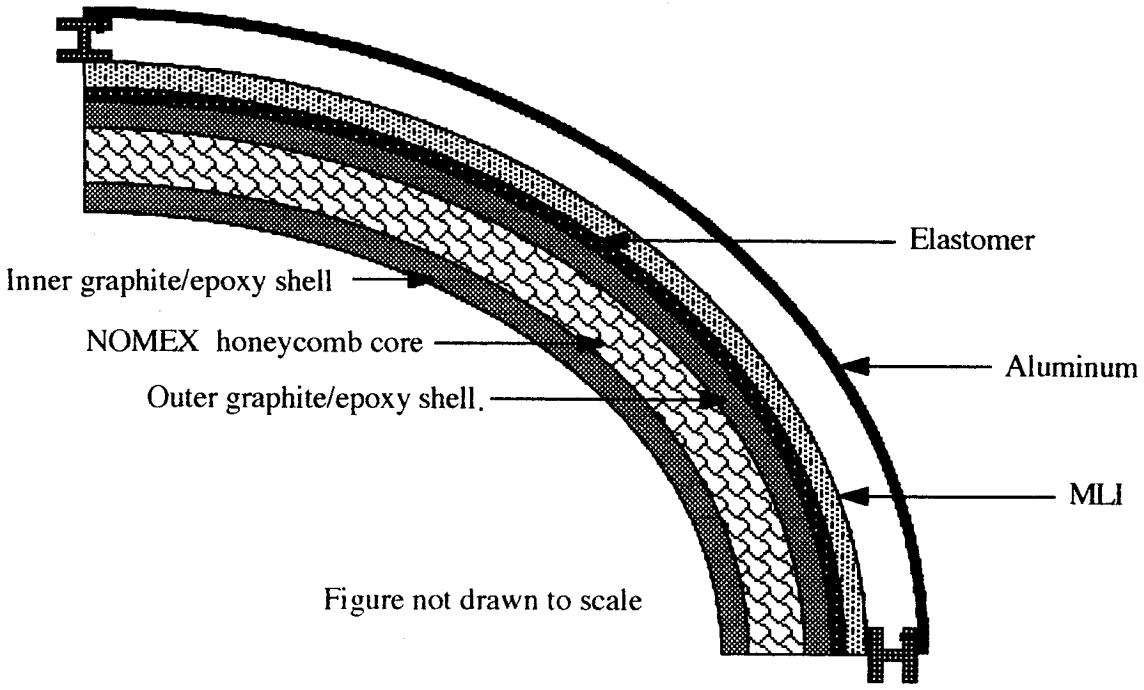

Figure 3.4 - Pressure Hull Cross Section

4. MOBILITY SUBSYSTEM

4.1 Configuration Selection. Numerous options were studied and compared before establishing a final mobility system configuration. The configuration options were broken down into frame, terrain interaction, and steering.

4.1.1 Frame Options. As stated earlier, the frame option was a choice between a uniframe configuration and a multi-segmented one (Figure 2.3). Because of the extreme importance placed on vehicle mobility, a segmented vehicle was selected at the expense of added complexity.

4.1.2 Terrain Interaction Options. Besides the conventional wheeled vehicle, tracks and walkers were evaluated. More exotic methods such as hoppers and rolling balls were even considered. Interestingly, prior to actual landings on the moon, the very same process took place among designers. It was believed that trafficability on the Moon's surface would be very poor. Consequently, many strange-looking walking machines were developed. However, from the experiences of the Apollo program, it is now known that any vehicle with round wheels will perform satisfactorily, provided the ground contact pressure is no greater than 7-10 kPa (Heiken et al). To be thorough, the more exotic schemes were still considered. They were not viable for our purposes. The walking vehicle concept was quickly rejected because of its complexity and its inability to meet the speed requirements. Much greater consideration was given to tracks or some variation thereof. The major advantage of a tracked vehicle is its increased maneuverability. Tracks provide better turn radii, traction, and slope climbing capabilities than do wheels. However, this increase in performance did not outweigh the drawbacks associated with its weight, complexity, and prohibitive power consumption for rover applications. Maintainability and reliability of the tracks in this environment was also a great concern. Thus a wheeled vehicle was deemed most appropriate.

Furthermore, it was decided that each wheel should be powered by its own electric motor placed within the wheel well.

4.1.3 Steering Options. Three methods of steering were evaluated. The standard Ackermann system used by automobiles provided one possibility. The second option was to use an articulated frame steering system. The third possibility was to use skid (or scuff) steering commonly seen on tracked vehicles (Figure 4.1).

The standard Ackermann configuration turns the front set of wheels, possibly via a rack and pinion arrangement. Another option is a double Ackermann system in which both front and rear wheels are turned. The standard Ackermann system was used as a baseline for comparison with the other steering systems.

Since an articulated frame design was being considered, it made sense to have an articulated frame steering system option. This involves powering a yaw axis at the frame connection and rotating the vehicle sections with respect to each other. One of its primary advantages is that the wheels of the front and the back segments traverse the same paths. The driver knows that if the front segment clears an obstacle, the back one will. Also, the body can be bent to maneuver out of conditions that would stop a uniframe vehicle. Articulated frame steering produces turn radii smaller than the standard Ackermann system.

A third option naturally evolved from the idea that each wheel should be individually powered by its own motor. Since each motor could be operated independently of the others and at different speeds, a skid steering system was considered. The skid steering concept involves driving the outer and inner sets of wheels at differential speeds (or directions). This scheme can generate turn radii much smaller than any of the other systems. However, this requires much more power than the other steering systems under consideration.

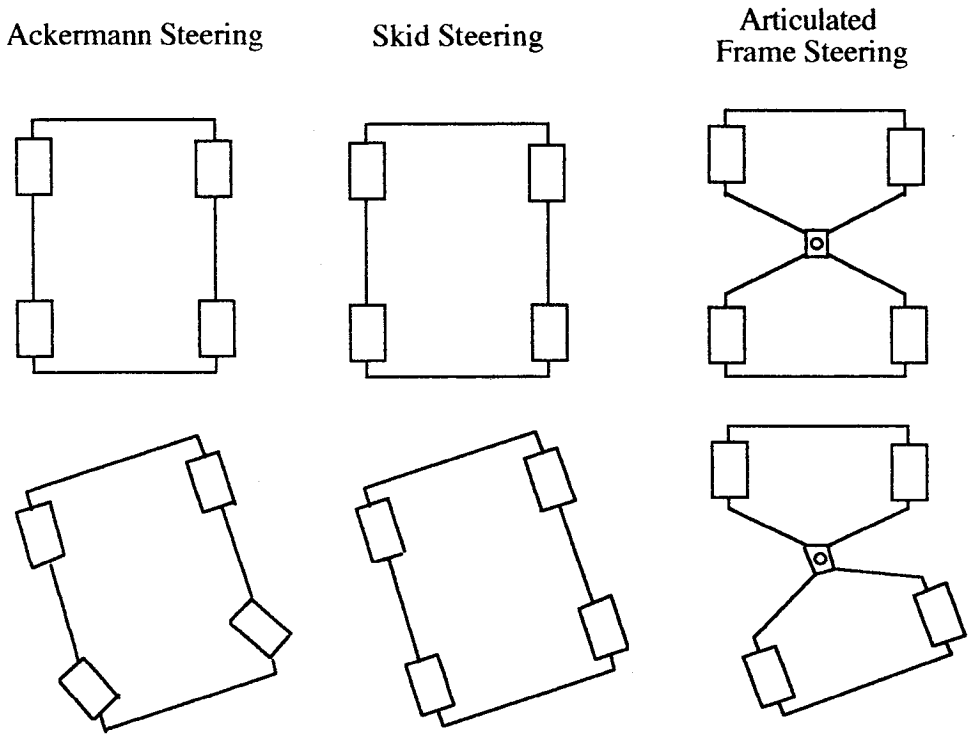

Figure 4.1 - Steering System Options

4.2 Final Configuration. The overall mobility system and the various components of the system are described in the following sections.

4.2.1 Saddle. Each pressure structure is supported by an aluminum saddle (Figure 4.2), which is a cradle used to distribute the loads caused by the wheels. The saddle is made up of longitudinal and transverse support beams attached to the pressure hull as well as plating. The saddle angle for optimum load distribution is 168° (Moss).

The two saddles are connected by an articulation joint (Figure 4.3). The joint controls yaw, and allows for free pitch and roll between the two pressure structures. The articulated turning of the rover is controlled by a motor attached to the yaw axis. The joint will be constructed of a high-strength steel. The joint will be subjected to stresses associated with maneuvering, but it will normally not have to pull the rear section since it will be driving with the same speed as the front section. Springs are place at the top of the flexible connection to balance the rover and keep it level. The joint will be housed in a flexible tube made of the same material as the flexible passageway. This will protect the joint from the effects of dust and thermal cycling.

4.2.2 "Pinned Wheel" Concept. An unusual wheel concept was chosen for improved mobility (Figure 4.4). Each side of each segment of the vehicle is supported by two wheels. The wheels are connected at their centers by a hollow cylindrical bar which is pinned at its midpoint. A hollow cylindrical cross-section was chosen because it is lightweight, and allows electrical connections to be housed inside. The bar is attached at the pin through a passive suspension system to the saddle. Note that the bar's ends are bent away from the pressure structure making Ackermann steering possible. The bar is free to rotate about the pin. This allows a large degree of vertical movement by the wheels while still maintaining constant ground contact. Figure 4.5 shows the extreme conditions that the wheels can handle. Figure 4.6 shows how the rover conforms to the terrain.

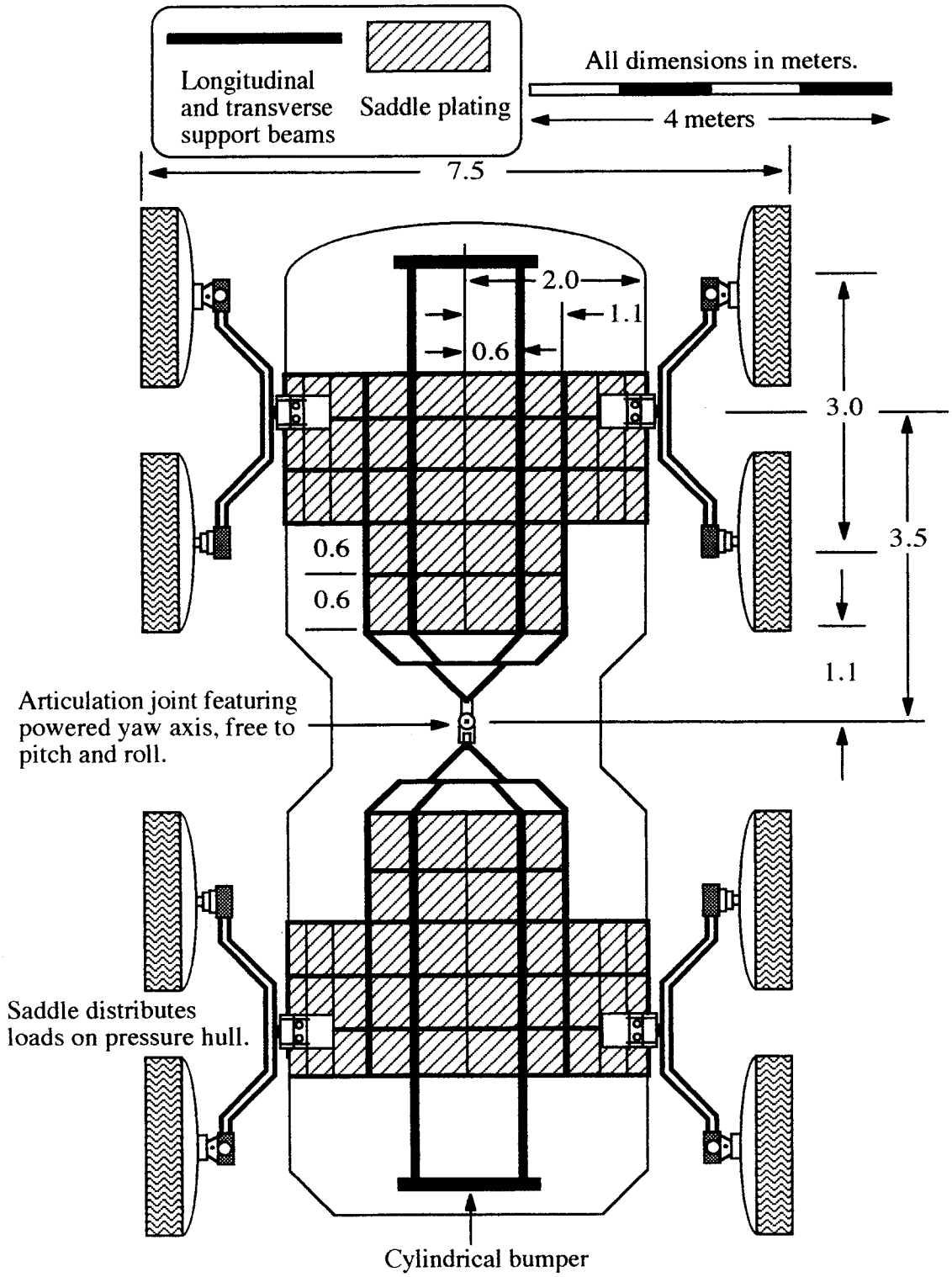

Figure 4.2 - Vehicle Substructure, Top View

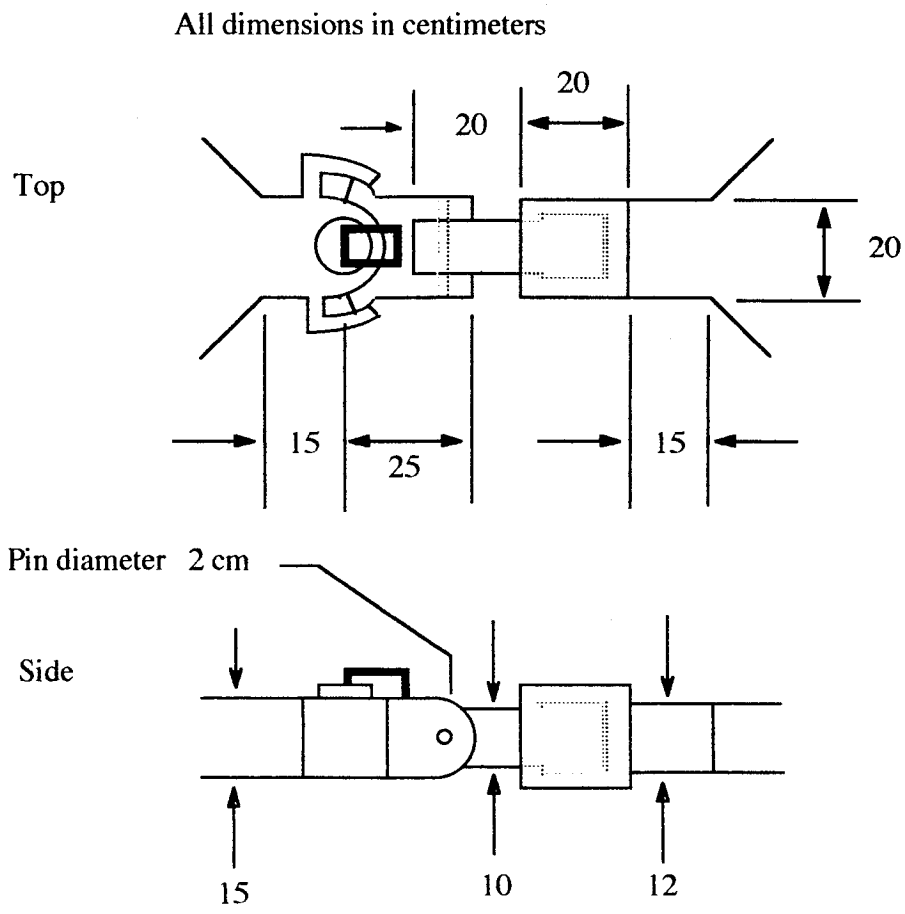

Figure 4.3 - Joint Schematic

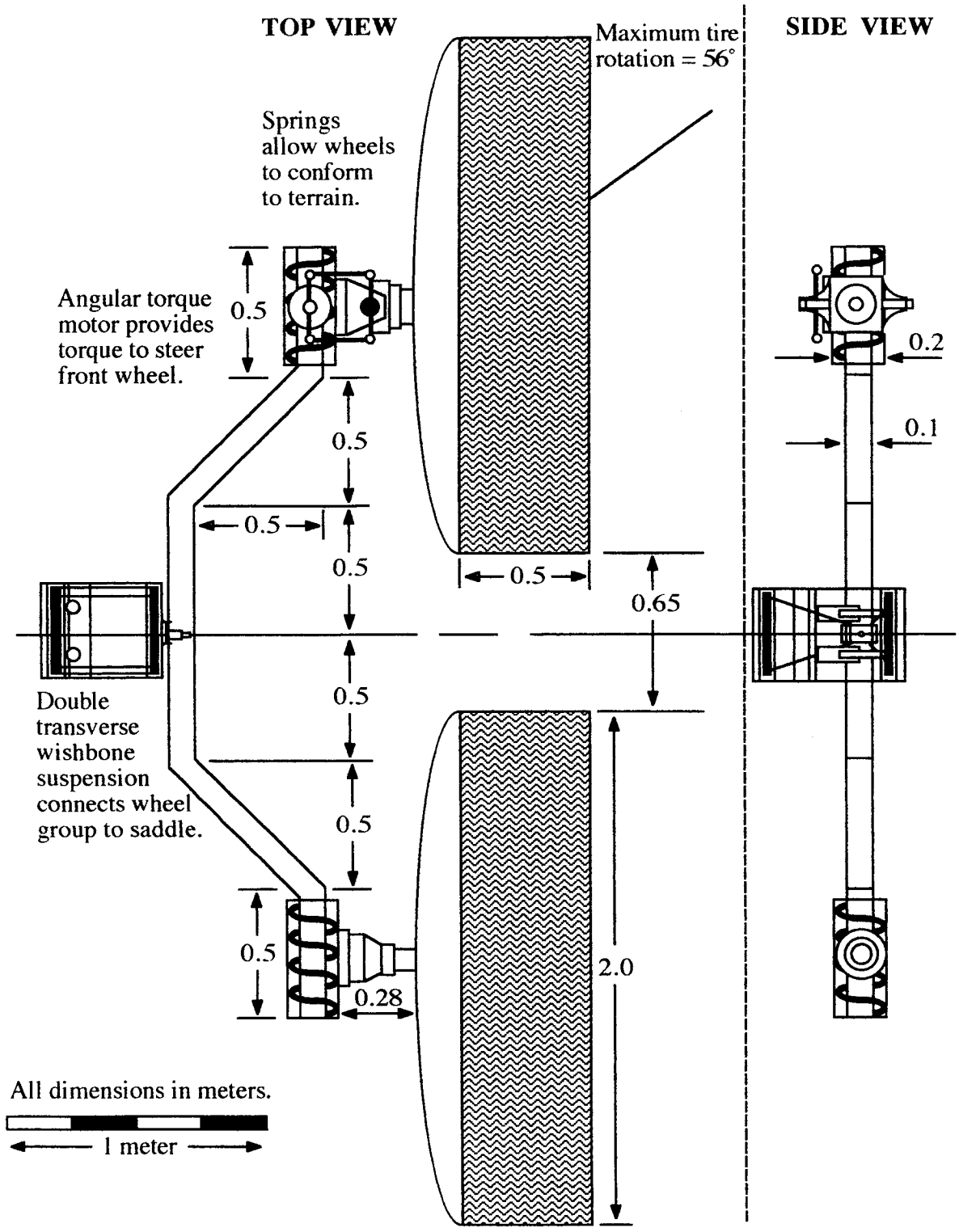

Figure 4.4 - Wheel Group

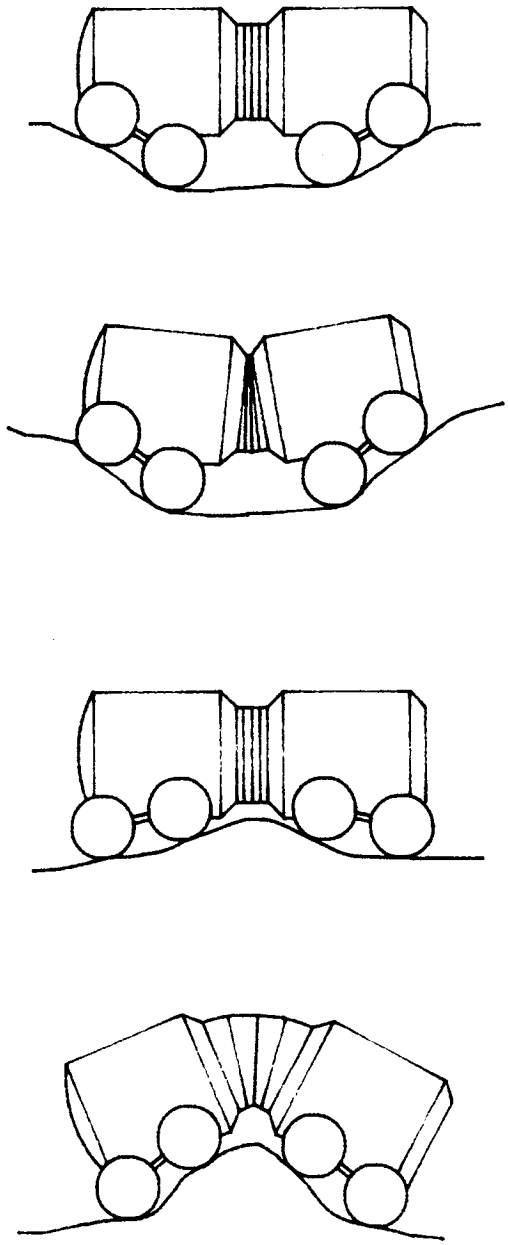

Figure 4.5 - Obstacle Extremes

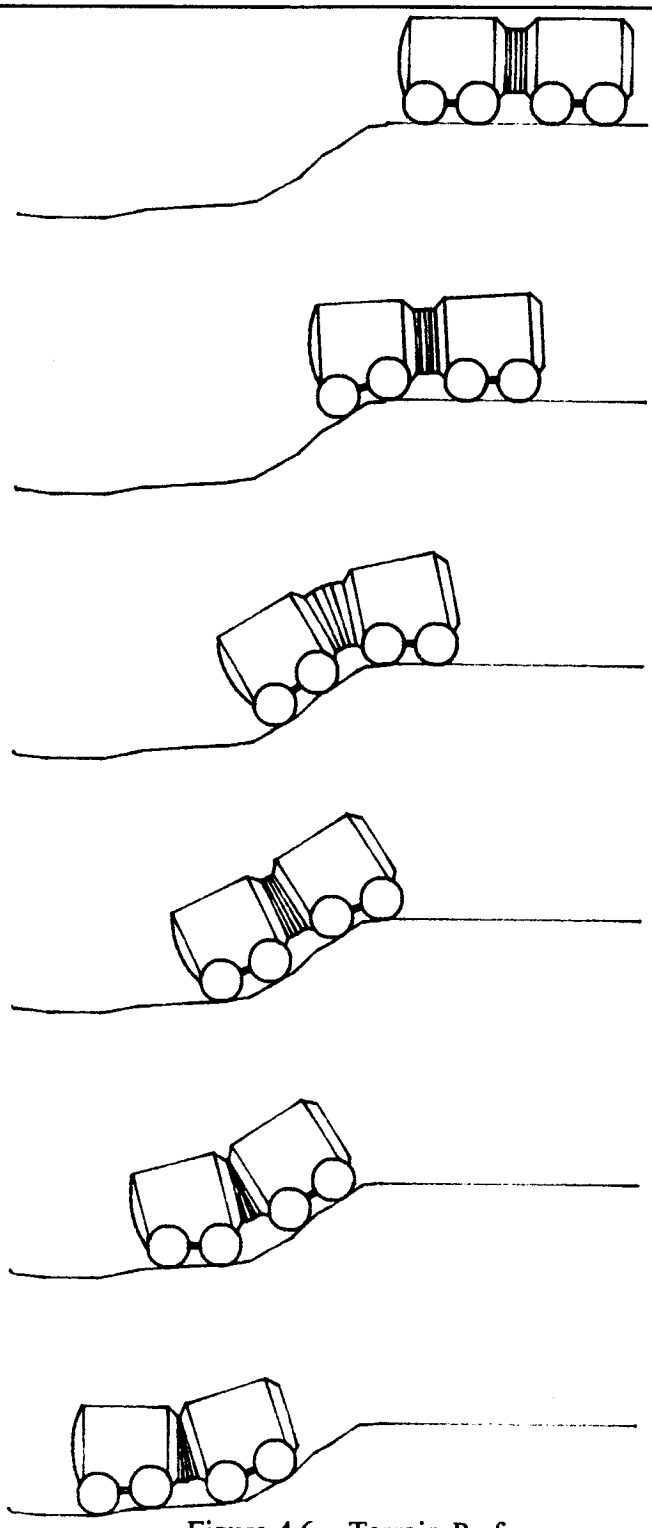

Figure 4.6 - Terrain Performance

4.2.3 Suspension System. The suspension system connects the saddle to the "pin wheel" bars and connects the bars to the wheels. It is designed to position the wheels on the ground with a maximum contact area. Furthermore it transmits drive, braking, and turning forces, and spring and shock absorber loads.

The proposed independent suspension system can be seen in Figures 4.4 and 4.7. It consists of a double transverse wishbone suspension (Figures 4.8 and 4.9) supporting the central pivot location of the "pinned wheel" arm. The upper and lower arms are of equal length to ensure that the connecting bar will not rotate about its longitudinal axis. A primary pair of components are two telescopic shock absorber-dampers balanced by springs. The purpose of the dampers is to dissipate some of the energy imparted to it in the form of heat. This leaves insufficient energy in the spring for violent rebounds, reducing the amplitude and frequency of oscillation. The upper end of the rod is pushed onto a ball thrust bearing housed in a rubber mounting. The bearing allows strut rotation while the rubber mounting accommodates angular movement and supports the body weight. The bottom end of the strut is pivoted to the lower arm by a ball and socket joint. Each suspension group is completely independent of the others, so the suspended body will not be influenced by small wheel

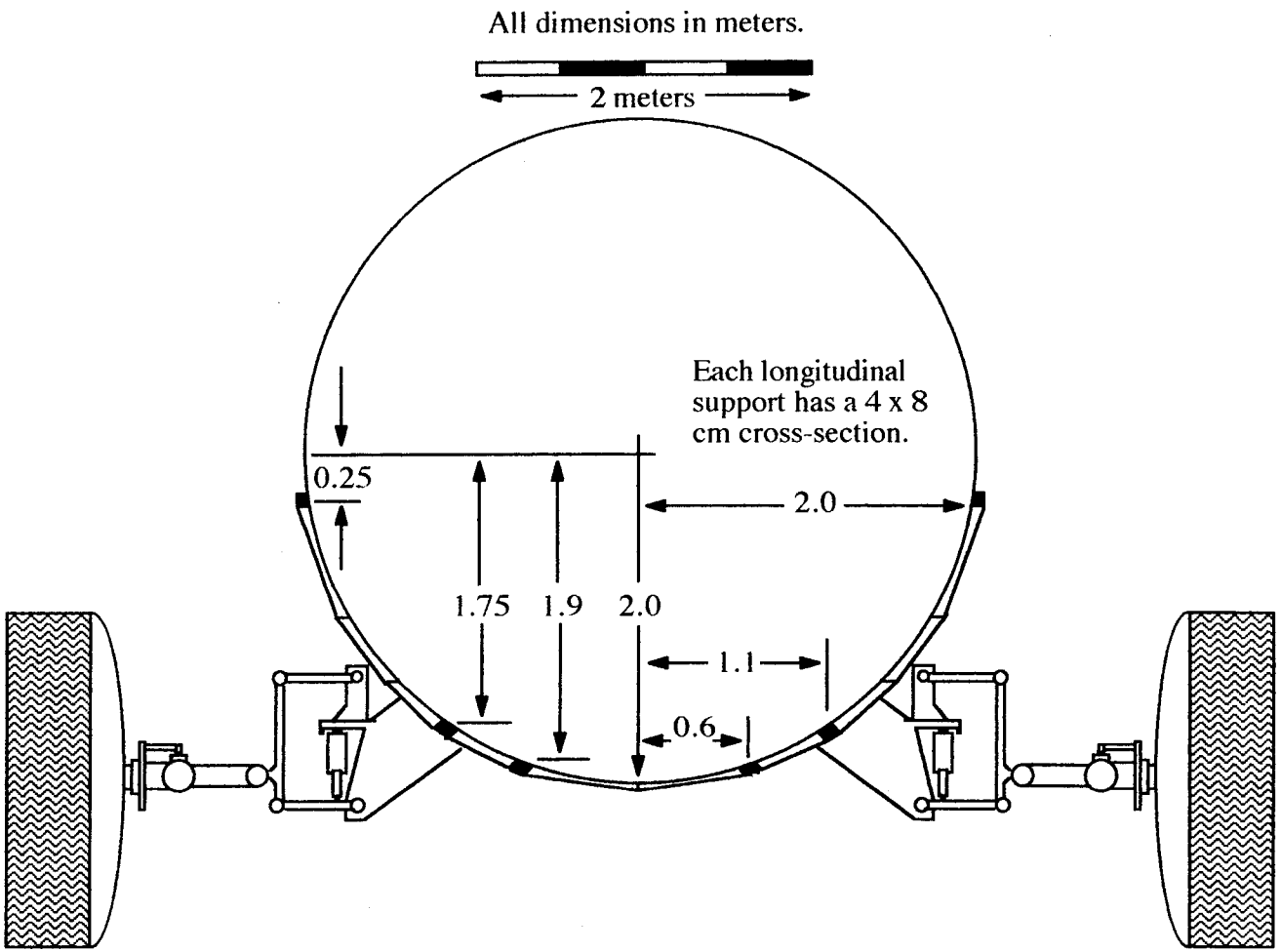

Figure 4.7 - Vehicle Substructure, Front View

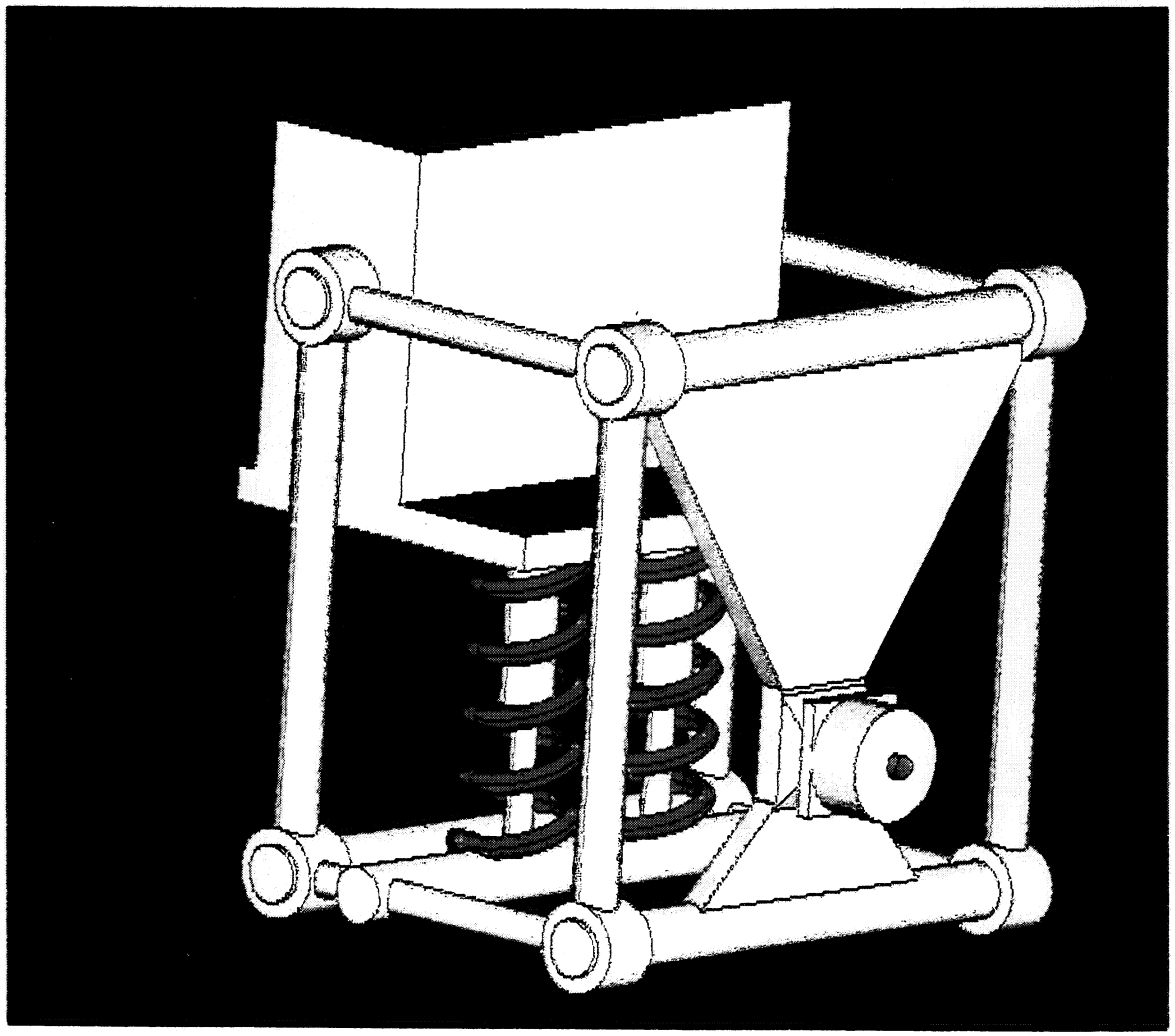

Figure 4.8 - Suspension Isometric

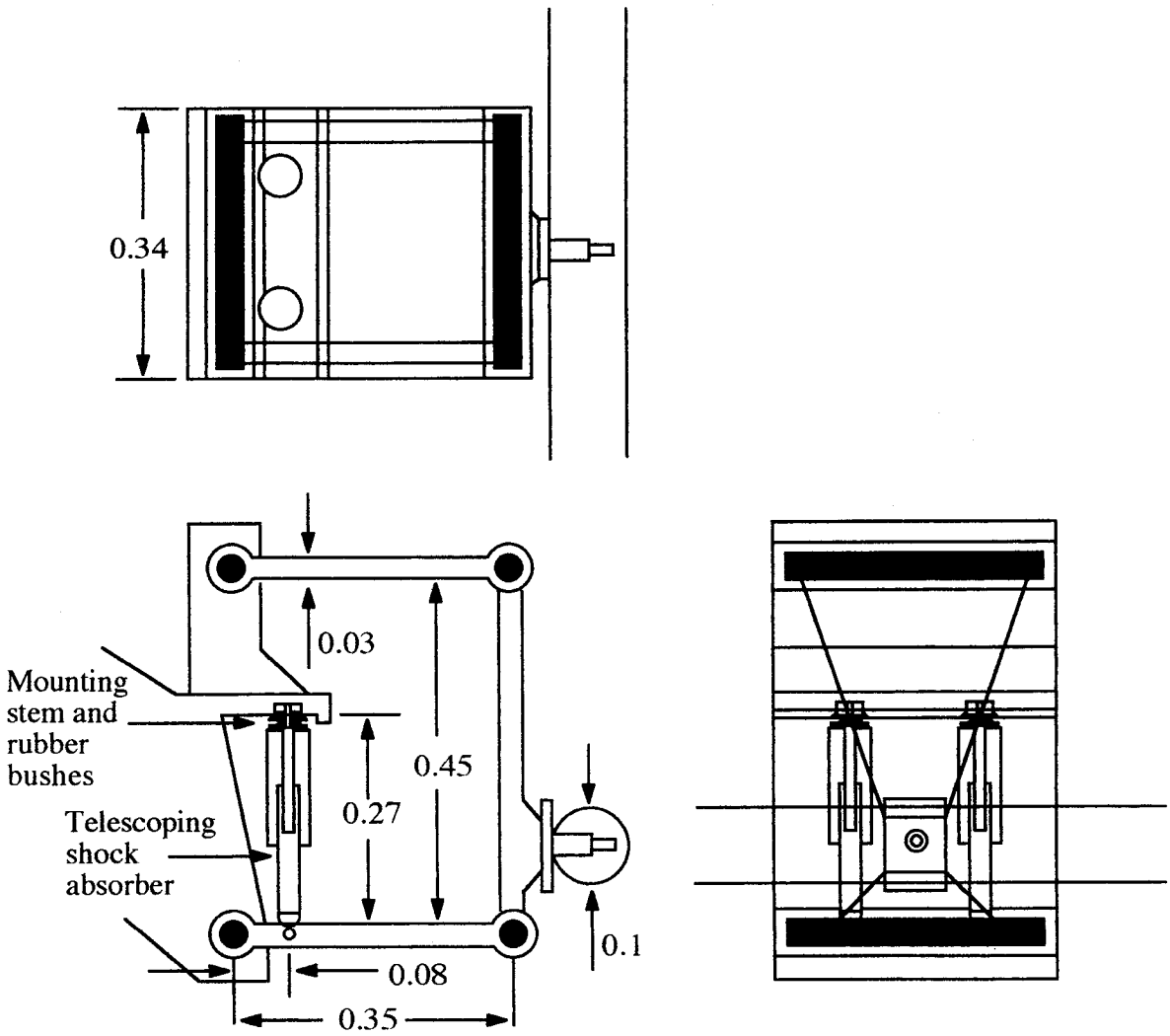

Figure 4.9 - Double Wishbone Suspension

deflections (Heisler). Figure 4.10 shows the maximum suspension displacements that can be achieved while still maintaining a level cabin. A larger step would cause cabin rotation, as would prolonged exposure to these terrain conditions (ie. a long ditch). In the case of Figure 4.10, the strut would force the wishbone members to return to their original rectangular shape, causing a counterclockwise rotation of the cabin.

At the end of each bar, the wheel is attached via a spring which allows rotation about the longitudinal axis of the bar. Thus the wheels are allowed to conform to various surface conditions and ground contact is maximized. The springs are balanced so that the wheels remain vertical on a horizontal surface.

4.2.4 Steering System. A dual steering system was chosen. Based on complexity and power consumption, it was decided that a combination of double Ackermann and articulated frame steering would be used. As the steering wheel is turned, an electronic control system turns the front and rear wheel pairs (Figure 4.11) (using motors mounted at the bar end) and the articulation joint to produce the appropriate geometry for an ideal, neutral steer turn (Figure 4.12). This geometry produces a minimum turn radius of 9.4 meters. However, after the articulated frame has been turned through its full angle, the ideal geometry may be sacrificed by turning the wheels further. This leads to a slight oversteer condition which will allow a tighter turn. In an oversteer, the vehicle will continue to turn while the steering wheel is held fixed. This will require that the driver be accustomed to controlling the vehicle during oversteer. A second option is to install an additional control system that can compensate for the oversteer. This insures that the response to steering control will be the same whether or not oversteer is present.

In an emergency the driver has the option of utilizing skid steering, since the wheels are already individually powered. Although in itself this would be too power-consuming, it can supplement the primary steering system if required.

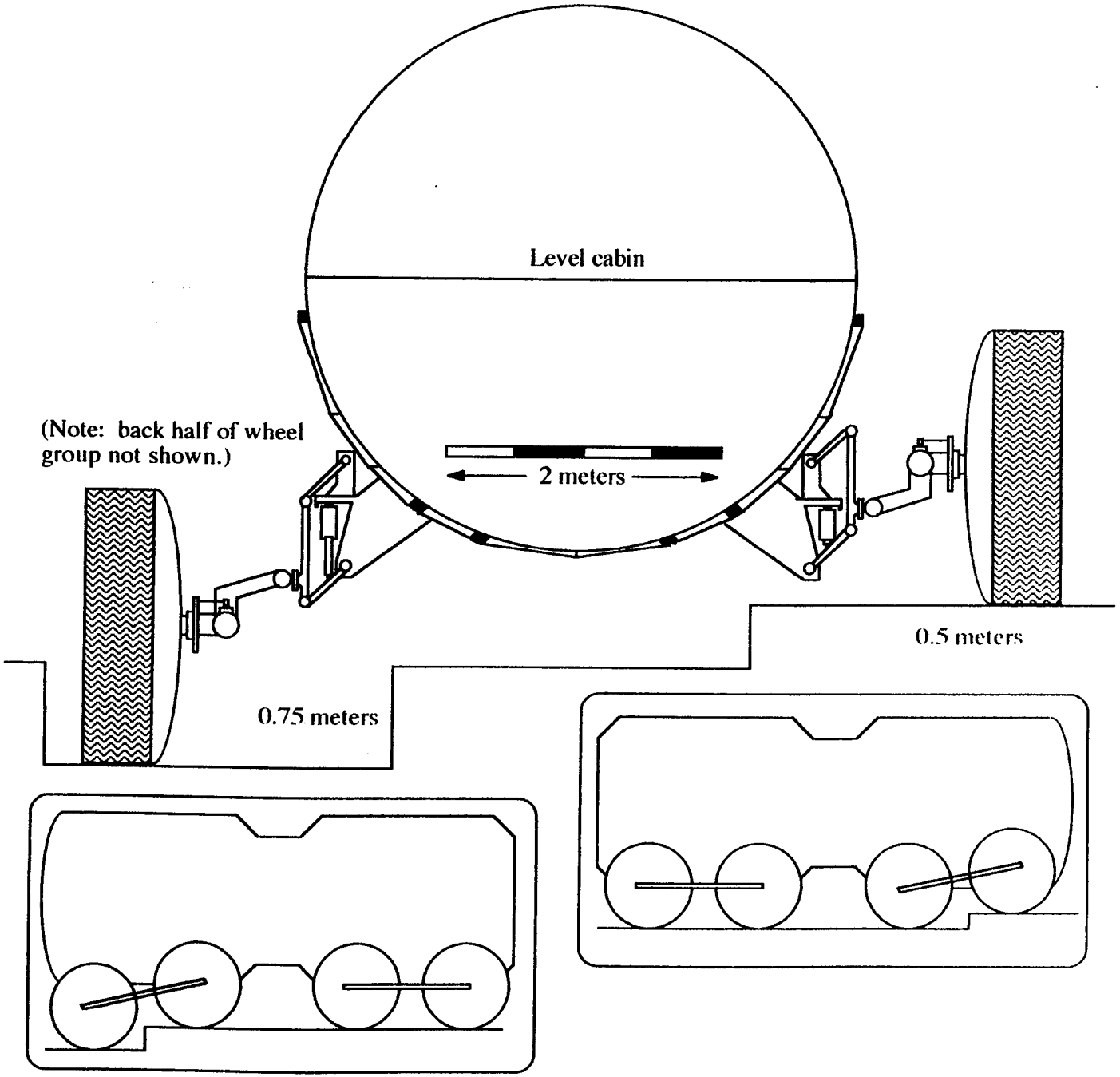

Figure 4.10 - Maximum Suspension Displacements (Level Cabin Condition)

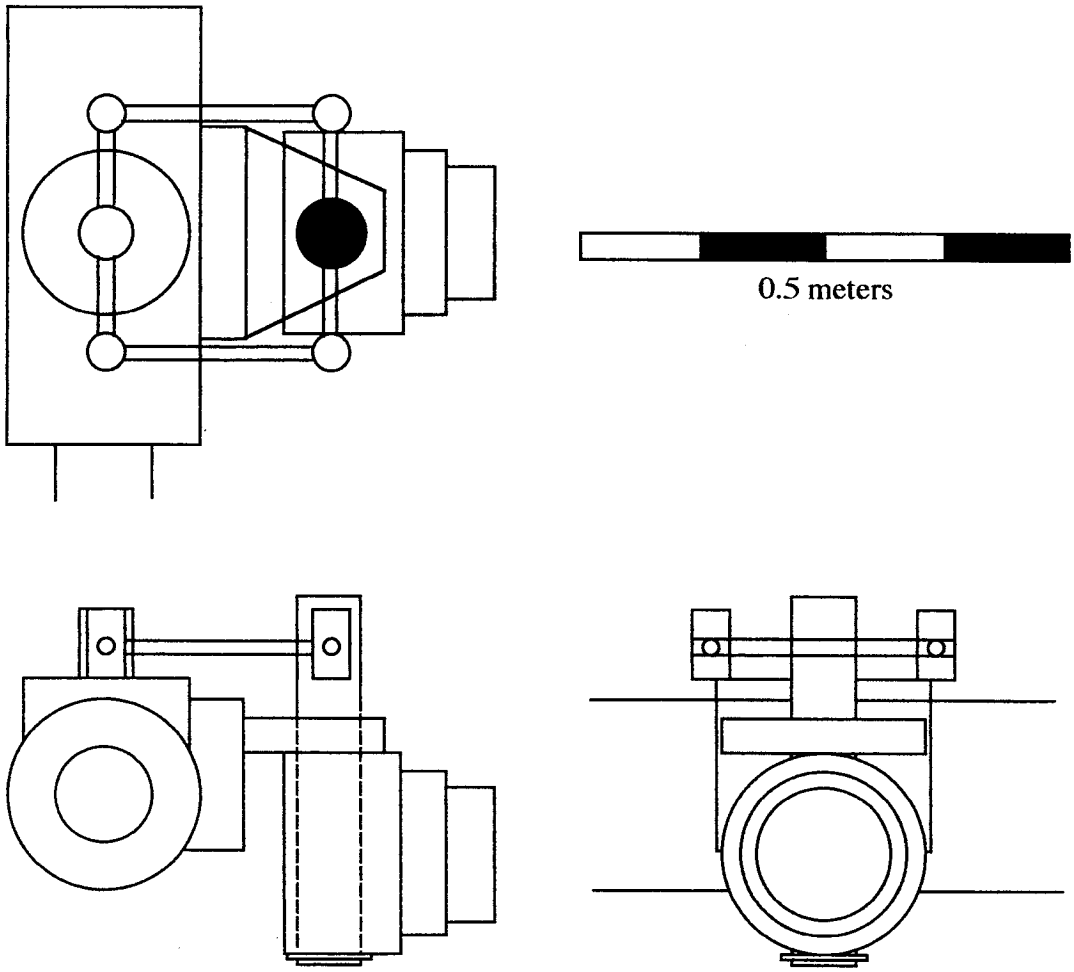

Figure 4.11 - Ackermann Steering System

* Note: the actual vehicle turn radius can be further reduced by continuing to turn the front and rear wheels beyond the point of maximum frame rotation. However, the inner wheels will be unable to align producing an oversteer condition.

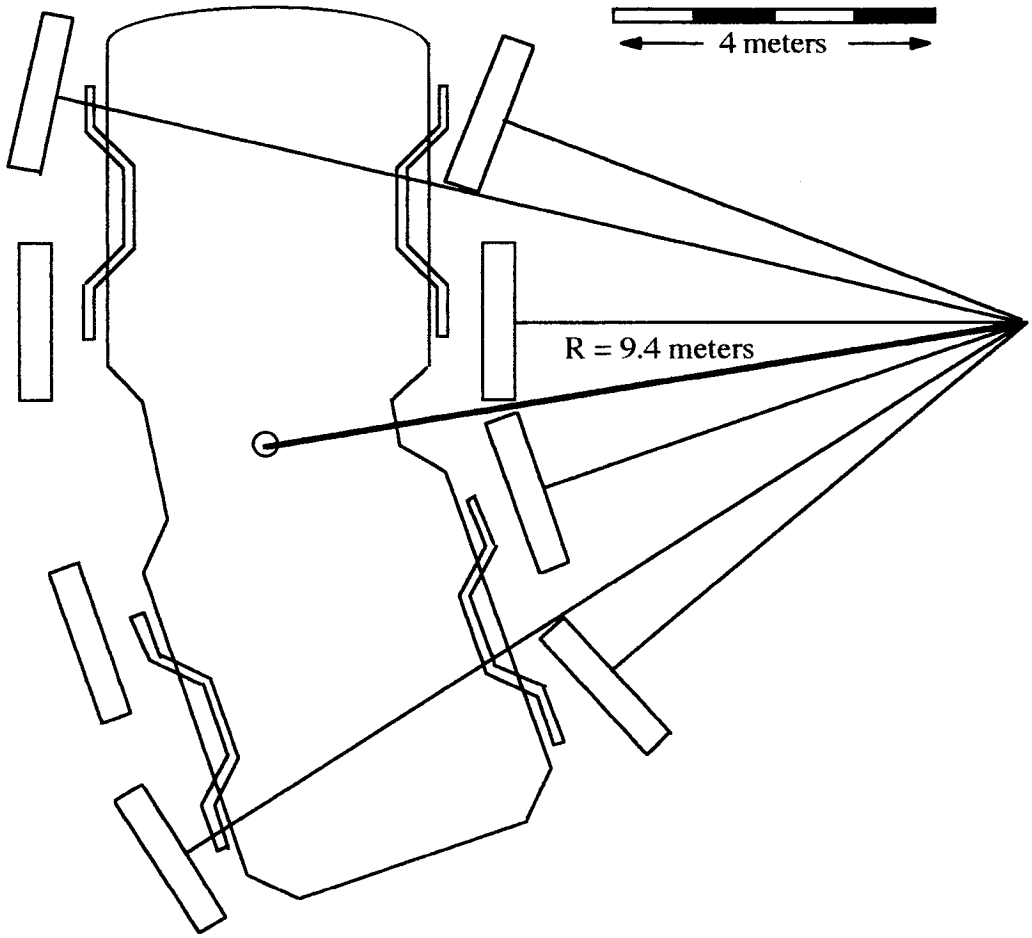

Figure 4.12 - Ideal (Neutral Steer) Turn

4.2.5 Wheel/Tire Assembly. The wheel/tire assembly consists of the wheel well containing the drive motor as well as the wheel, tire, and required gearing and support (Figure 4.13). The drive motor rotates a 0.45 meter radius rigid cylindrical frame that is inside the tire and rigidly connected to the back of the wheel. Slightly elastic rings fill the area between the frame and the tire. These rings support the tire to enhance traction. The face of the wheel is covered to protect the drive system from large amounts of lunar regolith disturbing its operation. Grousers (cleats) will be used to enhance mobility system performance.

4.2.5.1 Electric Motor. The drive motors and articulation motor of the PLR will have equal pull capabilities, so a single motor type may be used. Three-phase high performance DC brushless motors with variable speed drive will be used as the housed drive motors. These motors are mounted inside the hub of the wheel. The rated torque that can be produced is 900 Nm. Power at the rated torque is 1.5 kW. The maximum continuous stall torque provided will be a nominal value of 600 Nm (Inland). Smaller motors will be used for wheel turning, since they do not require such large torques. Hydraulic motors were not chosen due to the disadvantages they have for in-space applications.

Brushless permanent magnet motors offer many advantages over conventional electric motors. Little maintenance is required with the brushless motor because it does not have the problems of brush longevity and maintenance. In addition, they have the capability of reversing torque, which greatly enhances maneuverability (Mateuffel). A three-phase power source system is preferable since it lowers wear on the motor (Turner). DC electric motors have a higher torque to weight ratio, are more reliable, and are easier to control (Jones). Thus a DC brushless electric motor was selected.

Many advantages are found by using brushless systems with the proper servo amplifier. These include operation in harsh environments, a broad speed range, and many mechanical advantages. Figure 4.14 is a basic schematic of the system to be used. Hall

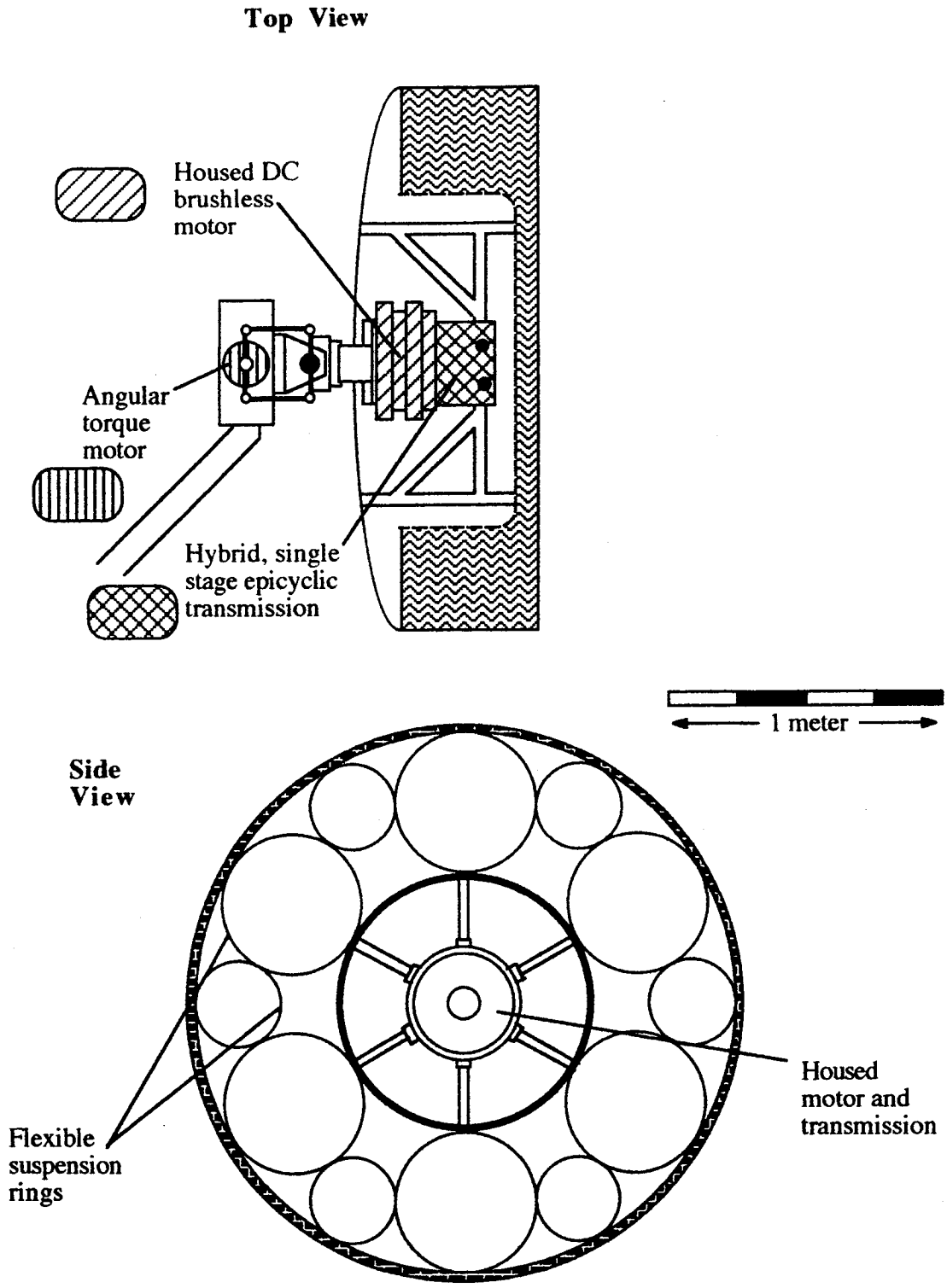

Figure 4.13 - Wheel Assembly

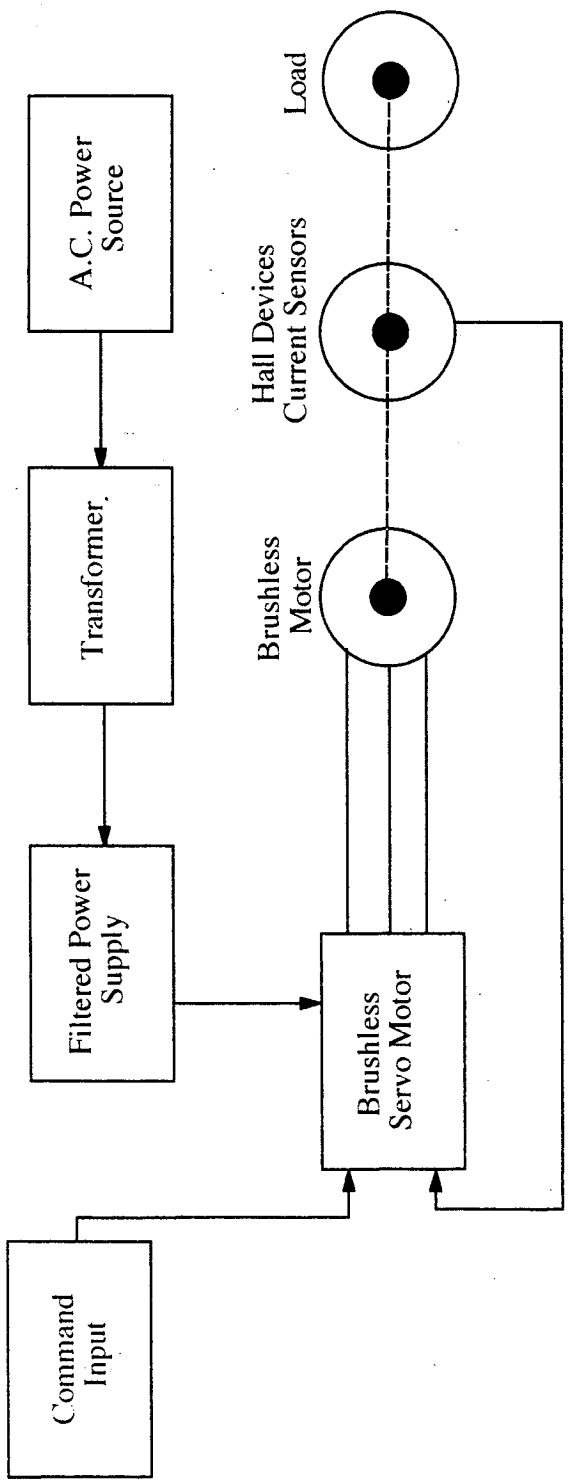

Figure 4.14 - DC Brushless Motor System Diagram

devices and current sensors are used for velocity and torque feedback to the amplifier. This feedback is compared with the input values and the servo amplifier adjusts the electrical output accordingly. This provides an overall reliable and rugged motor system.

A compact transmission which utilizes multiroller planetary friction drives is used (Figure 4.15). A 50:1 speed reduction is possible to provide ample torque for difficult maneuvers. The transmission has a 92-93% efficiency (Nasvytis).

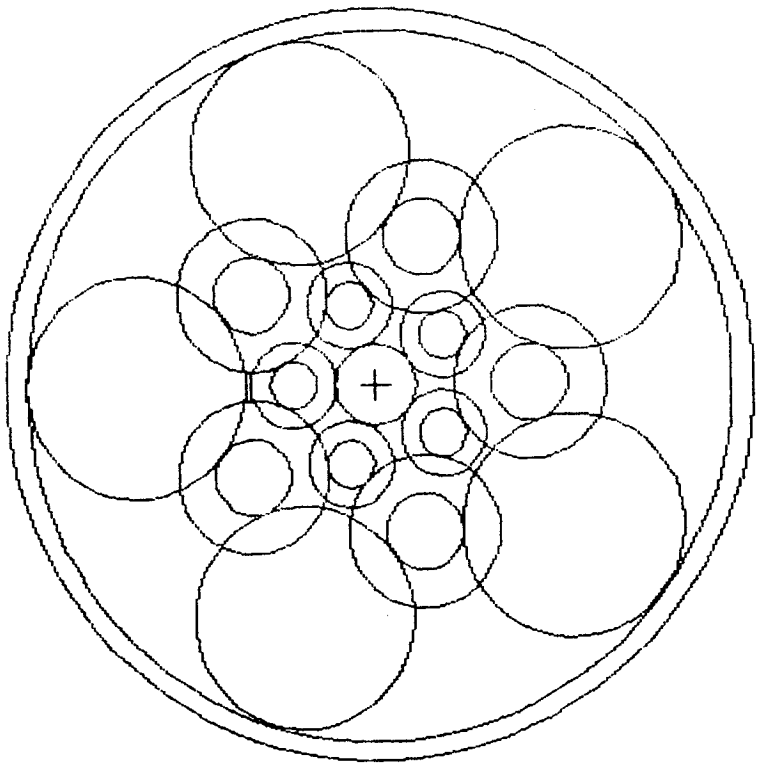

Figure 4.15 - Multiroller Planetary Drive System

4.3 Performance. The rover's mobility performance characteristics are presented in Table 2.2, reproduced here for convenience.

Table 2.2 - Mobility Performance Characteristics

Maximum Velocity	(4 wheels), 14.7 km/hr (8 wheels), 29.4 km/hr
Nominal Power Requirement	(4 wheels) 1.36 kW/wheel (8 wheels) 0.68 kW/wheel
Maximum Allowable Power	1.5 kW/wheel
Maximum Gross Pull	900 N/wheel
Maximum Vehicle Acceleration	0.64 m/s^2
Soil Compaction Resistance	
Normal Soil	22 N/wheel
Soft Soil	81 N/wheel
Hard Soil	4.0 N/wheel
Minimum Turn Radius (in percent of vehicle length)	
Neutral Steer	78.3%
Oversteer	60%
Range	2,000 km
Maximum Gradient	26.5°
Wheel Sinkage	
Normal Soil	1.03 cm
Soft Soil	2.86 cm
Hard Soil	0.21 cm
Climbable Step Height	0.53 M
Crossable Crevice	1.7 M

A nominal velocity of 10 km/hr (2.78 m/s) was assumed, which will easily meet the mission requirements. Normally, the rover will be driven with only four of the eight wheels powered. The rationale is that if the rover becomes stuck while using all-wheel drive, it will have difficulty freeing itself. However, if the rover becomes stuck while using only half of the wheels, powering the remaining wheels will probably free it.

Experimental analysis has shown that the coefficient of rolling resistance, f_r, is approximately 0.20 (Sponsler). The straight line power required is given by (Wong, J. Y.)

$$P_{st} = f_r W V_{st}.$$

This must be scaled depending on the number of powered wheels. This means that the power required per wheel (using four wheels) for straight-line motion at the nominal speed is 1.36 kW. With eight wheels powered, the power per wheel is 0.68 kW. The maximum power allocated to the drive motors is 1.5 kW. At this power, the rover can attain peak velocities of 14.7 km/hr and 29.4 km/hr, for four and eight powered wheels respectively. Turning power is difficult to estimate without experimental data for the specific steering system, terrain, and tires involved. It is estimated that the required turning power will be between 0.25 kW and 1 kW, depending on the speed of the rover and the terrain. Low speed turning will require more power than high speed turning, so turning power will not affect the maximum power required for mobility. This will be defined by the fastest forward speed, and the rover will not be traveling near this during maneuvers.

Bekker's models of obstacle performance indicate that the rover should be able to climb steps 0.53 meters high and cross crevices 1.7 meters in width. Keep in mind that the wheels are two meters in diameter, so these values are not unreasonable. However, the step height is based on a stationary wheel, and the actual wheels should be able to far outperform standard wheels with regard to climbable step height.

The following empirical formulas developed by Bekker (Heiken et al) were used to compute several of the performance parameters. The wheel sinkage, z, was calculated using

$$z\ (cm) = (W/Ak)^{1/n}.$$

The gross pull per wheel in newtons, H, was determined using

$$H = (Ac_b + W\tan\phi_b)\cdot[1-K/sL(1-e^{-sL/K})].$$

Figure 4.16 shows the variation of maximum gross pull per wheel with wheel slip. The operating envelope was chosen to allow maximum use of the soil's pulling capacity. This defined the necessary torque output of the motor. The soil compaction resistance per wheel in newtons, R_c, was found using

$$R_c = [bk/(n+1)]z^{n+1}.$$

Finally, the steepest slope a wheeled vehicle is capable of climbing may be estimated using

$$\text{Slope} = \tan^{-1}[(H-R_c)/H].$$

The input parameters for these equations are

W = wheel load (N) = 1,491

A = wheel footprint area (cm^2) = 1,755

L = wheel chord length of ground contact (cm) = 35.1

b = wheel width of ground contact (cm) = 50

k_c = cohesive modulus of soil deformation (N/cm^2) = 0.14

k_ϕ = frictional modulus of soil deformation (N/cm^3) = 0.82 (normal soil)

k = soil consistency (N/cm^3) = $k_c/b + k_\phi$ = 1.8

n = exponent of soil deformation = 1 (normal soil)

c_b = coefficient of soil wheel cohesion (N/cm^2) = 0.017

ϕ_b = soil/wheel friction angle (°) = 35

K = coefficient of soil slip (cm) = 1.8

s = wheel slip (dimensionless) = varies

It has been suggested that some of these parameters be adjusted for the critical condition of soft soil (Wong et al). These isolated areas could immobilize the vehicle and thus must be taken into account. Therefore the following adjustments will be made.

Soft soil k_ϕ = 0.5 N/cm^3

Soft soil n = 0.5

Hard soil k_ϕ = 6 N/cm^3

Hard soil n = 1.25

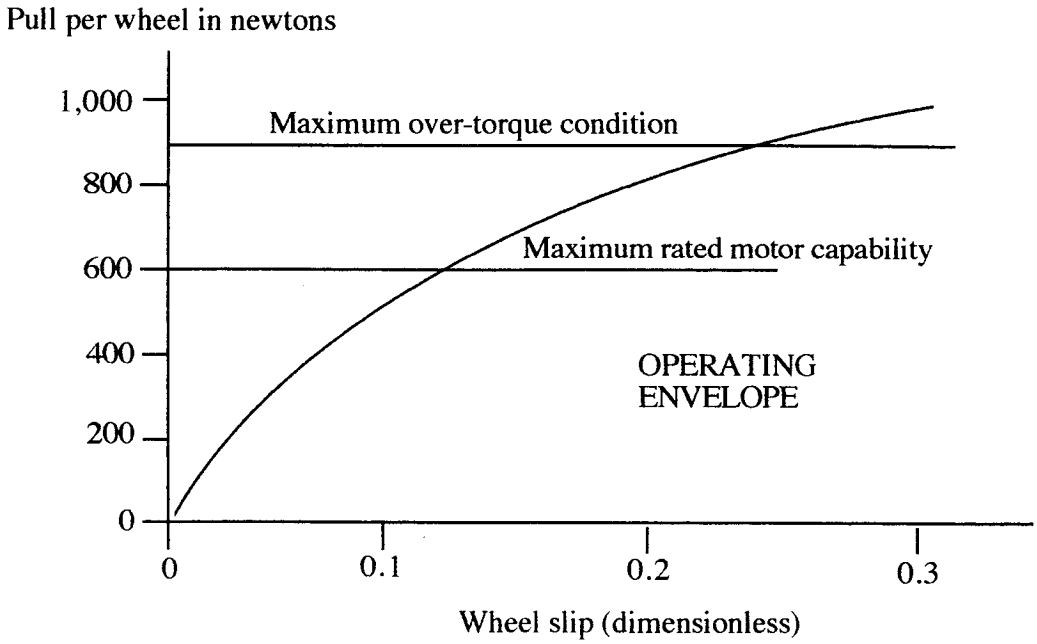

Figure 4.16 - Pull Per Wheel Versus Wheel Slip

5. POWER SUBSYSTEM

5.1 Power Required. The first step in selecting a power system for the pressurized lunar rover was to determine the amount of power required. Power estimates were made for all systems on the rover and are listed in Table 2.4. With these estimates, several mission profiles were planned. The first profile was the Survey Mission. This mission was planned around a 14 day period, where 50% of the time would be inactive time (eating, sleeping, etc.), 33% of the time would be survey work, and 17% of the time would be driving. The next profile was the Transport Mission. The profile was based on a four day period in which the vehicle was constantly driven. The third mission profile was the Search and Rescue Mission. This mission was based on a two day period where 80% of the mission will involve driving and searching and 20% of the mission involved the rescue. The power profiles for these three missions are shown in Figures 5.1 - 5.3.

Based on the maximum average power of 8.125 kW from the transport mission profile, it was determined that a continuous power of 8 kW is needed. The driving factor in determining the peak power required was the mobility system because it draws the greatest amount of power. Normally the rover is driven by four wheels. In the event that all eight wheels are needed to be driven at once, the total required power output would be 12 kW. This established the peak power requirement. Based on these figures, the power system will consist of a primary power source creating 8 kW and a 4 kW storage capacity.

5.2 Types of Power Systems. Several type of power generation were evaluated for the primary power source, including fuel cells, batteries, photovoltaic arrays, radioisotope thermoelectric generators (RTG), and dynamic isotope power systems (DIPS). Batteries were the first to be eliminated based on their short supply of power and long period of

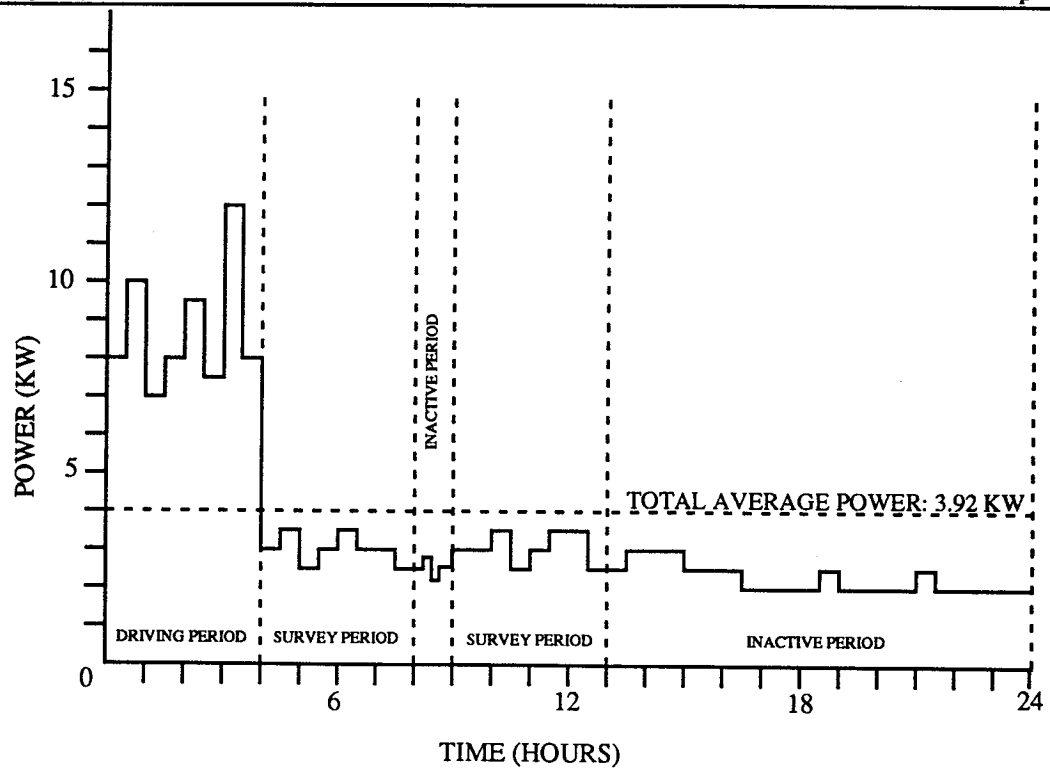

POWER REQUIREMENTS (W)

	PERIOD		
	INACTIVE	SURVEY	DRIVING
ECLSS	200	200	200
EXTERNAL FIXTURES	0	1000	200
INTERNAL REQUIREMENTS	1500	400	200
MOBILITY	0	0	6000
OPERATIONS	300	600	600
THERMAL CONTROL	800	800	800
TOTAL:	2800	3000	8000

Figure 5.1 - Power Profile: Survey Mission (Typical 24 hour period)

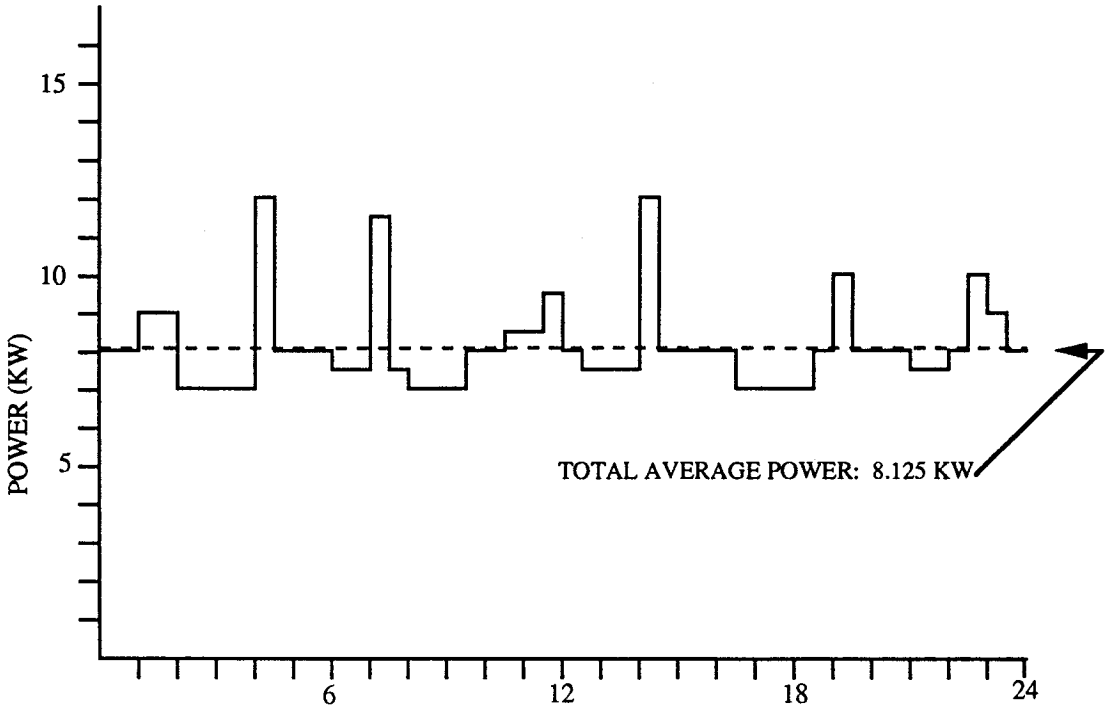

POWER REQUIREMENT(W)

ECLSS	200
EXTERNAL FIXTURES	200
INTERNAL REQUIREMENTS	200
MOBILITY	6000
OPERATIONS	600
THERMAL CONTROL	800
TOTAL:	8000

Figure 5.2 Power Profile: Transport Mission (Typical 24 hour period)

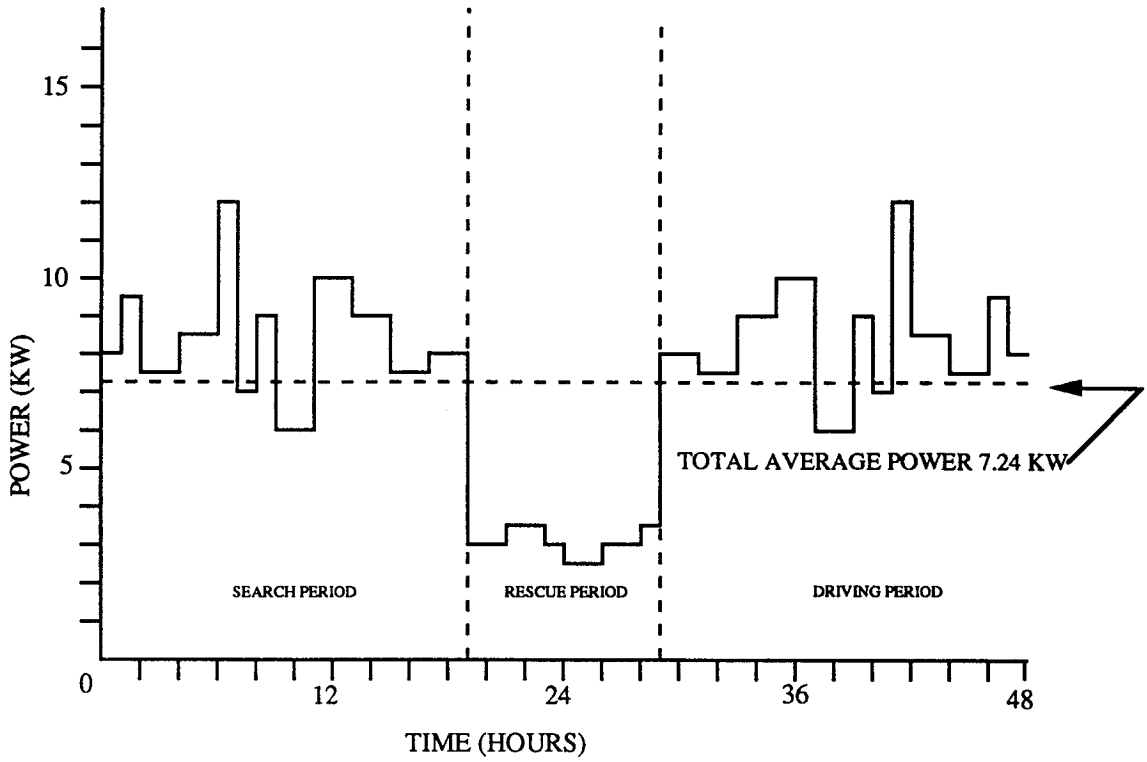

POWER REQUIREMENTS (W)

	SEARCH/ DRIVING	RESCUE
ECLSS	200	200
EXTERNAL FIXTURES	400	1000
INTERNAL REQUIREMENTS	200	800
MOBILITY	6000	0
OPERATIONS	600	600
THERMAL CONTROL	800	800
TOTAL:	8200	3400

Figure 5.3 - Power Profile: Search & Rescue Mission (Typical 48 hour period)

recharging. The photovoltaic array was eliminated due to a large array area required. To generate 8 kW of power, a non-steerable array would require a surface area of in excess of 80 m^2. The next option eliminated was the fuel cells. Even though fuel cells could easily produce the 8 kW, the mass requirement for such a system would be approximately 3,000 kg (NASA PSS ESBD 91.1). RTG was disregarded because its low energy conversion efficiency (5-10%) and high mass requirement. For the required power, the mass estimate of the RTG is well over 3,000 kg (Elias). The last system was the DIPS. Most DIPS cycles were found to have an energy conversion efficiency between 20 and 30%, while their mass estimates where fairly low (500-1,000 kg). In terms of availability and technology, most DIPS were very mature. With these factors, the DIPS became the choice for the primary power system of the rover. For auxiliary power, batteries with a photovoltaic array for recharging were chosen because of their simplicity.

5.3 DIPS. There are several DIPS cycles used in producing power. The first is the Brayton cycle. It uses a xenon-hydrogen mixture as its working medium. By using a gas, the need for a fluid management system is eliminated and fluid degradation does not become a problem (Stadnik). A second system is the Rankine cycle which uses toluene (a fluid) as its working medium. A third system is the Stirling cycle. The Stirling uses hydrogen as its working medium, again eliminating the need for a fluid management system. The energy conversion efficiency of the three system is: Brayton cycle 24%, Rankine cycle 21%, and Stirling cycle 40% (Walters). The technology for the Brayton and Rankine cycles is available now, while the Stirling cycle is still in the research and development phase (Walters). The Brayton cycle was chosen based on its working medium and availability.

5.4 Closed Brayton Cycle (CBC). Figure 5.4 is a functional diagram of the CBC. The heat source units (HSU) of the CBC (Figure 5.5) are one meter long with a diameter of 40 cm. Figure 5.6 shows the placement of the system within the pressure hull. They are

powered by the decay of Plutonium 238 modules, which have a diameter of 12 cm, length of 5 cm, mass of 6.55 kg, and specific energy release (q_v) of 0.9760 W/cm^3. Each HSU contains 17 modules. The thermal power output of each HSU, 4148 Wt, is calculated as follows:

$$E_{HSU} = 2/\pi \cdot q_v \cdot A_t \cdot L$$

where A_t is the transverse area and L is the length of the rod. The CBC has a conversion efficiency of 24.1%. Therefore, in order to obtain 8 kWe for the power system, an input of 32.2 kWt is needed, based on the following calculation:

$$E_{in} = E_{out}/\text{efficiency}$$

In order to obtain this amount of thermal power, eight HSU's are needed. Since the mass of each HSU is 25 kg, the total mass of the eight HSU's will be 200 kg.

The electrical power is created by the turboalternator compressor (TAC) assembly. The thermal power is transferred from the HSU to the TAC by the xenon-hydrogen working fluid. The gas is heated in the HSU and then enters the turbine end of the TAC. The temperature at the turbine is around 1150 K. The gas expands in the turbine and performs work, creating the electrical energy. The gas then passes through the recuperator where part of the excess energy is transferred to the cycle gas on its way to the HSU. The gas then leaves the recuperator and passes to the radiator were the excess heat is transferred directly to the radiator heat pipes, which then cycle the heat directly to space. The cooled gas is now at approximately 300 K. This gas travels from the radiator to the alternator (cooling it),

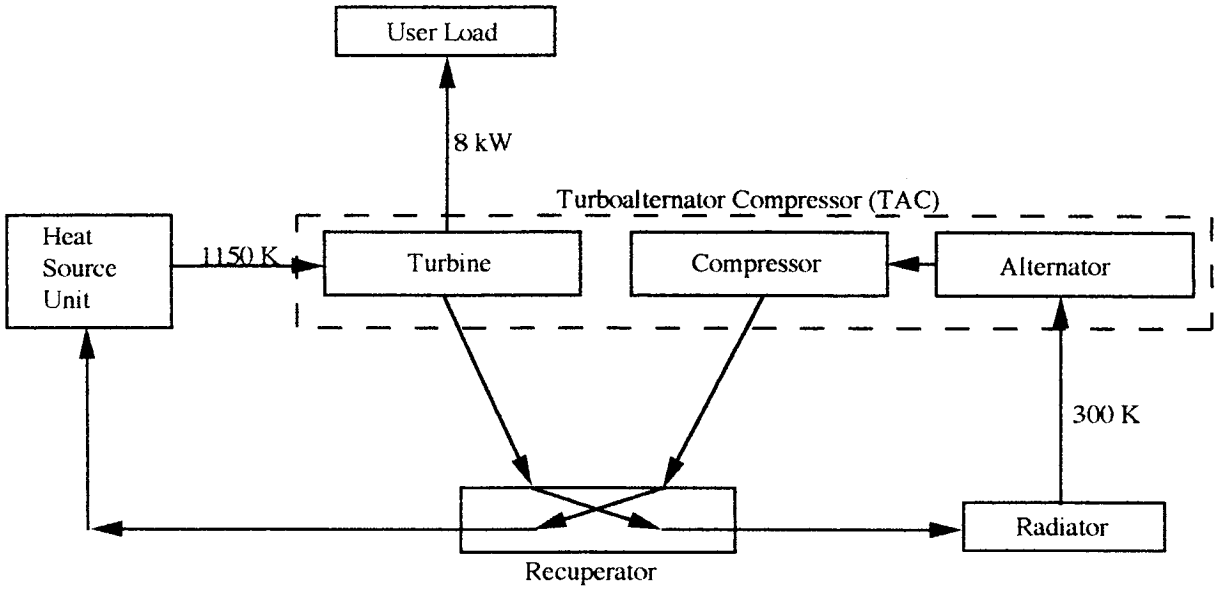

Figure 5.4 - Closed Brayton Cycle Functional Diagram

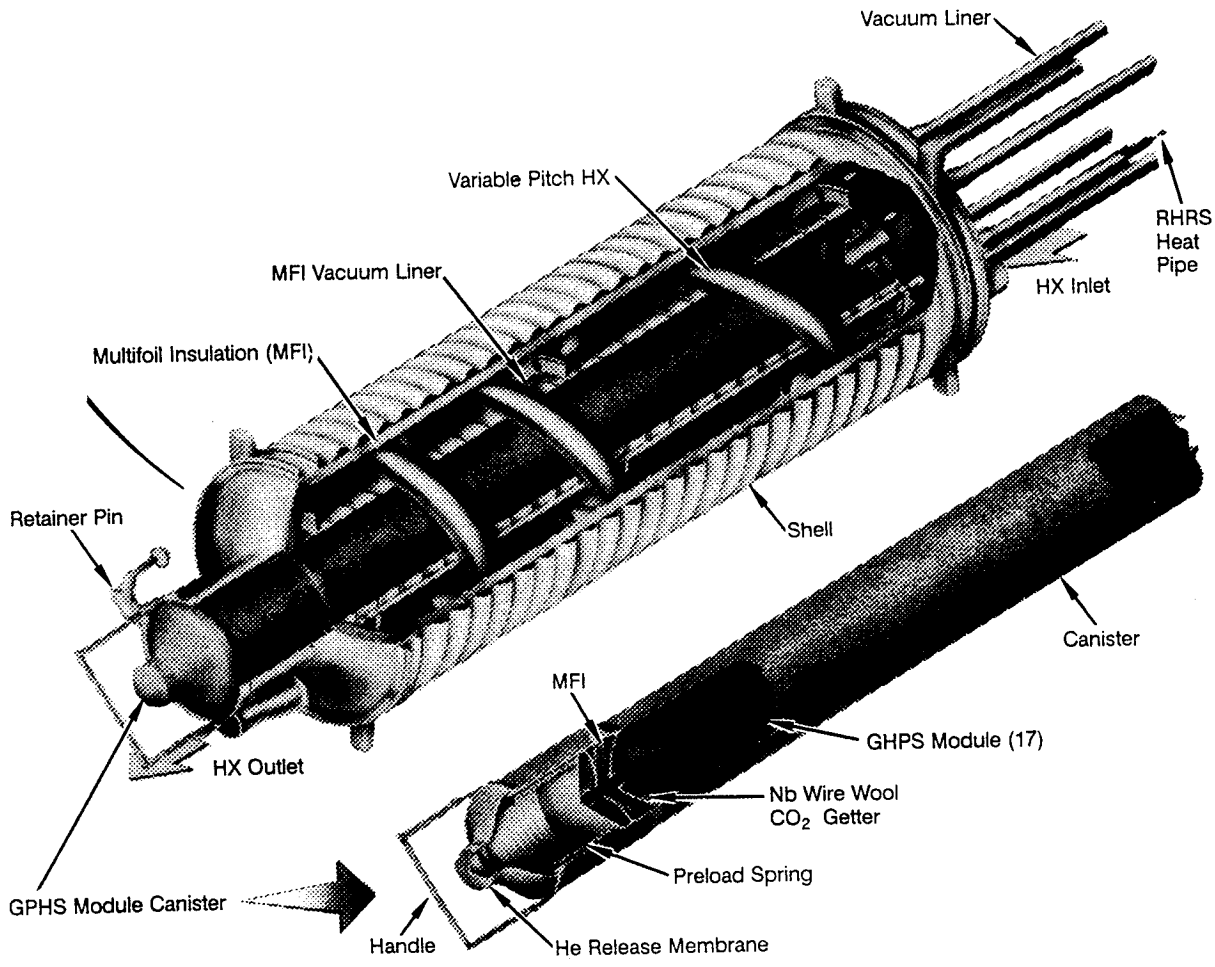

Figure 5.5 - DIPS Power Module Heat Source

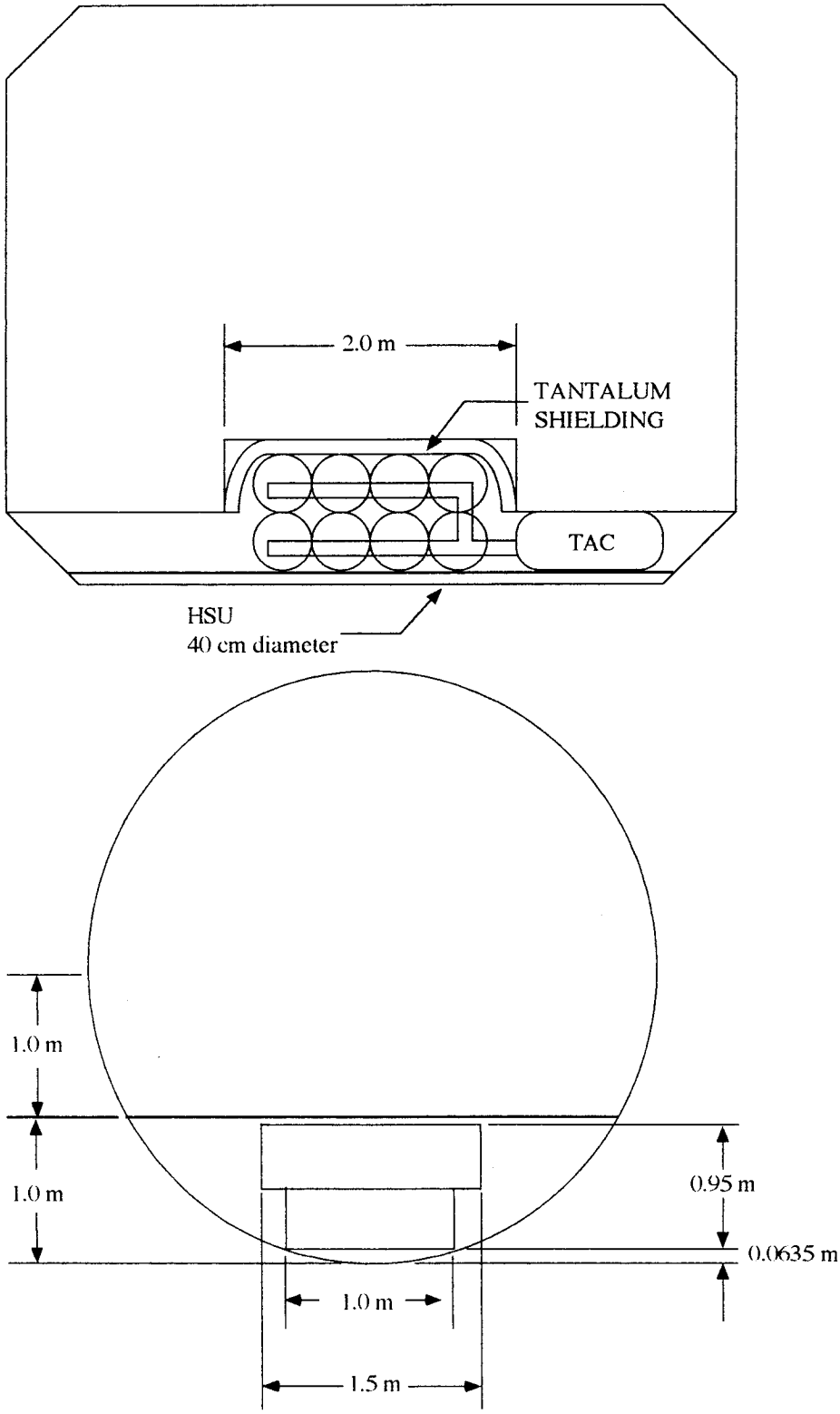

Figure 5.6 - Placement of Primary Power System

and then on to the compressor where the gas is compressed by a two to one ratio. From the compressor the gas travels again to the recuperator where it picks up excess heat from gas leaving the turbine. From the recuperator the gas travels back to the HSU and the cycle is complete (Johnson).

The radiator is a very important part of the CBC. The total radiator area is 15 m^2 with a mass of 75 kg. The radiator itself is carbon-carbon fin with copper/water heat pipes running through it. The HSU's also have a thermal control system of their own for when the system is not at full operating capacity or a problem occurs in the working fluid cycle. This system only operates when the HSU assembly temperature rises above 1300 K. The heat pipes are molybdenum with a rhenium coating and lithium as the working fluid (Schmitz). Shielding is required in order to protect the crew from the radiation given off by the HSU. The shield will be made of tantalum alloy, which will partially encase the HSU.

The volume breakdown of the CBC is as follows:

HSU	1.006 m^3
TAC	0.5 m^3
Shielding	0.4818 m^3
Total volume	1.9878 m^3

5.5 Secondary Energy Storage. A secondary energy storage system is needed to handle the peaks requirements above 8 kWe. The maximum peak power is 12 kW, which is 4 kW above the power put out by the CBC. It was estimated that these peaks would last no longer than an hour at a time. From the power profiles, the needed auxiliary power was estimated to be 4 kWhr. To satisfy this need, a sodium-sulfur battery system was chosen for the secondary power system, with a photovoltaic array to recharge the batteries. The Na/S

battery has a specific power of 250 Whr/kg (Withrow). With these figures, the total mass of the batteries would be:

mass of batteries = storage energy / specific power = 16.0 kg.

Once the batteries have been partially discharged, they can be recharged in one of two ways. The first is by the photovoltaic array made of GaAs/Ge. The second is by the primary power source, the CBC. When the total energy from the CBC is not being used, some of it can be redirected to charge the batteries. The size of the photovoltaic array was chosen to be 9 m^2. With an efficiency of 18.3%, the total power collected by the array will be 2.0159 kW. With this power, the batteries will be charged at a voltage of 240 V with a current of 8.4 amps. When the CBC is used to charge the batteries the voltage will still be 240 V but the current will vary according to the available power at the time.

5.6 Power Management and Distribution (PMAD). The purpose of the PMAD (Figure 5.7) is to distribute and convert the electrical energy produced by the CBC. The PMAD is made up of all the electrical components outside the CBC. The CBC produces 8 kWe of single phase AC power at around 200 volts. This power is regulated by a shunt regulator which dissipates all power not being used by the load. The power conditioning is done at the loads through converters designed for each (Schmitz).

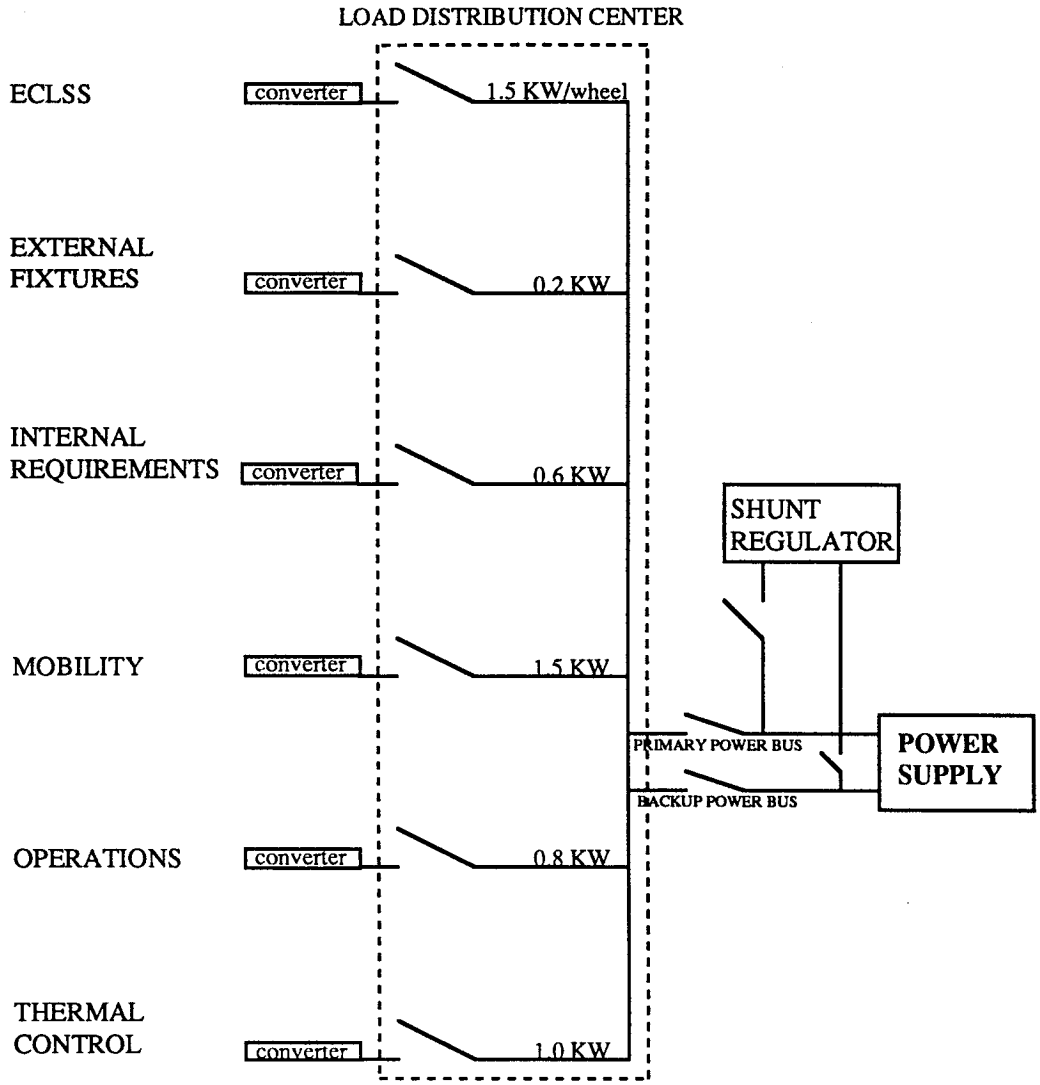

Figure 5.7 - Power Management and Distribution Functional Diagram

6. THERMAL CONTROL SUBSYSTEM

The temperature of the PLR is controlled by the balance of three thermal entities.

1) heat absorbed from thermal radiation (solar and lunar)
2) heat generated within the spacecraft
3) heat lost by radiation through the exterior surfaces

The first and third entities are considered the most important in design; however, the second cannot be ignored. Internal heat accumulation could pose a serious problem to a manned space vehicle. Common internal sources of heat are:

- waste heat and heat losses from power source
- electrical power and subsequent dissipation of heat by electrical resistance and mechanical friction of moving machinery
- human metabolism
- chemical processes

A functional diagram of the thermal control system is provided in Figure 6.1.

6.1 Options. There are basically three types of thermal control systems. The first is a passive system. In a passive system, there are usually no moving parts or heaters. The second type is a semi-passive system. It differs from the passive system because there are simple temperature-activated controls to close or open conductive paths, transport heat through heat pipes, and control the direction of radiation. Finally, there are active systems. They include pumped-loop systems, heaters controlled by thermostats, and mechanical refrigerators. Examples of all three are shown schematically in Figure 6.2.

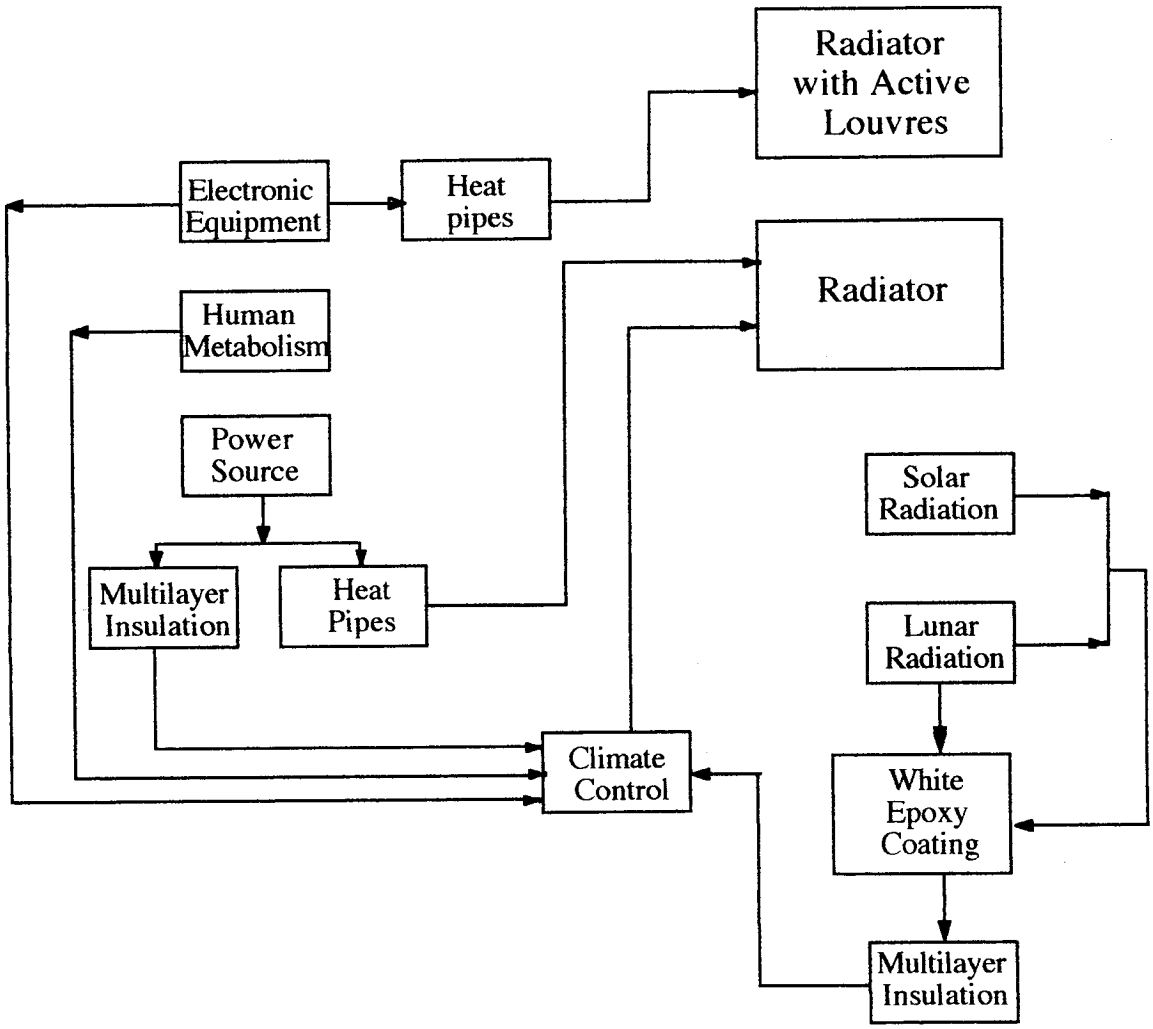

Figure 6.1 - Thermal Control Functional Diagram

Passive:

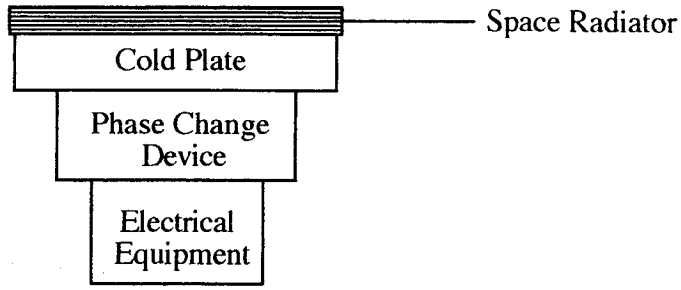

Semi-Passive:

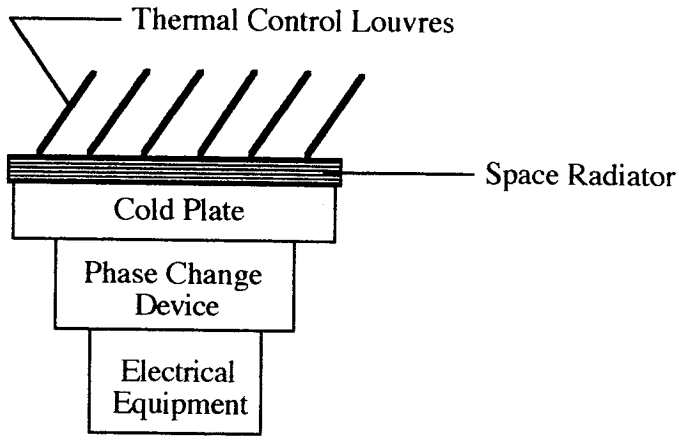

Active:

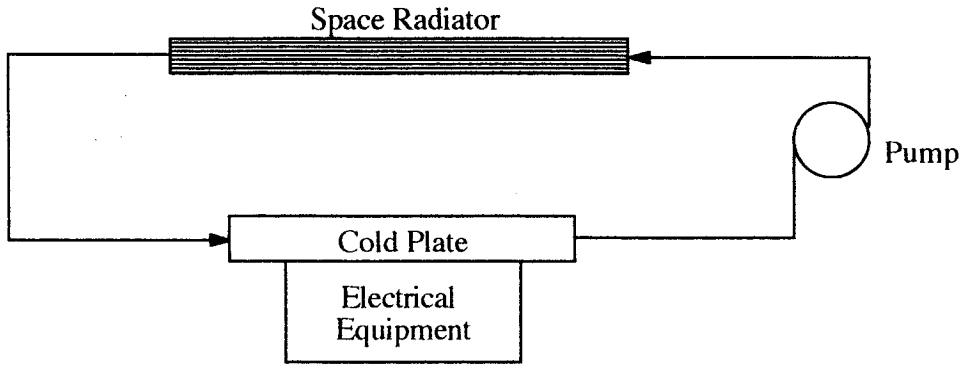

Figure 6.2 - Thermal Control Options (Wertz et al.)

A passive design is generally lighter, requires less electrical power, and costs less than an active design. Active designs are needed when there are small tolerances for temperature control. A reasonable design approach is to begin with a passive system and add additional elements as needed (Van Vliet).

6.2 Internal Thermal Control. Considering the size of the PLR, and the nature and time of a typical mission, all three of the basic thermal control systems will be used. Some temperature tolerances for the PLR are presented in Table 6.1 (Fortescue et al).

Table 6.1 - Temperature Tolerances

Electronic equipment (operating)	-10 to +40°C
Batteries	-5 to +40°C
Microprocessors	-5 to +40°C
Bearing mechanisms	-45 to +65°C
Solar cells	-45 to +65°C
Humans	+18 to +30°C

Internal heat dissipation will also need to be taken into consideration. Some sources of heat rejection and their amounts are (Walters, Eagle Engineering):

Human metabolism (4 men)	0.342 kW
Electronic equipment	3.0 kW
Power source	25 kW

6.2.1 Electrical Equipment. Most of the electrical equipment is located in two centralized areas; near the driving stations in the front module and the work stations in the rear module. In each of these two locations, a small, independent looping system will be set up. In both cases, heat will be transported from the equipment to the space radiator. The

radiator itself will be a second surface mirror (SSM). The heat transported to the SSM will be immediately rejected into space. A total of 1.5 m^2 of radiator area will be needed for the electrical equipment. A radiator area of 1.0 m^2 will be used for the equipment at the drive station and a 0.5 m^2 radiator will be required at the work stations. A generic functional diagram of this loop is given in Figure 6.3.

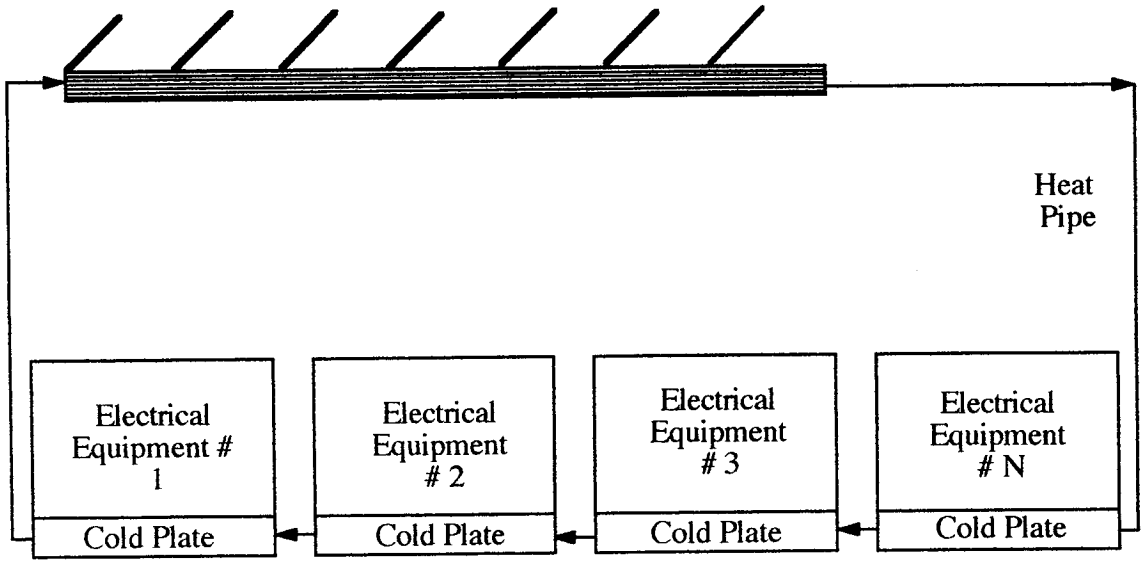

Figure 6.3 - Thermal Loop For Electrical Equipment

Thermally activated louvres will be placed on top of the SSM's. When the louvres are open, the radiator will function normally, but when closed, a heat shield will be formed. The rationale is that when the temperature is colder outside, the heat dissipated from the electrical equipment will stay inside the rover. Therefore less stress will be place upon the climate control system. The angle at which the louvres will be oriented will be linearly related to the external temperature. A schematic of this design as well as a control block diagram is shown in Figures 6.4 and 6.5 respectively.

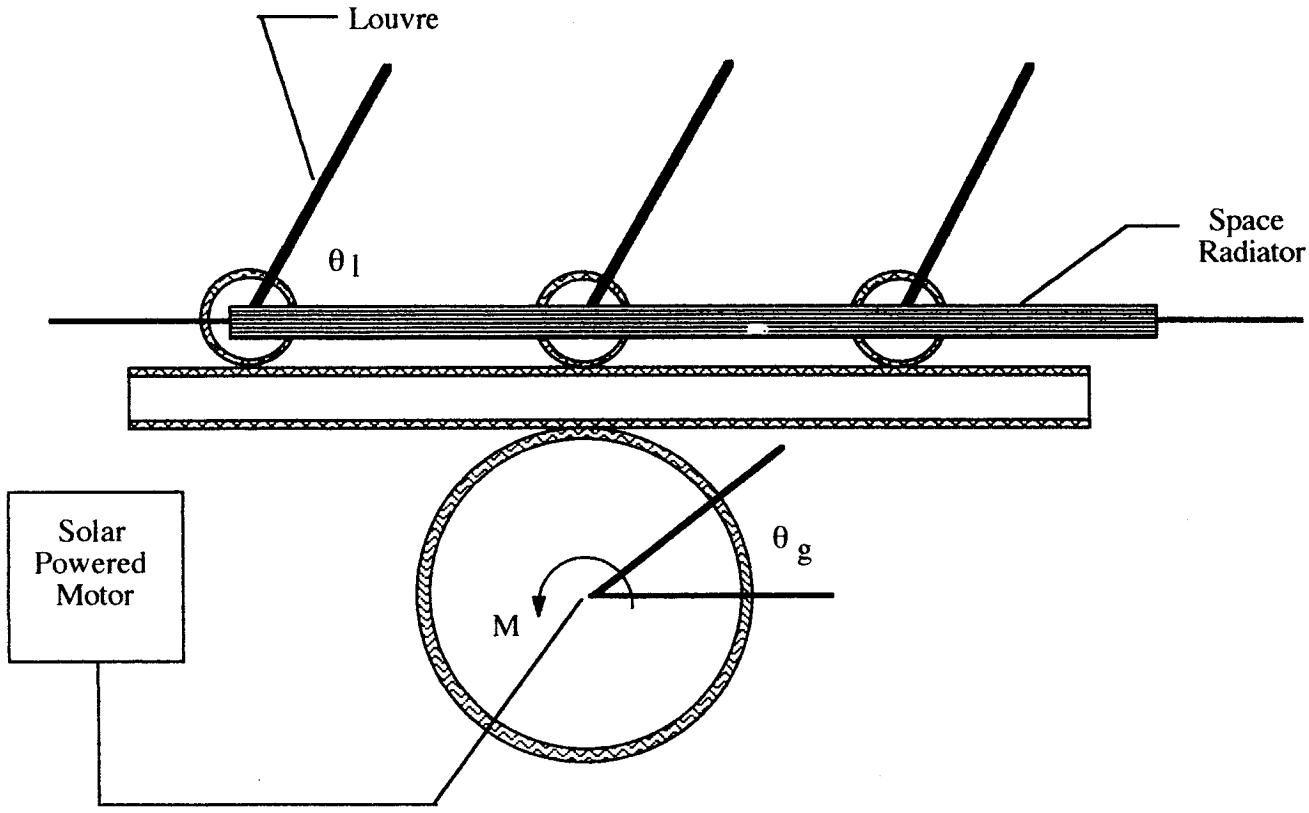

Figure 6.4 - Radiator with Active Louvres

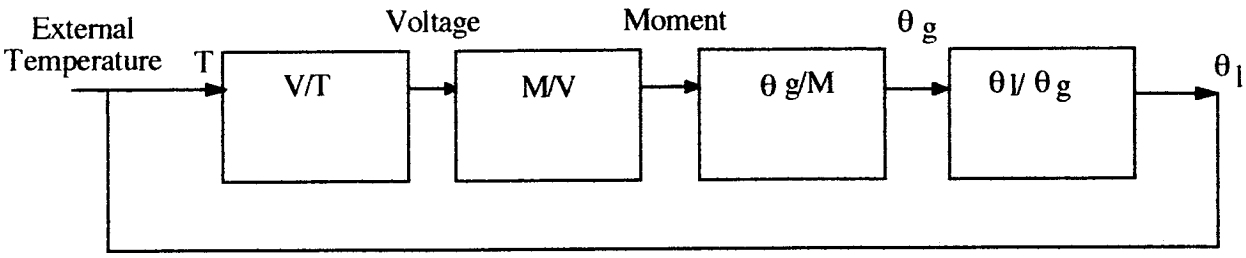

Figure 6.5 - Control Block Diagram of the Radiator with Active Louvres

6.2.2 Power System. The most critical part of the interior thermal design will be the rejection of the heat produced by the power system. The PLR will use a Closed Brayton Cycle. This system rejects approximately 25 kW of waste heat (Johnson). The power system will be located in the rear module (under the floor and near the back). The power system will need to be insulated. Thirty shields of multilayer insulation with a conductivity of 0.00029 W/mK would serve this purpose (Wertz et al).

Ideally, the heat should be rejected immediately to a space radiator from the power source, and the power source should be located as high as possible. However this conflicts with the vehicle's stability requirements. The radiator surface cannot be put on the underbelly of the PLR because the heat flow of the lunar surface would degrade its effectiveness. Also, the saddle for the mobility system would interfere, therefore that option was dropped. Alternatively, the radiator could be put on top of the rover. The only drawback of this scheme is that an elaborate heat pipe system is needed to transport the heat from the power system near the bottom of the rover to the space radiator on top.

The size of the radiator may be calculated using the Stefan-Boltzmann relation,

$$Q/A = \sigma\epsilon(T_1^4 - T_2^4)$$

where

Q = heat rejection = 25 kW

A = radiator area (unknown)

σ = Stefan-Boltzmann constant = 5.67×10^{-12} W/(cm^{2}K)

ϵ = emissivity of radiator = 0.85

T_1 = temperature of radiator (source) = 500 K

T_2 = external temperature (sink) = 227 K

From this calculation, a radiator with a 15 m^2 surface area will be needed to reject the heat from the power source.

6.2.3 Heat Pipes. The thermal control system will be required to reject the 25 kW of waste heat produced by the Closed Brayton Cycle. A critical factor in the heat rejection is that the heat must be transported over a three meter distance. This can be accomplished with heat pipes.

A heat pipe is a closed tube whose inner face is lined with a porous capillary wick. The wick is saturated with the liquid phase of the working fluid and the remaining volume of the tube contains the vapor phase. The heat applied at the evaporator (at the heat source) vaporizes the working fluid in that section. The resulting difference in pressure drives vapor from the evaporator to the condenser (at the space radiator) where it condenses, releasing latent heat of vaporization to a heat sink in that section of the pipe. Depletion of liquid by evaporation causes the liquid-vapor interface in the evaporator to enter into the wick surface and a capillary pressure is developed there. This pressure forces the liquid back to the evaporator for re-evaporation. This process carries on continuously.

The operating temperature of the heat pipes is relatively high (600 K). For such a high temperature, H_2O would be a good candidate for the working fluid. A compatible material for the container and wick must be selected for the H_2O working fluid. If a poor choice is made, harmful effects, such as corrosion and chemical reactions, may occur. Copper is highly suitable for the H_2O working fluid (Chi).

When designing a heat pipe, there are several limitations that must be taken into account. To prevent turbulent flow as well as compressibility effects, the flow must be less than Mach 0.2. This speed limitation yields a sonic limitation on the heat flux (Q_s).

There is also an entrainment limit on the heat flux (Q_e). Since the vapor and the liquid move in opposite directions in a heat pipe, a shear force exists at the liquid-vapor interface. If the vapor velocity is sufficiently high, a limit can be reached at which liquid will be entrained in the vapor. Once entrainment begins, a substantial increase in fluid circulation occurs until the liquid return system cannot accommodate the increased flow. This eventually leads to an abrupt dryout of the wick at the evaporator.

Another limiting factor on the heat flux is the capillary pressure (QL_c). For proper functioning, the pressure at the liquid side of the liquid-vapor interface must be different from that of the vapor side along the entire length of the heat pipe. The pressure difference is called the capillary pressure. If this pressure is lost, the circulation will cease.

The final limiting factor for the maximum heat flux is the boiling temperature (Q_b). The boiling limitation is basically a limitation of the radial heat flux at the evaporator and condenser. The limitation is set so that no vapor forms in the wick. If vapor bubbles did form in the wick, hot spots would be created which would obstruct the circulation of the liquid.

The limiting heat fluxes should be greater than the expected heat flux performance of the pipe. Following the graphical/analytical procedure for the design of heat pipes in S. W. Chi's, *Heat Pipe Theory and Practice*, heat pipes were designed for the transportation of waste heat from the power source to the radiator. Specifically, 20 heat pipes will be used to transport 1.25 kW of heat each. The heat pipe configuration is shown in Figure 6.6.

6.2.4 Internal Air Temperature. There are basically two situations to design for when considering the internal air temperature. From the functional diagram in Figure 6.1, lunar and solar radiation will be a factor during a lunar day. Large amounts of thermal radiation will penetrate the PLR. A climate control system (i.e a heat pump) will be required to control the temperature.

In the front Driving/Habitation Module, an intake fan will be located above the driving station. This will draw in the air and a temperature control device will correct the temperature. Then the air will be blown back to the rear of the cabin. A similar scheme will be utilized in the rear Work/EVA Module. In that module, the air will be taken in above the exercise station and put back into the cabin in front.

During a lunar night, there will be no solar radiation. Instead, the internal heat of the PLR will radiate outward. To design for this situation, a heat piping system emanating from the power system will be set up to transport waste heat to the rest of the rover. A thermal switch will be employed to open or close the conductive path of the pipes depending on the situation. The climate control system will still be utilized to guarantee the small temperature tolerances.

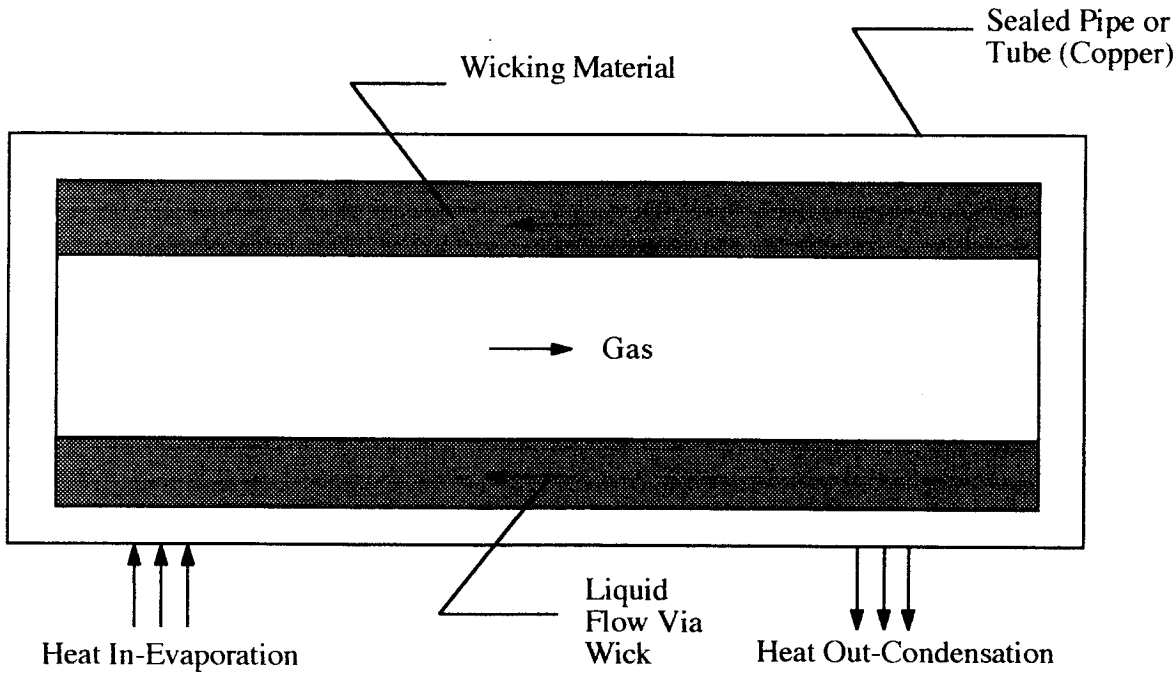

Copper pipe with copper wick
with water working fluid

outside diameter	2.54 cm
inside diameter	2.21 cm
vapor core diameter	1.02 cm
wick thickness	1.19 cm
end cap thickness	0.33 cm

copper wire screen wick
Mesh # 300

HEAT FLUX LIMITATIONS

Sonic Q_s	586 kW > 1.25 kW
Capillary Pressure QL_c	1.4 kW > 1.25 kW
Entrainment Q_e	58.3 kW > 1.25 kW
Boiling Q_b	1.32 kW > 1.25 kW

Figure 6.6 - Heat Pipe Schematic

6.3 External PLR Thermal Control. Most thermal spacecraft designs advocate the practice of completely insulating the craft from the external heat environment while controlling the rejection of heat in the interior of the craft (Van Vliet).

To calculate the heat flux through the PLR shell, the equilibrium skin temperature is used (Fortescue et al).

$$A_{PLR}\epsilon\sigma T^4 = A_S\alpha J_S + A_M\alpha J_A + A_M\epsilon F_{12}J_M$$

where

A_{PLR} = effective radiating area of the PLR

ϵ = emissivity of the PLR skin = 0.85

σ = Stephan-Boltzmann constant = 5.67×10^{-8} W/m^2

T = equilibrium skin temperature (K)

A_S = projected area of PLR towards the sun (m^2)

α = absorptivity = 0.2

J_S = solar radiation = 1400 W/m^2

A_M = projected area of PLR towards the Moon (m^2)

J_A = solar radiation due to lunar surface albedo (98 W/m^2)

F_{12} = view factor

J_M = lunar radiation = 1120 W/m^2

During the lunar day, the following estimates were used:

A_{PLR} = 81.7 m^2

A_S = 49.02 m^2

A_M = 44 m^2

F_{12} = 0.6

The calculation resulted in a skin temperature of 346 K. During the lunar night, the effects of the direct solar radiation as well as the reflected solar radiation are not present. The effective radiating area was increased to 163.4 m^2, the view factor was estimated to be 0.5, and A_M remained the same. The skin temperature for the lunar night was calculated to be 227 K.

The thermal conductance through the shell is found using:

$$q = 2\pi L(T_{inner} - T_{outer})/ (\Sigma [\ln(r_i/r_{i-1})]/k_i) \quad (i = 2,3,...7)$$

Inner G/E	r_2 = 4.0025 m r_1 = 4.0000 m	k = 8.73 W/mK
NOMEX honeycomb core	r_3 = 4.0175 m r_2 = 4.0025 m	k = 0.03 W/mK
Outer G/E	r_4 = 4.0200 m r_3 = 4.0175 m	k = 8.73 W/mK
Elastomer	r_5 = 4.0210 m r_4 = 4.0200 m	k = 0.035 W/mK
MLI	r_6 = 4.0718 m r_5 = 4.0210 m	k = 0.00029 W/mK
Aluminum bumper shield	r_7 = 4.1128 m r_6 = 4.1118 m	k = 200 W/mK
Overall Shell		k = 0.160 W/mK

The heat fluxes for extreme external conditions were found to be:

Maximum heat flux during lunar day = 8.30 W/m^2

Maximum heat flux during lunar night = 10.69 W/m^2

6.3.1 Multilayer Insulation. Multilayer insulation (MLI) consists of layers of aluminized Mylar alternated with coarse net material (Wertz et al). The net acts as a separator for the Mylar layers, thus trapping air. Usually, Kapton is used for the outermost and innermost layers. MLI has a thermal conductivity ranging from 0.00029-0.0004 W/mK depending upon the number of shields. A three centimeter thick layer of MLI will be used to insulate the structure from the external lunar and solar radiation.

MLI serves two other purposes. First it increases the effective heat capacity of the vehicle, reducing the harmful effects of thermal cycling. Second its light weight will reduce the need for highly active thermal control systems, thus increasing reliability with reductions in cost and mass.

6.3.2 White Epoxy Paint. The whole exterior surface of the shell will be coated with a white epoxy paint. The paint will not affect the thermal absorption of the surface, but will increase the emissivity. This results in a considerably lower α/ϵ ratio which can greatly reduce the temperature of the skin. For the paint chosen, if the exterior temperature were 422 K, due to the low α/ϵ (0.28), the skin equilibrium temperature would be 287 K (Wertz et al).

6.3.3 Windows. Special coatings will be necessary for the windows. To prevent the penetration of UV light, 0.1% Iron Oxide (Fe_2O_2) must be fused into the glass (Van Vliet). When sunlight transmits through glass, there is an internal temperature increase associated with it. This situation is more serious when dealing with windows on the moon. A thin film of gold will need to be sprayed onto the exterior surface of the window (Van Vliet). Heat penetration is considerably reduced while the window remains transparent.

6.3.4 Solar Cells. The effectiveness of solar cells diminishes with increasing temperature (Fortescue, et al). Also an appreciable amount of the solar radiation that hits

the cells are unusable because it is not within the range of wavelengths suitable for power conversion. This waste radiation only heats up the cells and degrades the effectiveness. A solution to the thermal problem is to coat the cells with silica. The silica increases the emittance, thus lowering the skin temperature. However, there is a 2% reduction in energy available for power conversion. To remedy the problem with the unusable radiation, filters will be used to block out the bad radiation, thus lowering the absorptance by as much as 50%. This will reduce the power output of the solar cells by slightly less than 10%, but the effectiveness will increase.

Table 6.2 - Thermal Control Subsystem Mass Statement

Component	**Mass (kg)**
Radiators	90
MLI	130
Heat pipes	100
Heat exchanger	50
Pump	20
Refrigerant	50

7. LIFE SUPPORT SUBSYSTEM

The purpose of the life support subsystem (LSS) is to maintain proper conditions for the crew and equipment inside the rover.

The first step in establishing the life support subsystem was to determine the design loads. These are shown in Table 7.1. Then the characteristics of the subsystem required for these loads were determined and shown in Table 7.2.

Table 7.1 - Life Support Subsystem Design Loads

Metabolic O_2	0.83 kg/man day
Metabolic CO_2	1.00 kg/man day
Potable H_2O	1.86 kg/man day
Metabolic H_2O	0.35 kg/man day
Handwash H_2O	1.81 kg/man day
Shower H_2O	3.63 kg/man day
Perspiration and Respiration H_2O	1.82 kg/man day
Urinal Flush H_2O	0.49 kg/man day
Urine H_2O	1.50 kg/man day
Food Solids	0.73 kg/man day
Food H_2O	0.45 kg/man day
Food Packaging	0.45 kg/man day
Fecal Solids	0.03 kg/man day
Charcoal required	0.06 kg/man day
Trash	0.82 kg/man day
Trash Volume	0.0028 m^3/man day

Table 7.2 - Life Support Subsystem Characteristics

Subsystem	Mass (kg)	Power (W)
Temperature and Humidity Control	50	60
Atmospheric Control and Supply	80	10
Atmospheric Revitalization	20	10
Fire Detection and Support	10	--
Water Recovery and Management	120	30
Waste Management	20	20
Extra-Vehicular Activity & Support	20	30
Total	**320**	**160**

The next step was to establish the degree of loop closure, i.e. how many of the expendable resources, if any, should be reclaimed. After examining the available technology as well as the weight and power penalties involved, a partially closed system was chosen. A completely closed loop system for such a small scale does not exist. Furthermore, unlike an open system, a single unit failure would jeopardize the entire closed loop. Since the mission is only 14 days, only the water and air will be reclaimed. The technology of the future should be able to perform this duty without a major power or weight penalty. The LSS operates under the parameters listed in Table 7.3.

Note that the total pressure of the cabin varies from 68.3 to 101.325 kPa. The cabin will be pressurized to 101.325 kPa when docking with the lunar base which will also be pressurized to 101.325 kPa. When departing from the lunar base, the cabin will be depressurized to 68.3 kPa so that the prebreathing before EVA is minimized.

Table 7.3 - Life Support Subsystem Parameters

Parameter	Nominal Conditions
CO_2 Pressure	33.3 Pa
O_2 Pressure	18.6-22.06 kPa
Total Pressure	101.325 kPa
Temperature	65-75 °F
Dew Point	40-60 °F
Ventilation	4.6-12.2 m/min
Potable Water	3.08-3.67 kg/man-day
Hygiene Water	5.44 kg/man-day
Wash Water	12.7 kg/man-day

The LSS functional schematic is shown in Figure 7.1. The carbon dioxide is removed from the cabin air and then the carbon is separated from the oxygen through reduction. Meanwhile, the waste water undergoes oxygen generation where the hydrogen and oxygen are separated by electrolysis. The oxygen is sent back to storage while the hydrogen is combined with the oxygen from the CO_2 reduction, and water condensate is stored and recovered. The water is then used for non-potable functions. Thus the air and water are both reclaimed.

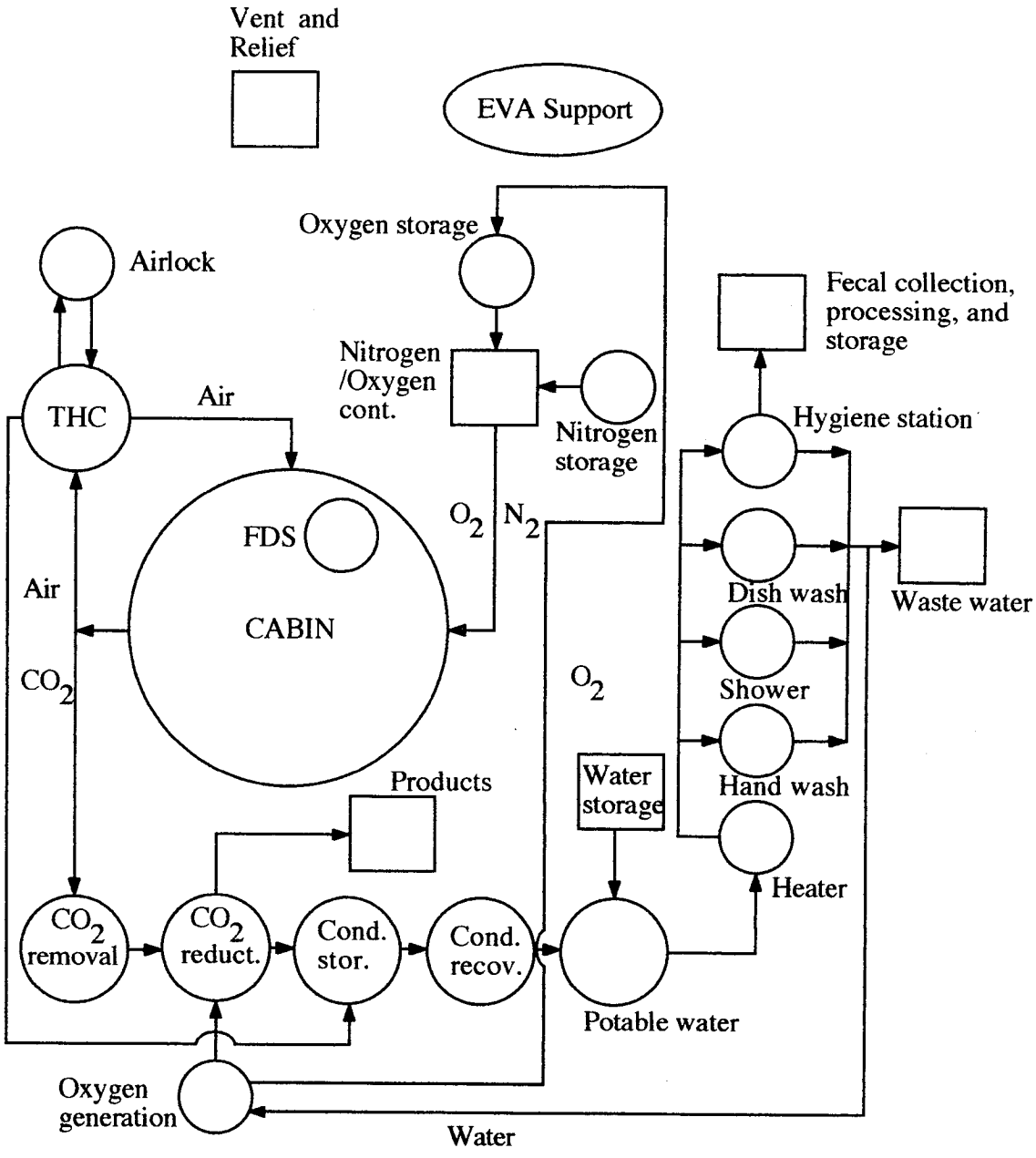

Figure 7.1 - Life Support Subsystem Functional Diagram

8. GUIDANCE, NAVIGATION, AND CONTROL SUBSYSTEM

8.1 Guidance and Navigation. The rover's guidance and navigation requirements will be met by an inertial guidance system and the use of satellite observations. The satellite will map areas in which the rover will operate. The inertial guidance system will overlay the position coordinates so that relative positions may be known and seen from a top-view.

The inertial guidance system is shown in Figure 8.1. The ball bearings on all the axes allow the gimbals to rotate with respect to each other and the case itself. The inertial guidance system is set with respect to the local horizon coordinate system at position (x_0,y_0,z_0,t_0). The gyroscopes are used to keep the gimbals in that position during the mission. When a gyroscope detects a disturbance tilt, it generates an electrical response which is processed and then directed to a gimbal motor. This motor applies a torque to rotate the appropriate gimbal in the proper direction to remove the tilt. The gyroscopes are placed orthogonal to each other so a disturbance in any axis may be discovered and the system may be kept stable.

The accelerometers are also placed orthogonal to each other. With the use of a spring scale, the accelerometers are able to detect the rover's acceleration. Integrating yields the velocity and position (relative to the starting point). The navigation computer will keep track of the rover's movements and overlay the coordinates on a satellite map of the region.

The gyroscopes sometimes produce errors in position coordinates when acted on by torques. Therefore an optical tracker will be used to provide redundancy and safety. Two celestial objects, a substantial angular distance apart, are necessary to keep the three-axis gimbal system stable. Ideally, three trackers should be used, so adjustments to all three axes may be made simultaneously and the system can pick up a celestial body entering the view while another celestial body is leaving. However, only one tracker is used because of their bulkiness. It is switched alternatively to the selected celestial bodies. Figure 8.2 shows the optical tracker. The functions of sensing the celestial body, adjusting the telescope into

C-2

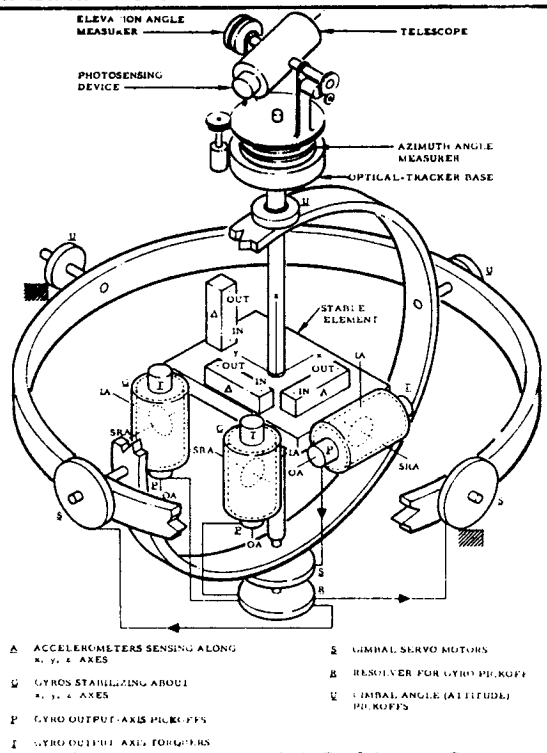

Figure 8.1 - Inertial Guidance System

(as taken from Slater)

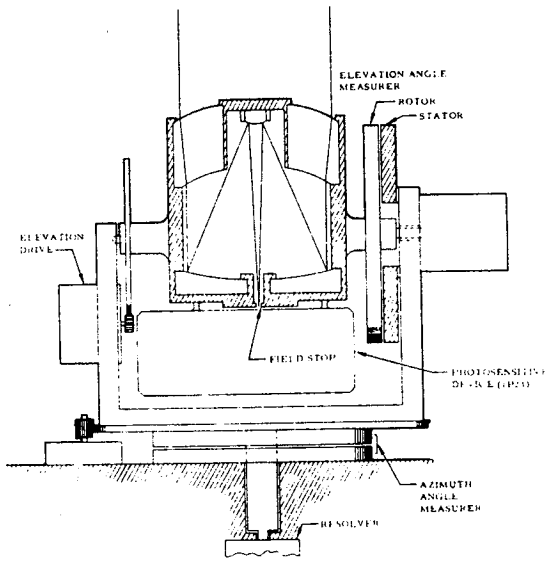

Figure 8.2 - Optical Tracker

(as taken from Slater)

alignment with it, and calculating the angles are all done by the on-board computer, with the use of a photosensitive device placed behind the focal plane of the telescope.

The driver will be able to see any obstacle within three meters of the rover through the front windows. Also lights and cameras are placed in strategic locations to see any blind spots. To help the driver determine if a rock is "clearable", a laser will be positioned on the front of the rover. When on relatively flat land, if the driver sees red light being reflected off of a rock, he will know that the rock is not clearable. Another problem in navigating will be to clear rocks when going over hills and large bumps. For example, while the rover is ascending a hill and the rear cylinder has not reached the hill yet, the pinned bar will tend to rotate the front of the rover down, decreasing the ground clearance at the front end of the rover. In case of a rock obstacle, a cylindrical bumper/roller made of elastomer will be placed in front of the rover. If a rock hits it, it will turn the front part of the rover about the pin. This will help the rover clear the rock and at the same time protect the underbody.

8.2 Control. A manual system is used to control the rover. The steering wheel will control the front two wheels (of the forward cylinder) and the rear two wheels (of the rear cylinder). It will be supported with the articulated joint, with skid steering available in an emergency. The driving mechanism will consist of three pre-programmed modes. These modes will depend on how many powered wheels are needed (i.e. four, six, and eight powered wheels). Also there will be a manual override capability with eight individual controls to power each wheel.

While steering, the computer will calculate all the necessary angles for a turn of perfect geometry, using the articulated joint and Ackermann steering until the maximum articulation angle is achieved. If a tighter turn is required, it can be achieved using oversteer (see §4).

9. COMMUNICATIONS SUBSYSTEM

The missions of the rover require several different communications links. These links will be combined into one subcarrier scheme, amplified by a common power amplifier and broadcast by one antenna.

Earth-to-lunar links are nearly constant in range (about 385,000 kilometers). Due to the effects of lunar radio noise, atmospheric absorptions, etc., the equivalent noise temperature of 400 K is assumed.

It is assumed that there will be a network of three lunar stations which will allow full coverage of the moon for voice transmission (Filipowsky).

9.1 The S-Band System. The communications system requires a ranging system for accurate range measurements. This is accomplished by the repeated transmission of a long pseudo-random code. The code bandwidths are very wide, so they must be broadcast in the C-band or the S-band.

Also, there are two approaches to dealing with the separate links of the communications system. The VHF approach involves transmitting each individual link with its own antenna. These frequencies are allocated in the UHF and VHF regions. The S-band approach combines the separate signals into one signal, whose wide bandwidth requires allocation in the S-band. This eliminates the need for multiple antennas.

By combining the ranging system with the unified approach, the communications subsystem becomes more compact and requires less power. The various signals are combined with a modulator, then amplified by a 20 W amplifier for transmission at 2.3 GHz by a parabolic reflector antenna. The signal can then be transmitted to either a lunar base, or directly to earth.

9.2 Voice Links. The voice link (Figure 9.1) allows direct communications between the astronauts and the lunar base, with the option of communication with earth, if necessary. For redundancy, two separate two-way voice links are provided. It has been shown that a three kHz band transmitted at 30 dB will produce easily understandable speech (telephone lines use the same bandwidth, but at a higher signal contrast). The range equation can be used to determine the transmission power.

$$Pr = kT_{op}B_{tr}\sigma_i 4\pi R^2 M/GA\eta$$

where

k = Boltzmann constant

T_{op} = average operating radio noise temperature

B_{tr} = transmission bandwidth

σ_i = input signal contrast

R = distance from source

M = safety factor

G = gain of broadcasting antenna

A = area of receiving antenna

η = antenna efficiency

By assuming a safety factor of 10, a 26 dB gain, and an 85 ft diameter receiving antenna with an efficiency of 60%, the voice link will require 1.32 W of power.

The voice link will allow normal conversation between the astronauts and the base, with a 2.6 second round trip delay between the rover and earth, requiring a slightly altered conversation scheme. Also, a special frequency is allotted for emergency messages.

The rover is equipped with a voice control center which will also serve as an intercom. It accepts inputs from standard microphones located throughout the rover and provides outputs to loudspeakers. The power requirement for voice transmission is about 2W, which may need to be modified depending on ground equipment.

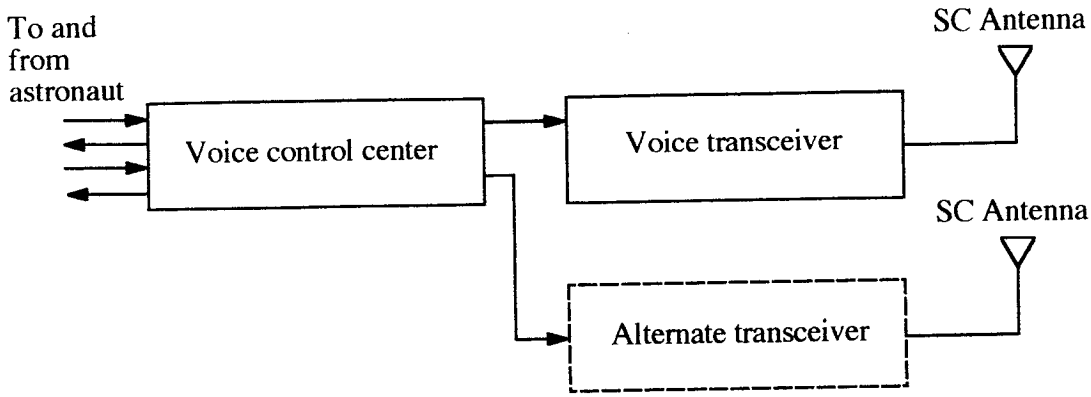

Figure 9.1 - Two-way Voice Link

9.3 Telemetry Link. The telemetry link (Figure 9.2) transmits all data information from the rover to the base. This data includes scientific data (from measurements), biomedical data, housekeeping and structural data, and computer processed data. This data will be transmitted in real time when the rover is in line-of-sight with the base. For long-range missions, the telemetry can be stored onboard and transmitted at high speed when near the base. The telemetry will be processed at the base, then transmitted to earth.

Telemetry data will be handled with PCM transmission, a type of digital transmission that is very flexible and allows a high degree of accuracy. The telemetry will also carry some analog data. The analog data will be combined with the digital data to produce a composite signal which is then transmitted.

The signal power contrast will be about 13 dB (which will result in an error rate of about 1 in 10^{-5}), and the signal will transmit about 108 bits/day, or 2500 bits/sec.

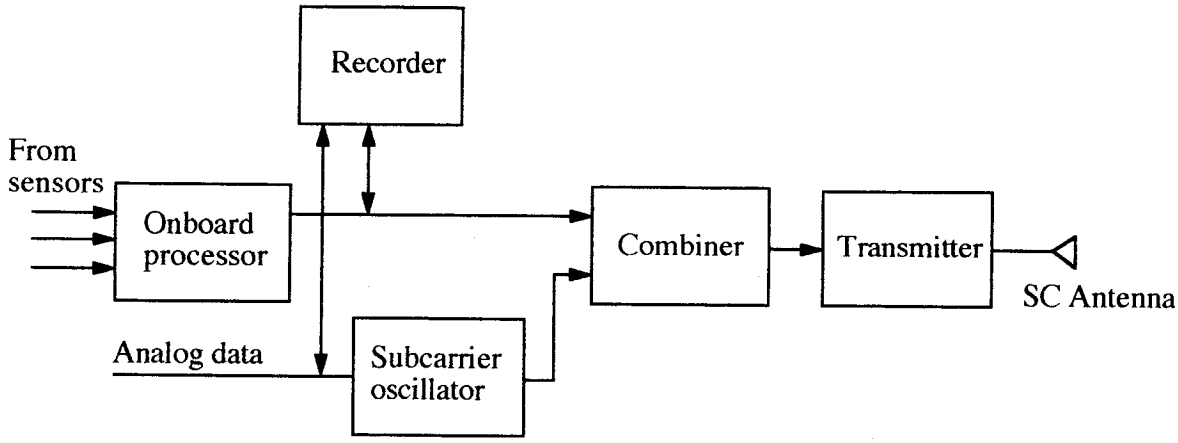

Figure 9.2 - Telemetry Link

9.4 Command Link. The command link (Figure 9.3) serves as the data up-link for the mission. It allows direct command from the base, with an option for command from earth. The data is transmitted digitally in a special command link code. The data is coded to prevent faulty messages or false commands. The signal is decoded aboard the rover, and verified via telemetry back to the command link. Command reception triggers a command directly to the appropriate system.

The decoder will require 17 W of power and the receiver will require 1.5 W.

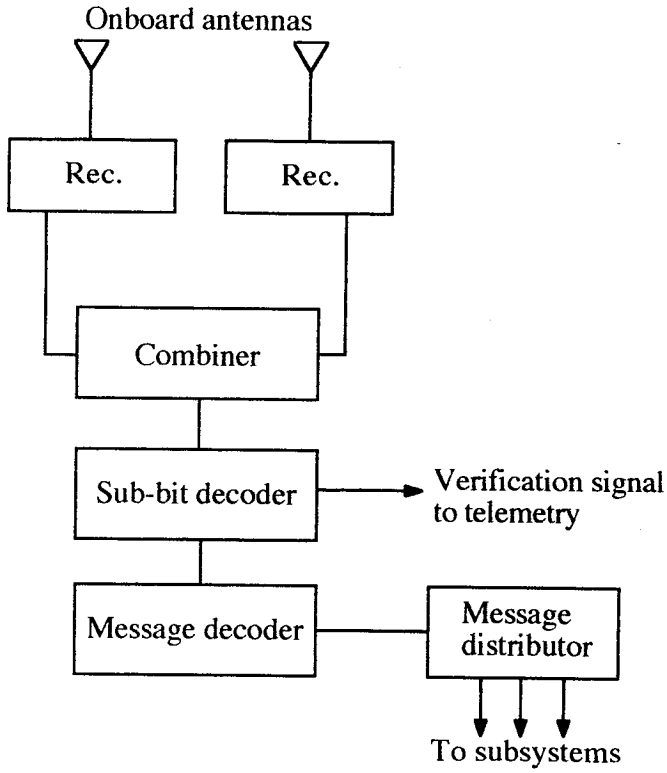

Figure 9.3 - Digital Command Link

9.5 Television Link. The rover's television link (Figure 9.4) is one of the less critical parts of the communications system. A slow scan of about 300 lines at 10 frames/sec will suffice for most applications. By utilizing a digital scanning method, frame rate can be sacrificed for resolution (and vice versa), to better suit specific applications. Figure 9.5 shows picture quality levels for various signal-noise ratios (Sonnet). The ratios in the figure show peak signal-noise ratios, not average ratios, which are about 3 dB less. It can be seen that 26 dB will be sufficient for good picture transmission, and the link will need about 12W of power.

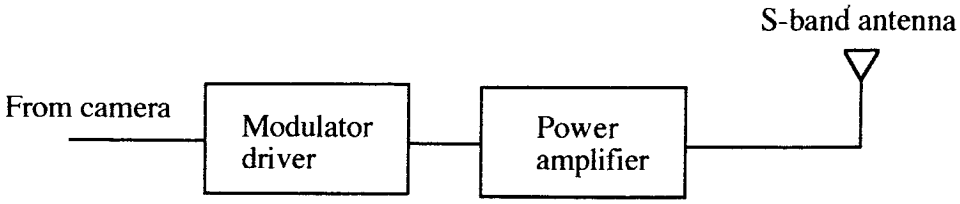

Figure 9.4 - TV Link

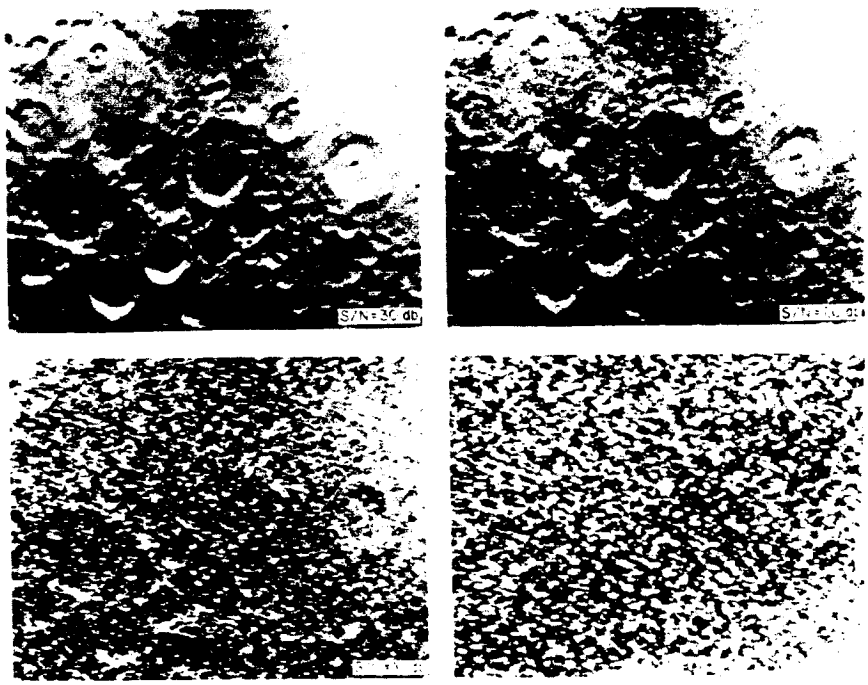

Figure 9.5 - Picture Quality Levels

Picture quality for different *peak* signal to rms noise ratio.

9.6 EVA Link. Extravehicular activity will require special EVA communications links (Figure 9.6). This will be for short distances, around 100 to 1,000 meters. The EVA link will consist of a combination of a two-way voice link and biomedical telemetry. This can work on a voice-actuated switch; when the voice channel is not being used, telemetry

will be transmitted. This can be broadcast to the astronauts by an omnidirectional (0 dB gain) antenna on a VHF band, which will require minimal power.

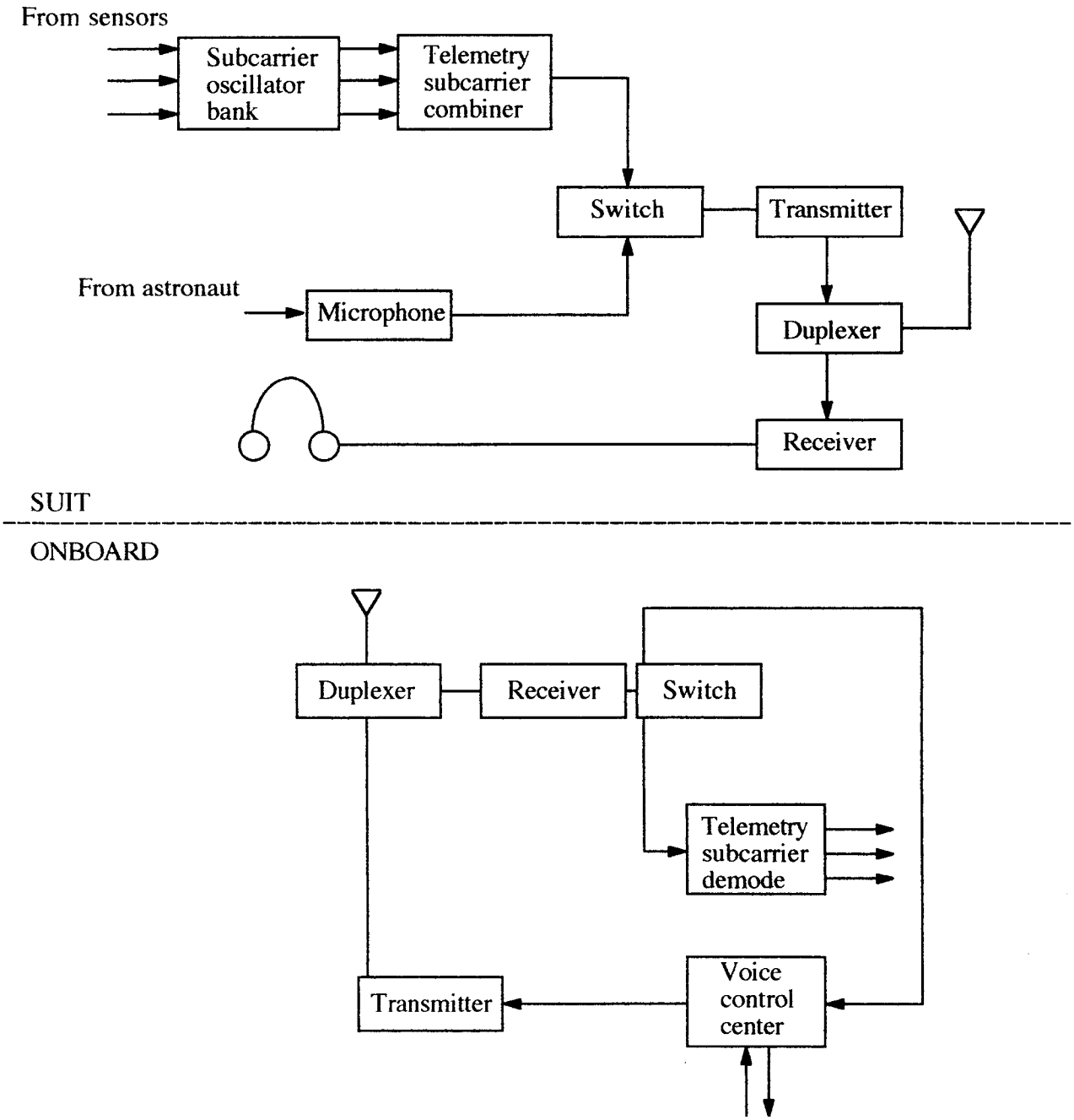

Figure 9.6 - Extra-vehicular Link

9.7 Antennas. As previously mentioned, the EVA link will be transmitted by a small, low-power omnidirectional antenna, which will be mounted on the front half of the rover. All other communications links will be transmitted by a parabolic reflector dish. It has been shown that a 26 dB gain is adequate for picture, voice, and telemetry transmission. The gain of an antenna is related to its area by the following equation:

$$G = 4\pi\eta A/L^2$$

where L = wavelength of transmission.

With a 2.3 GHz signal broadcast by an antenna of 50% efficiency, the dish must have a diameter of 1.174 meters to produce a 26 dB gain. To account for antenna degradation, a 1.2 meter parabolic reflector was selected, which will also be mounted on the front of the rover.

10. REFERENCES

Bekker, M. G. *Introduction To Terrain Vehicle Systems.* Ann Arbor: The University of Michigan Press, 1969.

Bennett, G. L. *A Look at the Soviet Space Nuclear Power Program.* Proceedings of the 24th Intersociety Energy Conversion Engineering Conference, Volume 2, 1989.

Blankenship, Charles P. and Hayduk, Robert J. *Large Space Structures-Structural Concepts and Materials.* SAE Paper 872499.

Budinski, Kenneth G. *Engineering Materials, Properties and Selection.* New Jersey: Prentice Hall, Inc., 1992.

Chi, S. W. Heat Pipe Theory and Practice. New York: McGraw-Hill Book Company 1976.

Cook, Steve. *HLLV Evolution*, report presented at NASA Meeting, Langley Virginia, 1991.

CRC Practical Handbook of Materials Science. Section 12, *Polymeric Materials.*

Dochat, G. R. and Dhar, M. *Free Piston Space Stirling Technology Program.* Proceedings of the 24th Intersociety Energy Conversion Engineering Conference, Volume 2, 1989.

Dupont. *Design and Fabrication Techniques for Honeycomb of NOMEX Aramid Sandwich Structures.*

Dwiggins, Boyce H. *Automotive Steering System.* Albany: Delmar Publishers, 1968.

Eagle Engineering, Maintenance and Supply Options N88-29837.

Caroon, Wayne L. Euro-Composites. Elkwood, VA.

Filipowski, Richard F. and Muehldorf, Eugen I. *Space Communications Systems.* New Jersey: Prentice Hall, 1965.

Fortescue, Peter and Stark, John Ed., *Spacecraft Systems Engineering.* John Wiley & Sons, 1991, New York

Green, Jack. *The Geology of the Lunar Base.* North American Aviation, Inc., Space and Information Systems Division, 1961.

Hall, John B., Ferebee, Melvin J., and Sage, Karen H. *Environmental Control and Life Support Systems Technology Options for Space Station Application.* SAE Paper 851376.

Hatsopoulos, G. N. and Gyftopoulos, E. P. *Thermionic Energy Conversion; Volume 1, Processes and Devices.* Massachusetts: M.I.T. Press, 1975.

Haynes, D. A. Space Exploration Initiative, NASA Langley Research Center.

Heiken, Grant H., Vaniman, David T., and French, Bevan M. *Lunar Sourcebook; A User's Guide To The Moon.* Cambridge: Cambridge University Press, 1991.

Heisler, Heinz. *Vehicle And Engine Technology, Volume 1.* London: Edward Arnold (Publishers) Ltd, 1985.

Heitchus, Regis D. *Space Systems Technology.* Reinhold Book Corporation, 1968.

Humphries, William R., Reuter, James L., and Schunk, Richard G. *Space Station Environmental Control and Life SUpport System Distribution and Loop Closure Studies.* SAE Paper 860942.

Humphries, William R., Reuter, James L., and Schunk, Richard G. *Space Station Freedom Environmental Control and Life Support System Design - A Status Report.* SAE Paper 901211.

Johnson, R.A. "A Dynamic Power System Portable Generator for the Moon or Mars." IECEC-91 Paper No. 910210

Jones, Clyde S., Doran, Billy, Nola, Frank. *Traction Drive System Considerations for a Lunar Roving Vehicle.* SAE Paper 700023.

Kander, R. G. Department of Materials Science & Engineering, V.P.I. & S.U.

Lawrence, L. Jr. and Lett, P. W. *Characterization of Lunar Surfaces and Concepts of Manned Lunar Roving Vehicles.* SAE Paper 630078.

Limpert, Rudolf. *Vehicle System Components: Design and Safety.* New York: John Wiley & Sons.

Loken, H. Y. *Dupont Aramids for Advanced Composites*, Industrial Composites Seminar. Society for the Advancement of Materials & Process Engineering, Midwest Chapter, March 9, 1982.

Lundeberg, J. F. *Meteoroid Design Criteria.* SAE Paper 650786.

Mateuffel, E. W. *Direct Current Brushless Torquer.* Final Report, Contract NAS8-20591, MSFC, Huntsville, Alabama, December 1967.

McKaig. *Lunar Scientific Missions.* SAE Paper 660449.

Mobile Robots III. Proceedings - International Society for Optical Engineering, SPIE, 1989.

Moss, Dennis R. *Pressure Vessel Design Manual.* Houston: Gulf Publishing Company, 1987.

Mutch, Thomas A. *Geology of the Moon, A Stratigraphic View.* Princeton: Princeton University Press, 1970.

NASA Document. *Planet Surface Systems Element Systems Database 91.1.* 1991.

NASA Technical Memorandum 4170. *Exploration Studies Technical Report, Volumes I & III.* 1989.

Nealy, John E., Wilson, John W., and Townsend, Lawrence W. *Preliminary Analyses Of Space Radiation Protection For Lunar Base Surface Systems.* SAE Paper 891487.

Off-highway Vehicles, Tractors & Equipment: Conference of Automobile Division of Institution of Mechanical Engineers, Mechanical Engineers Publications, Ltd., 1976.

Paul, D. III. *Challenge of Alternate Approaches To the Achievement of Lunar Exploration and Exploitation.* SAE Paper 650833.

Powell, F. T., Wynveen, R. A., and Lin, C. *Environmental Control and Life Support Technologies for Advanced Manned Missions.* SAE Paper 860994.

Sandbank, C. P. *Digital Television.* John Wiley & Sons, 1990.

Slater, J. M. *Inertial Guidance Sensors.* Reinhold Publishing Corporation, 1964.

Sponsler, W. B. *Preliminary Mobility Tests of a Scale Model Lunar Roving Vehicle.* SAE Paper 660147.

Stadnik, A. G. *DIPS Power Conversion Cycle Selection.* Proceedings of the 24th Intersociety Energy Conversion Engineering Conference, Volume 2, 1989.

Sykes, George F., Milkovich, Scott M. and Herakovich, Carl T. *Simulated Space Radiation Effects on a Graphite Epoxy Composite.* Polymeric Materials: Science and Engineering v.52, 1985.

Thornel Carbon Fibers, Thornel, Amoco.

Tiffany, O. L. and Zwitzeff, E. M. *Scientific Exploration of the Moon Using a Roving Vehicle.* SAE Paper 660145.

Townsend, Lawrence W., Wilson, John W., and Nealy, John E. *Space Radiation Shielding Strategies and Requirements For Deep Space Missions.* SAE Paper 891433.

Turner, David. *A Cost-Effective Brushless D.C. Motor.* SAE Paper 860475.

Van Vliet, Robert M. *Passive Temperature Control in the Space Environment.* The Macmillan Company, 1965, New York

Walters, C.E. *Thulium Heat Source for High-Endurance and High-Energy-Density Power System.* IECEC-91 Paper No. 910234.

Wertz, James R. and Larson, Wiley J. Ed., *Space Mission Analysis Design.*

Wong, J. Y. *Theory of Ground Vehicles.* John Wiley & Sons, 1978.

Wong, Richard E. *Manned and Unmanned Roving Vehicles for Lunar Exploration.* SAE Paper 680373.

Wong, Richard E. and Galan, Louis. *Design For The Lunar Environment.* SAE Paper 680099.

Wong, Richard E. and Galan, Louis. *Lunar Mobile Laboratory - Design Characteristics.* SAE Paper 660146.